ON SUPERRADIANT PHASE TRANSITIONS IN GENERALISED DICKE MODELS

— Quantum and Thermal Phase Transitions in the Lambda-Model —

vorgelegt von

Diplom-Physiker

Mathias Hayn

aus Berlin

Von der Fakultät II – Mathematik und Naturwissenschaften
der Technischen Universität Berlin
zur Erlangung des akademischen Grades
Doktor der Naturwissenschaften
Dr. rer. nat.

genehmigte Dissertation

PROMOTIONSAUSSCHUSS:

Vorsitz:	Prof. Dr. Ulrike Woggon, Technische Universität Berlin
Erster Gutachter:	Prof. Dr. Tobias Brandes, Technische Universität Berlin
Zweiter Gutachter:	Prof. Dr. Cristiano Ciuti, Université Paris Diderot — CNRS

Tag der wissenschaftlichen Aussprache: 9. November 2016

Berlin 2017

Für Anton, Luisa & Sophie

ABSTRACT

In this doctoral thesis, the thermodynamic phases und phase transitions of a generalised Dicke model are studied and characterised. Both, finite and vanishing temperatures are considered.

The Dicke model of quantum optics describes collective phenomena which occur when light interacts with a many-atom system. In the thermodynamic limit, a so-called Hepp–Lieb superradiant phase transition sets in. A superradiant phase develops for low temperatures or strong coupling between light and atoms, which is characterised by a macroscopic excitation of the light field and a spontaneous, collective polarisation of the atoms.

This thesis discusses a generalised version of the Dicke model, which is described by a quantum mechanical system consisting of three-level atoms in Lambda-configuration and two modes of a resonator.

By means of the Holstein–Primakoff transformation, the Hamiltonian of this system is written in terms of four interacting, non-linear oscillators, which can be linearised in the thermodynamic limit, yielding the ground-state energy as well as the low-energy excitations. The phase diagram consisting of two superradiant phases separated by continuous and first-order phase transitions is derived.

In order to clarify the question whether or not the superradiant phase transition of this generalised Dicke model can be observed experimentally for real atoms, the significance of the diamagnetic term is discussed. In contrast to the original Dicke model, superradiant phase transitions are possible in principle. This is due to the first-order phase transitions. In addition, a no-go theorem for continuous superradiant phase transitions is presented. The argument is based on the Thomas–Reiche–Kuhn sum rule.

Last, we study the superradiant phase transition of the generalised Dicke model at finite temperatures. Therefore, the partition sum is computed and analysed in the thermodynamic limit using Laplace's method. At finite temperatures, the properties of the phase diagram and phases remain. However, here all phase transitions are of first order.

ZUSAMMENFASSUNG

Gegenstand dieser Doktorarbeit ist die Untersuchung und Charakterisierung der thermodynamischen Phasen und Phasenübergänge in einem generalisierten Dicke-Modell bei endlichen Temperaturen und im Grenzfall verschwindender Temperaturen.

Das Dicke-Modell der Quantenoptik dient zur Beschreibung von kollektiven Phänomenen in der Wechselwirkung von Licht mit vielen Atomen. Es weist im thermodynamischen Limes einen Phasenübergang auf; den sogenannten Hepp–Lieb Superradianzphasenübergang. Hier kommt es bei tiefen Temperaturen bzw. starker Kopplung zwischen Licht und Atomen zur Bildung einer superradianten Phase, welche durch eine makroskopische Anregung im Lichtfeld und eine spontane kollektive Polarisierung aller Atome gekennzeichnet ist.

In dieser Arbeit wird eine generalisierte Version des Dicke-Modells betrachtet: Die Atome werden durch quantenmechanische Systeme bestehend aus drei Energiezuständen in der sogenannten Lambda-Konfiguration beschrieben und das Lichtfeld besteht aus zwei Moden eines Resonators.

Mithilfe der Holstein–Primakoff-Darstellung wird der Hamilton-Operator des Systems auf die Form von vier wechselwirkenden nichtlinearen Oszillatoren gebracht. Im thermodynamischen Limes wird dieses System linearisiert und die Grundzustandsenergie, sowie die niedrig-energetischen Anregungsenergien analytisch bestimmt. Das Phasendiagramm mit zwei superradianten Phasen getrennt durch Phasenübergänge erster und zweiter Ordnung wird aufgestellt.

Ein weiterer Aspekt dieser Doktorarbeit ist, ob der superradiante Phasenübergang dieses generalisierten Dicke-Modells in Systemen mit echten Atomen experimentell nachgewiesen werden kann. Hierbei wird auf die Bedeutung des diamagnetischen Terms eingegangen und gezeigt, dass hier, im Gegensatz zum ursprünglichen Dicke-Modell, aufgrund des Auftretens eines Phasenübergangs erster Ordnung ein superradianter Phasenübergang möglich ist. Des Weiteren wird ein Beweis für die Unmöglichkeit von kontinuierlichen superradianten Phasenübergängen bei realen Atomen vorgestellt. Grundlage dafür ist die Thomas–Reiche–Kuhn-Summenregel.

Als letzter Punkt wird auf die Frage eingegangen, wie sich der Quantenphasenübergang des generalisierten Dicke-Modells auf endliche Temperaturen überträgt. Dazu wird die Zustandssumme im thermodynamischen Limes in einer Sattelpunktsnäherung berechnet und analysiert. Man sieht, dass auch bei endlichen Temperaturen der Charakter des Phasendiagramms und der Phasen erhalten bleibt, wobei hier alle Phasenübergänge von erster Ordnung sind.

CONTENTS

1 INTRODUCTION

The Dicke model of quantum optics in its original form introduced by Robert Henry Dicke in 1954 (Dicke, 1954) describes the interaction of a many-atom system with the electromagnetic field, light in particular. It supports the prominent phenomenon of Dicke superradiance, i. e. the collective spontaneous radiation of light which is focused both in space (along a direction defined by the experimental setup) and time. In addition, in the thermodynamic limit, the Dicke model develops a phase transition, the superradiant Hepp–Lieb phase transition, which was first described in 1973 by Elliot Hershel Lieb & Klaus Hepp (Hepp and Lieb, 1973b). This continuous phase transition separates a phase at high temperatures and small atom-light coupling from a phase at low temperatures and strong atom-light coupling. In the former, all atoms occupy their respective ground state and no excitations in the light field are present. The latter phase is the so-called superradiant phase, which is characterised by a macroscopic excitation of the atoms and the light field, and a collective spontaneous polarisation of the atoms.

Phase transitions are one of the most striking phenomena in physics. For a wide range of control parameters, e. g. temperature or pressure, a substance has qualitatively the same physical properties. But some of these properties differ strongly for the respective phases. The appearance of phase transitions are traced back to large fluctuations of energy and particle number of the system at certain temperatures or other control parameters. These fluctuations are due to the coupling of the system to its environment. At zero temperature, thermal fluctuations are absent. However, then quantum fluctuations can take over and give rise to quantum phase transitions. Both, thermal and quantum phase transitions, emerge in the Dicke model.

The superradiant phase transition is some kind of peculiar, since it does not show for systems consisting of real atoms. Theoretically, this is described by the so-called no-go theorem. However, the group of Tilman Esslinger realised the superradiant phase transition for an effective Dicke model in 2010 (Baumann, Guerlin, et al., 2010). Among others, this triggered a great deal of publications on the Dicke model and its generalisations.

The aim of this thesis is to analyse a generalised version of the original Dicke model: The individual atoms are described by three-level systems in a Lambda-configuration, i. e. two, in general, non-degenerate ground states which couple via two modes of a resonator respectively to one excited state. The first question which naturally

arises is if there is a superradiant phase transition; probably yes. But does the superradiant phase exhibits the same properties as in the original model and of what order is the phase transition? Aside from that, might it be even possible that the no-go theorem is not applicable here and a superradiant phase transition does occur for real atoms in this generalised level scheme. We will discuss all these questions in the quantum limit, i. e. at zero temperature. However, the influence of finite temperatures on the phase transition and the properties of the phases is addressed as well.

In addition, the STIRAP[1] scheme and dark-state physics are hallmarks of the Lambda-configuration. The STIRAP scheme is used in experiments for a complete transfer of population from one quantum state to another quantum state. In order to allow for a transfer between transitions which are forbidden due to selection rules, STIRAP is achieved via an intermediate state which is never populated during the transfer. In the case of the Lambda-configuration, the intermediate state is the excited state and the two states on which the transfer is performed are the two ground states. Since the excited state is never populated, it can never decay and thus not radiate via a coupling to a light field. For this reason, the excited state is called dark state here. Since the dark state plays a prominent role in STIRAP and the physics of atoms in Lambda-configuration, we expect to find some kind of emergence of it in the phases or phase transitions.

Before we analyse the generalised Dicke model in detail, we give a derivation of the original and the generalised versions of the Dicke model. This derivation is based on a microscopic Hamiltonian. Furthermore, an introduction to the phenomena of Dicke superradiance, and the superradiant phase transition of Hepp and Lieb and its quantum limit is given. But first of all, we quantise the electromagnetic field and its interaction with charges, in order to get the proper constants in the microscopic atomic Hamiltonian. This step is crucial when we study the effect of the diamagnetic term and the no-go theorem for real atoms.

1.1 QUANTISATION OF THE ELECTROMAGNETIC FIELD

The classical theory of electromagnetism is based on Maxwell's equations and the Lorentz force law from which all electromagnetic phenomena like radiation, Faraday's cage, light diffraction and reflection, induction, and so forth can be deduced. However, to formulate a quantum theory of electromagnetism, the Maxwell–Lorentz equations are not a good starting point. The canonical way of quantising a classical theory is by promoting the generalised coordinates and their conjugate momenta to operators which obey a canonical commuta-

1 Stimulated Raman Adiabatic Passage, cf. e.g. Ref. (Bergmann, Theuer, and Shore, 1998).

tion relation (Dirac, 1958; Altland and Simons, 2010). In addition, the classical Hamiltonian function becomes an operator and is the central object in Schrödinger's equation.

Thus we need to find the classical Hamiltonian of the electromagnetic field. On the other hand, the Hamiltonian is obtained from the Lagrangian by a Legendre transformation. So the schedule is as follows:

(*i*) Find the Lagrangian of the electromagnetic field which generates the correct equations of motion, i. e. the Maxwell–Lorentz equations,

(*ii*) identify the generalised coordinates and the corresponding conjugate momenta,

(*iii*) set up the Hamiltonian, and

(*iv*) canonical quantise the Hamiltonian.

This is done in the next subsections.

1.1.1 *The Lagrangian of Electromagnetism*

One fundamental principle of analytical mechanics is Lagrangian mechanics. Given the Lagrangian of a system, one can derive the equations of motion which govern the movement of point particles as well as the dynamics of fields, i. e. systems with continuous degrees of freedom (Goldstein, 1980). The latter applies to e. g. all kind of wave phenomena, especially to the electromagnetic field.

The Lagrangian L for systems of charged particles interacting with an electromagnetic field is given by

$$L\big(\{\mathbf{r}_n\},\{\dot{\mathbf{r}}_n\},\mathbf{A},\Phi,\partial_t\mathbf{A},\partial_t\Phi\big) = \sum_{n=1}^{\mathcal{N}} \frac{1}{2} m_n \dot{\mathbf{r}}_n^2 + \int_{\mathbb{R}^3} d^3r\, \mathcal{L}, \tag{1.1}$$

with the Lagrangian density

$$\mathcal{L} = \frac{\varepsilon_0}{2}\left[\mathbf{E}(\mathbf{r})^2 - c^2\mathbf{B}(\mathbf{r})^2\right] + \mathbf{j}(\mathbf{r})\cdot\mathbf{A}(\mathbf{r}) - \rho(\mathbf{r})\Phi(\mathbf{r}). \tag{1.2}$$

Here, $\mathbf{r}_n$ is the position of the n^{th} particle with charge q_n and mass m_n, $\dot{\mathbf{r}}_n = \frac{d}{dt}\mathbf{r}_n$ is the corresponding velocity, ε_0 is the vacuum permittivity, $\mathbf{E}$ and $\mathbf{B}$ are the electric and magnetic field, respectively, c is the speed of light in vacuum, $\mathbf{j}$ and ρ are the current and charge density, respectively, and $\mathbf{A}$ and Φ are the vector and scalar potential, respectively. The sum extends over the number $\mathcal{N}$ of charged particles.

The current and charge densities are sources for the electromagnetic field and originate from the charged particles,

$$\mathbf{j}(\mathbf{r}) = \sum_{n=1}^{\mathcal{N}} q_n \dot{\mathbf{r}}_n \delta(\mathbf{r} - \mathbf{r}_n), \tag{1.3}$$

$$\rho(\mathbf{r}) = \sum_{n=1}^{\mathcal{N}} q_n \delta(\mathbf{r} - \mathbf{r}_n), \tag{1.4}$$

where $\delta(\mathbf{r})$ is Dirac's delta distribution.

Lastly, the connection of the electromagnetic fields $\mathbf{E}$ & $\mathbf{B}$ and the electromagnetic potentials $\mathbf{A}$ & Φ is given by

$$\mathbf{E}(\mathbf{r}) = -\nabla\Phi(\mathbf{r}) - \partial_t \mathbf{A}(\mathbf{r}), \tag{1.5a}$$

$$\mathbf{B}(\mathbf{r}) = \nabla \times \mathbf{A}(\mathbf{r}). \tag{1.5b}$$

The Lagrangian of Eq. (1.1) is justified, since its Euler–Lagrange equations reproduce both the Lorentz force law and the Maxwell equations (Jackson, 1999; Cohen-Tannoudji, Dupont-Roc, and Grynberg, 1989). In addition, it is invariant under Lorentz transformations and makes the corresponding action gauge invariant.

ELECTROMAGNETISM IN FOURIER SPACE The Maxwell equations and the potential equations, Eq. (1.5), involve different kind of space derivatives like gradient, divergence, and rotation. These are not that difficult to handle. However, the equations are much more simpler in Fourier or reciprocal space where space derivatives become multiplications with numbers.

If $f(\mathbf{r})$ is a field or component of a vector field, then the corresponding field $\tilde{f}(\mathbf{k})$ in Fourier space reads

$$\tilde{f}(\mathbf{k}) = \int_{\mathbb{R}^3} d^3r\, f(\mathbf{r}) e^{-i\mathbf{k}\cdot\mathbf{r}}, \tag{1.6}$$

or the other way around

$$f(\mathbf{r}) = \int_{\mathbb{R}^3} \frac{d^3k}{(2\pi)^3}\, \tilde{f}(\mathbf{k}) e^{i\mathbf{k}\cdot\mathbf{r}}. \tag{1.7}$$

We denote fields in Fourier space, i. e. the Fourier transform, by a tilde. Besides, note that the $1/2\pi$ normalisation factor is asymmetrically put into the $\mathbf{k}$ integral.

We give two examples of Fourier transforms which will be needed later on. First, the Fourier transform of the charge density, Eq. (1.4), is given by

$$\tilde{\rho}(\mathbf{k}) = \sum_{n=1}^{\mathcal{N}} q_n e^{-i\mathbf{k}\cdot\mathbf{r}_n}. \tag{1.8}$$

Secondly, we calculate the Fourier transform of $\phi(\mathbf{r}) = 1/r$, the Coulomb potential, explicitly,

$$\tilde{\phi}(\mathbf{k}) = \int_{\mathbb{R}^3} d^3r \, \frac{e^{-i\mathbf{k}\cdot\mathbf{r}}}{r} \tag{1.9}$$

$$= \int_0^\infty dr \int_0^\pi d\vartheta \, \sin\vartheta \int_0^{2\pi} d\varphi \, r \, e^{-ikr\cos\vartheta} \tag{1.10}$$

$$= 2\pi \int_0^\infty dr \int_{-1}^1 ds \, r \, e^{-ikrs} \tag{1.11}$$

$$= \lim_{\mu\to 0} \frac{2\pi}{ik} \int_0^\infty dr \, \left(e^{ikr} - e^{-ikr}\right) e^{-\mu r} \tag{1.12}$$

$$= -\lim_{\mu\to 0} \frac{2\pi}{ik} \left(\frac{1}{ik-\mu} - \frac{1}{-ik-\mu} \right) = \frac{2\pi}{ik} \frac{2ik}{k^2} \tag{1.13}$$

$$\tilde{\phi}(\mathbf{k}) = \frac{4\pi}{k^2}. \tag{1.14}$$

The Fourier transform $\tilde{f}$ is in general complex. However, all fields in the Lagrangian are real valued. In order to guarantee for real valued fields in Eq. (1.7), the Fourier transform $\tilde{f}(\mathbf{k})$ has to satisfy the relation[2]

$$\tilde{f}^*(\mathbf{k}) = \tilde{f}(-\mathbf{k}). \tag{1.17}$$

I. e., we get the Fourier transform for negative $\mathbf{k}$ by complex conjugation.

The Fourier transforms of the electromagnetic fields, Eq. (1.5), are given by the relations

$$\tilde{\mathbf{E}}(\mathbf{k}) = -i\mathbf{k}\,\tilde{\Phi}(\mathbf{k}) - \partial_t \tilde{\mathbf{A}}(\mathbf{k}), \tag{1.18}$$

$$\tilde{\mathbf{B}}(\mathbf{k}) = i\mathbf{k} \times \tilde{\mathbf{A}}(\mathbf{k}). \tag{1.19}$$

Before we write the Lagrangian density, Eq. (1.2), in Fourier space, we first note that for two fields $f(\mathbf{r})$ & $g(\mathbf{r})$ and their corresponding Fourier transforms $\tilde{f}(\mathbf{k})$ & $\tilde{g}(\mathbf{k})$ it holds

$$\int_{\mathbb{R}^3} d^3r \, f(\mathbf{r}) g(\mathbf{r}) = \int_{\mathbb{R}^3} d^3r \, \frac{1}{(2\pi)^6} \int_{\mathbb{R}^3} d^3k \int_{\mathbb{R}^3} d^3k' \, \tilde{f}(\mathbf{k}) \tilde{g}(\mathbf{k}') \, e^{i(\mathbf{k}+\mathbf{k}')\cdot\mathbf{r}} \tag{1.20}$$

$$= \int_{\mathbb{R}^3} \frac{d^3k}{(2\pi)^3} \int_{\mathbb{R}^3} d^3k' \, \tilde{f}(\mathbf{k}) \tilde{g}(\mathbf{k}') \delta(\mathbf{k}+\mathbf{k}') \tag{1.21}$$

$$= \int_{\mathbb{R}^3} \frac{d^3k}{(2\pi)^3} \, \tilde{f}(\mathbf{k}) g(-\mathbf{k}). \tag{1.22}$$

---

[2]

$$f^*(\mathbf{r}) \overset{(1.7)}{=} \int_{\mathbb{R}^3} \frac{d^3k}{(2\pi)^3} \, \tilde{f}^*(\mathbf{k}) e^{-i\mathbf{k}\cdot\mathbf{r}} \overset{\mathbf{k}\to-\mathbf{k}}{=} \int_{\mathbb{R}^3} \frac{d^3k}{(2\pi)^3} \, \tilde{f}^*(-\mathbf{k}) e^{i\mathbf{k}\cdot\mathbf{r}} \tag{1.15}$$

$$\overset{!}{=} f(\mathbf{r}) \overset{(1.7)}{=} \int_{\mathbb{R}^3} \frac{d^3k}{(2\pi)^3} \, \tilde{f}(\mathbf{k}) e^{i\mathbf{k}\cdot\mathbf{r}} \tag{1.16}$$

Thus, we have the relation

$$\int_{\mathbb{R}^3} d^3r\, f(\mathbf{r}) g(\mathbf{r}) = \int_{\mathbb{R}^3} \frac{d^3k}{(2\pi)^3}\, \tilde{f}(\mathbf{k}) \tilde{g}^*(\mathbf{k}), \tag{1.23}$$

which is known as Plancherel theorem (Champeney, 1973). Then, the Lagrangian in Eq. (1.1) can be written as

$$L = \sum_{n=1}^{N} \frac{1}{2} m_n \dot{\mathbf{r}}_n^2 + \int_{\mathbb{R}^3} \frac{d^3k}{(2\pi)^3}\, \tilde{\mathcal{L}}_1, \tag{1.24}$$

where the Lagrangian density $\tilde{\mathcal{L}}$ in Fourier space is given by

$$\begin{aligned} \tilde{\mathcal{L}}_1 &= \frac{\varepsilon_0}{2} \left[|\tilde{\mathbf{E}}(\mathbf{k})|^2 - c^2 |\tilde{\mathbf{B}}(\mathbf{k})|^2 \right] + \tilde{\mathbf{j}}^*(\mathbf{k}) \cdot \tilde{\mathbf{A}}(\mathbf{k}) - \tilde{\rho}^*(\mathbf{k}) \tilde{\Phi}(\mathbf{k}) \\ &= \frac{\varepsilon_0}{2} \left[|i\mathbf{k}\tilde{\Phi}(\mathbf{k}) + \partial_t \tilde{\mathbf{A}}(\mathbf{k})|^2 - c^2 |\mathbf{k} \times \tilde{\mathbf{A}}(\mathbf{k})|^2 \right] \\ &\qquad + \tilde{\mathbf{j}}^*(\mathbf{k}) \cdot \tilde{\mathbf{A}}(\mathbf{k}) - \tilde{\rho}^*(\mathbf{k}) \tilde{\Phi}(\mathbf{k}). \end{aligned} \tag{1.25}$$

We already noticed that the Fourier transform is in general complex. So at first glance it may seem that we have twice as many degrees of freedom in Fourier space than in real space. On the other hand, we have noticed in Eq. (1.17) that the Fourier transform needs to be defined in one *half space* only; the Fourier transform at $\mathbf{k}$ in the second half space can be obtained by complex conjugation of the Fourier transform at the corresponding point $\mathbf{k}$ in the first half space. Thus we can restrict the integrals in Fourier space to the half space

$$\mathbb{K} = \left\{ \mathbf{k} = (k_1, k_2, k_3) \in \mathbb{R}^3 \,|\, k_1 \geqslant 0 \right\}. \tag{1.26}$$

Then the integral in L ranges over $\mathbb{K}$,

$$L = \sum_{n=1}^{N} \frac{1}{2} m_n \dot{\mathbf{r}}_n^2 + \int_{\mathbb{K}} \frac{d^3k}{(2\pi)^3}\, \tilde{\mathcal{L}}_2 \tag{1.27}$$

and the Lagrangian density is given by

$$\begin{aligned} \tilde{\mathcal{L}}_2 = \varepsilon_0 &\left[|i\mathbf{k}\tilde{\Phi}(\mathbf{k}) + \partial_t \tilde{\mathbf{A}}(\mathbf{k})|^2 - c^2 |\mathbf{k} \times \tilde{\mathbf{A}}(\mathbf{k})|^2 \right] \\ &+ \tilde{\mathbf{j}}^*(\mathbf{k}) \cdot \tilde{\mathbf{A}}(\mathbf{k}) + \tilde{\mathbf{j}}(\mathbf{k}) \cdot \tilde{\mathbf{A}}^*(\mathbf{k}) - \tilde{\rho}^* \tilde{\Phi}(\mathbf{k}) - \tilde{\rho} \tilde{\Phi}^*(\mathbf{k}). \end{aligned} \tag{1.28}$$

The two extra terms in the Lagrangian density $\tilde{\mathcal{L}}_2$, Eq. (1.28), compared to the Lagrangian density $\tilde{\mathcal{L}}_1$, Eq. (1.25), stem from the restriction of the range of the integral to the half space.

We see that there is no kinetic term $\partial_t \Phi$ for the scalar potential in the Lagrangian. This is no problem when the Euler–Lagrange equations are set up for the coordinate Φ (which will give Gauß's law). However, in the end we want to construct the Hamiltonian, where we need the conjugate momenta of all coordinates. The conjugate momentum of a coordinate q is obtained from the partial derivative

$\partial L/\partial(\partial_t q)$. Since $\partial_t \Phi$ does not enter L, there is no corresponding conjugate momentum, or it is identically zero. This means, that Φ is no dynamical variable. To eliminate Φ from the Lagrangian, we first set up the Euler–Lagrange equation for $\tilde{\Phi}$,

$$0 = \frac{\partial \tilde{\mathcal{L}}_2}{\partial \tilde{\Phi}^*(\mathbf{k})} - \frac{\partial \tilde{\mathcal{L}}_2}{\partial(\partial_t \tilde{\Phi}^*(\mathbf{k}))} = -\varepsilon_0 \left[i\mathbf{k}\tilde{\Phi}(\mathbf{k}) + \partial_t \tilde{\mathbf{A}}(\mathbf{k}) \right] \cdot i\mathbf{k} - \tilde{\rho}(\mathbf{k}), \quad (1.29)$$

then solve for $\tilde{\Phi}$,

$$\tilde{\Phi}(\mathbf{k}) = \frac{1}{k^2} \left[i\mathbf{k} \cdot \partial_t \tilde{\mathbf{A}}(\mathbf{k}) + \frac{\tilde{\rho}(\mathbf{k})}{\varepsilon_0} \right], \quad (1.30)$$

and lastly, replace $\tilde{\Phi}$ in the Lagrangian.

THE COULOMB GAUGE The electromagnetic field at each point in space is characterised by $\mathbf{E}$ and $\mathbf{B}$, i. e. by six degrees of freedom. The four Maxwell equations relate these degrees of freedom, such that only four independent degrees of freedom for the electromagnetic field remain. These four degrees of freedom fully describe the theory.

We have considered the Lagrangian of the electromagnetic field in terms of the scalar and the vector potential plus their corresponding *velocities*. We have already eliminated the scalar potential since it is no dynamical variable. Thus, so far our theory is based on six degrees of freedom, i. e. compared to the theory described by the $\mathbf{E}$ and $\mathbf{B}$ field, there are two excessive degrees of freedom. The two degrees of freedom can be further eliminated by fixing a gauge. The most appropriate gauge in our case is the Coulomb or transverse gauge. In the Coulomb gauge, one sets

$$\nabla \cdot \mathbf{A}(\mathbf{r}) = 0, \quad (1.31)$$

or in Fourier space

$$\mathbf{k} \cdot \tilde{\mathbf{A}}(\mathbf{k}) = 0. \quad (1.32)$$

The name *transverse* gauge becomes clear from the second equation, where the longitudinal (parallel to $\mathbf{k}$) part of $\tilde{\mathbf{A}}$ is set to zero and only the transverse part is left.

Due to this discrimination of transverse and longitudinal components of the vector potential, we decompose *all* Fourier transformed vector fields $\tilde{\mathbf{v}}$ in the Lagrangian in a transversal $\tilde{\mathbf{v}}_\perp$ and a longitudinal $\tilde{\mathbf{v}}_\parallel$ part,

$$\tilde{\mathbf{v}}(\mathbf{k}) = \tilde{\mathbf{v}}_\parallel(\mathbf{k}) + \tilde{\mathbf{v}}_\perp(\mathbf{k}), \quad (1.33)$$

where the longitudinal and transverse parts are given by

$$\tilde{\mathbf{v}}_\parallel(\mathbf{k}) = \frac{\mathbf{k}}{k} \cdot \tilde{\mathbf{v}}(\mathbf{k}) \frac{\mathbf{k}}{k} \equiv \tilde{v}_\parallel(\mathbf{k}) \frac{\mathbf{k}}{k} \text{ and} \quad (1.34)$$

$$\tilde{\mathbf{v}}_\perp(\mathbf{k}) = \tilde{\mathbf{v}}(\mathbf{k}) - \tilde{\mathbf{v}}_\parallel(\mathbf{k}), \quad (1.35)$$

respectively.

Performing this decomposition, the Lagrangian density, Eq. (1.28), becomes

$$\tilde{\mathcal{L}}_2 = \varepsilon_0 \left[|i\mathbf{k}\,\tilde{\rho}(\mathbf{k})/(k^2\varepsilon_0) + \partial_t \tilde{\mathbf{A}}_\perp(\mathbf{k})|^2 - c^2 |\mathbf{k} \times \tilde{\mathbf{A}}_\perp(\mathbf{k})|^2 \right] + \tilde{\mathbf{j}}^*_\perp(\mathbf{k}) \cdot \tilde{\mathbf{A}}_\perp(\mathbf{k}) + \tilde{\mathbf{j}}_\perp(\mathbf{k}) \cdot \tilde{\mathbf{A}}^*_\perp(\mathbf{k}) - 2\frac{\tilde{\rho}^*(\mathbf{k})\tilde{\rho}(\mathbf{k})}{k^2\varepsilon_0}. \quad (1.36)$$

If we expand the moduli squared, we finally obtain the Lagrangian

$$L = \sum_{n=1}^{\mathcal{N}} \frac{1}{2} m_n \dot{\mathbf{r}}_n^2 - V_C + \int_{\mathbb{K}} \frac{d^3k}{(2\pi)^3}\, \tilde{\mathcal{L}}_3, \quad (1.37)$$

where V_C is the electrostatic Coulomb energy of all charges,

$$V_C = \frac{1}{\varepsilon_0} \int_{\mathbb{K}} \frac{d^3k}{(2\pi)^3} \frac{|\tilde{\rho}(\mathbf{k})|^2}{k^2}, \quad (1.38)$$

which can be written as

$$V_C = \frac{1}{2\varepsilon_0} \int_{\mathbb{R}^3} \frac{d^3k}{(2\pi)^3} \frac{|\tilde{\rho}(\mathbf{k})|^2}{k^2} \quad (1.39)$$

$$\overset{(1.8)}{=} \frac{1}{2\varepsilon_0} \sum_{n,m=1}^{\mathcal{N}} q_n q_m \int_{\mathbb{R}^3} \frac{d^3k}{(2\pi)^3} \frac{1}{k^2}\, e^{-i\mathbf{k}\cdot(\mathbf{r}_n - \mathbf{r}_m)} \quad (1.40)$$

$$\overset{(1.14)}{=} \sum_{n=1}^{\mathcal{N}} \frac{q_n^2}{16\pi^3\varepsilon_0} \int_{\mathbb{R}^3} d^3k\, \frac{1}{k^2} \quad (1.41)$$

$$+ \frac{1}{\varepsilon_0} \sum_{\substack{n,m=1 \\ n>m}}^{\mathcal{N}} q_n q_m \int_{\mathbb{R}^3} \frac{d^3k}{(2\pi)^3} \int_{\mathbb{R}^3} d^3r \frac{e^{-i\mathbf{k}\cdot(\mathbf{r}_n - \mathbf{r}_m + \mathbf{r})}}{4\pi r} \quad (1.42)$$

$$= V_{SE} + \frac{1}{4\pi\varepsilon_0} \sum_{\substack{n,m=1 \\ n>m}}^{\mathcal{N}} q_n q_m \int_{\mathbb{R}^3} d^3r\, \frac{1}{r} \delta(\mathbf{r}_n - \mathbf{r}_m + \mathbf{r}) \quad (1.43)$$

$$V_C = V_{SE} + \frac{1}{4\pi\varepsilon_0} \sum_{\substack{n,m=1 \\ n>m}}^{\mathcal{N}} q_n q_m \frac{1}{|\mathbf{r}_n - \mathbf{r}_m|}. \quad (1.44)$$

We see that the Coulomb energy V_C can be separated into two parts; one constant (but diverging) self energy part, V_{SE}, and one part which stems from the electrostatic interaction of all charges.

The Lagrangian density $\tilde{\mathcal{L}}_3$ is given by

$$\tilde{\mathcal{L}}_3 = \varepsilon_0 \left[\partial_t \tilde{\mathbf{A}}^*(\mathbf{k}) \cdot \tilde{\mathbf{A}}(\mathbf{k}) - c^2 k^2 \tilde{\mathbf{A}}^*(\mathbf{k}) \cdot \tilde{\mathbf{A}}(\mathbf{k}) \right] + \tilde{\mathbf{j}}^*(\mathbf{k}) \cdot \tilde{\mathbf{A}}(\mathbf{k}) + \tilde{\mathbf{j}}(\mathbf{k}) \cdot \tilde{\mathbf{A}}^*(\mathbf{k}), \quad (1.45)$$

and we have omitted the subscript $\perp$ of the vector potential and from now on, the Coulomb gauge is assumed, i. e. $\tilde{\mathbf{A}} \cdot \mathbf{k} = 0$.

Due to the Coulomb gauge, the vector field $\tilde{\mathbf{A}}(\mathbf{k})$ has two independent components only. We denote these two components at the point $\mathbf{k}$ with $\boldsymbol{\varepsilon}_1(\mathbf{k})$ and $\boldsymbol{\varepsilon}_2(\mathbf{k})$, respectively. Thus, $\tilde{\mathbf{A}}$ can be written as

$$\tilde{\mathbf{A}}(\mathbf{k}) = \boldsymbol{\varepsilon}_1(\mathbf{k})\tilde{A}_{\varepsilon_1}(\mathbf{k}) + \boldsymbol{\varepsilon}_2(\mathbf{k})\tilde{A}_{\varepsilon_2}(\mathbf{k}), \quad \boldsymbol{\varepsilon}_1 \perp \boldsymbol{\varepsilon}_2. \tag{1.46}$$

Going back to real space, the corresponding Lagrangian is

$$\begin{aligned} L = &\sum_{n_1}^{\mathcal{N}} \frac{1}{2} m_n \dot{\mathbf{r}}_n^2 - V_C \\ &+ \int_{\mathbb{R}^3} d^3r \left(\frac{\varepsilon_0}{2} \left[\left(\partial_t \mathbf{A}(\mathbf{r})\right)^2 - c^2 \left(\nabla \times \mathbf{A}(\mathbf{r})\right)^2 \right] + \mathbf{j}(\mathbf{r}) \cdot \mathbf{A}(\mathbf{r}) \right). \end{aligned} \tag{1.47}$$

1.1.2 *The Classical Hamiltonian of Electrodynamics*

So far we have constructed the Lagrangian in the Coulomb gauge of charges interacting with the electromagnetic field. The next step is to find the corresponding Hamiltonian. Therefore, we compute the conjugate momenta $\mathbf{p}_n$ and $\tilde{\boldsymbol{\Pi}}$ of the coordinates $\mathbf{r}_n$ and $\tilde{\mathbf{A}}$. The conjugate momenta for the charges are given by

$$\mathbf{p}_n = \nabla_{\dot{\mathbf{r}}_n} L = m_n \dot{\mathbf{r}}_n + q_n \mathbf{A}(\mathbf{r}_n), \tag{1.48}$$

where we took into account that the velocities $\dot{\mathbf{r}}_n$ enter the current density, Eq. (1.3). In terms of the conjugate momenta, the current density reads

$$\mathbf{j}(\mathbf{r}) = \sum_{n=1}^{\mathcal{N}} \left(q_n \frac{\mathbf{p}_n}{m_n} \delta(\mathbf{r} - \mathbf{r}_n) - \frac{q_n^2}{m_n} \mathbf{A}(\mathbf{r}_n) \delta(\mathbf{r} - \mathbf{r}_n) \right). \tag{1.49}$$

The conjugate momenta of the fields $\tilde{A}_{\varepsilon_s}$ is given by (Goldstein, 1980; Cohen-Tannoudji, Dupont-Roc, and Grynberg, 1989)

$$\tilde{\Pi}_{\varepsilon_s}(\mathbf{k}) = \frac{\partial L}{\partial \left(\partial_t \tilde{A}^*_{\varepsilon_s}(\mathbf{k})\right)} = \varepsilon_0 \partial_t \tilde{A}_{\varepsilon_s}(\mathbf{k}). \tag{1.50}$$

In real space this becomes

$$\boldsymbol{\Pi}(\mathbf{r}) = \varepsilon_0 \partial_t \mathbf{A}(\mathbf{r}). \tag{1.51}$$

Now, we obtain the Hamiltonian by a Legendre transformation (Goldstein, 1980),

$$\begin{aligned} H = &\sum_{n=1}^{\mathcal{N}} \mathbf{p}_n \cdot \dot{\mathbf{r}}_n \\ &+ \int_{\mathbb{K}} \frac{d^3k}{(2\pi)^3} \sum_{s=1}^{2} \left[\tilde{\Pi}_{\varepsilon_s}(\mathbf{k}) \partial_t \tilde{A}^*_{\varepsilon_s}(\mathbf{k}) + \tilde{\Pi}^*_{\varepsilon_s}(\mathbf{k}) \partial_t \tilde{A}_{\varepsilon_s}(\mathbf{k}) \right] - L. \end{aligned} \tag{1.52}$$

If we substitute the *velocities* for the conjugate momenta,

$$H = \sum_{n=1}^{N} \left[\frac{\mathbf{p}_n^2}{m_n} - \frac{q_n}{m_n} \mathbf{p}_n \cdot \mathbf{A}(\mathbf{r}_n) - \frac{1}{2m_n} \Big(\mathbf{p}_n - q_n \mathbf{A}(\mathbf{r}_n) \Big)^2 \right] + V_C$$
$$+ \int_{\mathbb{K}} \frac{d^3k}{(2\pi)^3} \left[\frac{1}{\varepsilon_0} \sum_{s=1}^{2} \left(\tilde{\Pi}_{\varepsilon_s} \tilde{\Pi}^*_{\varepsilon_s} + \tilde{\Pi}^*_{\varepsilon_s} \tilde{\Pi}_{\varepsilon_s} - \tilde{\Pi}^*_{\varepsilon_s} \tilde{\Pi}_{\varepsilon_s} \right) + \varepsilon_0 c^2 k^2 \tilde{\mathbf{A}}^* \cdot \tilde{\mathbf{A}} \right]$$
$$- \sum_{n=1}^{N} \left(\frac{q_n}{m_n} \mathbf{p}_n \cdot \mathbf{A}(\mathbf{r}_n) - \frac{q_n^2}{m_n} \mathbf{A}^2(\mathbf{r}_n) \right) \tag{1.53}$$

$$H = \sum_{n=1}^{N} \left[\frac{1}{2} \frac{\mathbf{p}_n^2}{m_n} - 2q_n \frac{\mathbf{p}_n \cdot \mathbf{A}(\mathbf{r}_n)}{2m_n} + \frac{1}{2} \frac{q_n^2}{m_n} \mathbf{A}(\mathbf{r}_n)^2 + V_C \right.$$
$$\left. + \int_{\mathbb{K}} \frac{d^3k}{(2\pi)^3} \left[\frac{1}{\varepsilon_0} \sum_{s=1}^{2} \tilde{\Pi}^*_{\varepsilon_s}(\mathbf{k}) \tilde{\Pi}_{\varepsilon_s}(\mathbf{k}) + \varepsilon_0 c^2 k^2 \tilde{\mathbf{A}}^*(\mathbf{k}) \cdot \tilde{\mathbf{A}}(\mathbf{k}) \right] \right], \tag{1.54}$$

the Hamiltonian in the Coulomb gauge is given by

$$H = \sum_{n=1}^{N} \frac{1}{2m_n} \left[\mathbf{p}_n - q_n \mathbf{A}(\mathbf{r}_n) \right]^2 + V_C$$
$$+ \underbrace{\int_{\mathbb{K}} \frac{d^3k}{(2\pi)^3} \left[\frac{1}{\varepsilon_0} \tilde{\mathbf{\Pi}}^*(\mathbf{k}) \cdot \tilde{\mathbf{\Pi}}(\mathbf{k}) + \varepsilon_0 c^2 k^2 \tilde{\mathbf{A}}^*(\mathbf{k}) \cdot \tilde{\mathbf{A}}(\mathbf{k}) \right]}_{= H_f}. \tag{1.55}$$

The term on the second line is the Hamiltonian, H_f, of the free electromagnetic field, i.e. without any charges.

1.1.3 *Canonical Quantisation in the Coulomb Gauge*

Now we go from classical electrodynamics to quantum electrodynamics. The actual quantisation is done by promoting the coordinates and fields to operators (Dirac, 1958; von Neumann, 1932; Altland and Simons, 2010),

$$\mathbf{r}_n \longrightarrow \hat{\mathbf{r}}_n, \qquad \mathbf{p}_n \longrightarrow \hat{\mathbf{p}}_n, \text{ for the charges and} \tag{1.56}$$
$$\tilde{\mathbf{A}}(\mathbf{k}) \longrightarrow \hat{\mathbf{A}}(\mathbf{k}), \quad \tilde{\mathbf{\Pi}}(\mathbf{k}) \longrightarrow \hat{\mathbf{\Pi}}(\mathbf{k}), \text{ for the electromagnetic field.} \tag{1.57}$$

Here we have omitted the tilde (~) on the field operators $\hat{\mathbf{A}}$ and $\hat{\mathbf{\Pi}}$ to simplify the notation.

These operators are not commuting in general, but rather have to fulfil the canonical commutation relations,

$$\left[(\hat{\mathbf{r}}_n)_j, (\hat{\mathbf{p}}_m)_k \right] = i\hbar \, \delta_{n,m} \delta_{j,k} \tag{1.58}$$

for the charges [$(\hat{\mathbf{r}}_n)_j$ is the j^{th} component of the position operator of the n^{th} charge; $(\hat{\mathbf{p}}_m)_k$ is defined in a similar way] and

$$\left[\hat{A}_{\varepsilon_1}(\mathbf{k}), \hat{\Pi}_{\varepsilon_2}(\mathbf{k}')\right] = 0 \tag{1.59a}$$

$$\left[\hat{A}_{\varepsilon_1}(\mathbf{k}), \hat{\Pi}^\dagger_{\varepsilon_2}(\mathbf{k}')\right] = i\hbar\,\delta_{\varepsilon_1,\varepsilon_2}\delta(\mathbf{k}-\mathbf{k}') \tag{1.59b}$$

for the electromagnetic field (Cohen-Tannoudji, Dupont-Roc, and Grynberg, 1989). All other commutators give zero. We note that the vectors $\mathbf{k}$ and $\mathbf{k}'$ in Eqs. (1.59) are in the same half space $\mathbb{K}$. The operator $\hat{\Pi}^\dagger$ is the Hermitian adjoint operator of $\hat{\Pi}$.

One can formulate these commutation relations in real space as well. Since they contain the so-called transverse delta function [see e. g. (Cohen-Tannoudji, Dupont-Roc, and Grynberg, 1989)], the corresponding expressions are more complex, though.

So we have quantised the classical system by replacing the Poisson brackets of classical mechanics by the quantum mechanical commutator, $\{\cdot,\cdot\} \to \frac{1}{i\hbar}[\cdot,\cdot]$, (Dirac, 1958; von Neumann, 1932; Altland and Simons, 2010) both for the charges and the electromagnetic field.

CREATION AND ANNIHILATION OPERATORS This last paragraph completes the quantisation of the electromagnetic field. For this purpose, we define the two operators

$$\hat{a}_\varepsilon(\mathbf{k}) = \sqrt{\frac{\varepsilon_0}{2\hbar\omega_k}}\left[\omega_k \hat{A}_\varepsilon(\mathbf{k}) + i\frac{1}{\varepsilon_0}\hat{\Pi}_\varepsilon(\mathbf{k})\right], \tag{1.60}$$

$$\hat{a}^\dagger_\varepsilon(\mathbf{k}) = \sqrt{\frac{\varepsilon_0}{2\hbar\omega_k}}\left[\omega_k \hat{A}^\dagger_\varepsilon(\mathbf{k}) - i\frac{1}{\varepsilon_0}\hat{\Pi}^\dagger_\varepsilon(\mathbf{k})\right] \tag{1.61}$$

composed of operators of the electromagnetic field only. In addition, we have introduced the dispersion relation

$$\omega_k = ck. \tag{1.62}$$

We see, that the commutation relations of these two operators,

$$\begin{aligned}\left[\hat{a}_{\varepsilon_1}(\mathbf{k}), \hat{a}^\dagger_{\varepsilon_2}(\mathbf{k}')\right] = \\ \frac{\varepsilon_0}{2\hbar\omega_k}\Bigg(-i\frac{\omega_k}{\varepsilon_0}\underbrace{\left[\hat{A}_{\varepsilon_1}(\mathbf{k}), \hat{\Pi}^\dagger_{\varepsilon_2}(\mathbf{k}')\right]}_{=i\hbar\delta_{\varepsilon_1,\varepsilon_2}\delta(\mathbf{k}-\mathbf{k}')} + i\frac{\omega_{k'}}{\varepsilon_0}\overbrace{\left[\hat{\Pi}_{\varepsilon_1}(\mathbf{k}), \hat{A}^\dagger_{\varepsilon_2}(\mathbf{k}')\right]}^{=-i\hbar\delta_{\varepsilon_1,\varepsilon_2}\delta(\mathbf{k}-\mathbf{k}')}\Bigg) \\ = \delta_{\varepsilon_1,\varepsilon_2}\delta(\mathbf{k}-\mathbf{k}')\end{aligned} \tag{1.63}$$

are the commutation relations for the annihilation and creation operators (all other commutators are zero). Thus, the operators $\hat{a}_\varepsilon(\mathbf{k})$ and $\hat{a}^\dagger_\varepsilon(\mathbf{k})$ are interpreted as annihilation and creation operators, respectively. They annihilate and create a photon with momentum $\hbar\mathbf{k}$ and polarisation ε.

Besides, we note that the matrix elements of the creation and annihilation operators are not dimensionless, as can be seen from Eq. (1.63).

The inversion of Eq. (1.60) reads

$$\hat{A}_\varepsilon(\mathbf{k}) = \sqrt{\frac{\hbar}{2\varepsilon_0\omega_k}}\left(\hat{a}^\dagger_\varepsilon(\mathbf{k}) + \hat{a}_\varepsilon(\mathbf{k})\right), \tag{1.64}$$

$$\hat{\Pi}_\varepsilon(\mathbf{k}) = i\sqrt{\frac{\hbar\omega_k\varepsilon_0}{2}}\left(\hat{a}^\dagger_\varepsilon(\mathbf{k}) - \hat{a}_\varepsilon(\mathbf{k})\right). \tag{1.65}$$

So the product of the two $\hat{\Pi}$ operators gives

$$\hat{\Pi}^\dagger_\varepsilon(\mathbf{k})\hat{\Pi}_\varepsilon(\mathbf{k}) = \varepsilon_0\frac{\hbar\omega_k}{2}\left(\hat{a}_\varepsilon(\mathbf{k})\hat{a}^\dagger_\varepsilon(\mathbf{k}) - \hat{a}_\varepsilon(\mathbf{k})^2 - \hat{a}^\dagger_\varepsilon(\mathbf{k})^2 + \hat{a}^\dagger_\varepsilon(\mathbf{k})\hat{a}_\varepsilon(\mathbf{k})\right) \tag{1.66}$$

and the product of the two $\hat{A}$ operators is

$$\hat{A}^\dagger_\varepsilon(\mathbf{k})\hat{A}_\varepsilon(\mathbf{k}) = \frac{\hbar}{2\varepsilon_0\omega_k}\left(\hat{a}_\varepsilon(\mathbf{k})\hat{a}^\dagger_\varepsilon(\mathbf{k}) + \hat{a}_\varepsilon(\mathbf{k})^2 + \hat{a}^\dagger_\varepsilon(\mathbf{k})^2 + \hat{a}^\dagger_\varepsilon(\mathbf{k})\hat{a}_\varepsilon(\mathbf{k})\right), \tag{1.67}$$

so that the electromagnetic-only part of the Hamiltonian [see (1.55)] becomes

$$\hat{H}_f = \int_{\mathbb{K}}\frac{d^3k}{(2\pi)^3}\sum_{s=1}^{2}\hbar\omega_k\left[\hat{a}_{\varepsilon_s}(\mathbf{k})\hat{a}^\dagger_{\varepsilon_s}(\mathbf{k}) + \hat{a}^\dagger_{\varepsilon_s}(\mathbf{k})\hat{a}_{\varepsilon_s}(\mathbf{k})\right] \tag{1.68}$$

$$= \int_{\mathbb{R}^3}\frac{d^3k}{(2\pi)^3}\sum_{s=1}^{2}\hbar\omega_k\left[\hat{a}^\dagger_{\varepsilon_s}(\mathbf{k})\hat{a}_{\varepsilon_s}(\mathbf{k}) + 1/2\right], \tag{1.69}$$

i. e. a sum of non-interacting harmonic oscillators with frequencies ω_k. The full Hamiltonian, consisting of both charges and electromagnetic fields, reads

$$\hat{H} = \sum_{n=1}^{\mathcal{N}}\frac{1}{2m_n}\left[\hat{\mathbf{p}}_n - q_n\sum_{s=1}^{2}\varepsilon_s\hat{A}_{\varepsilon_s}(\hat{\mathbf{r}}_n)\right]^2 + V_C(\{\hat{\mathbf{r}}_n\}) + \hat{H}_f. \tag{1.70}$$

PERIODIC BOUNDARY CONDITIONS So far, there is no constraint on the movement of the charges. However, in most experiments the charges are restricted to a finite volume. This may be due to traps or interaction with other particles. In this situation, periodic or box boundary conditions are advantageous. We apply periodic boundary conditions. These imply

$$f(\mathbf{r}) \stackrel{!}{=} f(\mathbf{r} + \ell_j\mathbf{e}_j), \quad j \in \{1,2,3\} \tag{1.71}$$

for every field f. This may be artificial for small volumes, but becomes exact in the thermodynamic limit when the volume goes to infinity.

Periodic boundary conditions restrict the values of $\mathbf{k} = (k_1, k_2, k_3)$ to[3]

$$k_j = \frac{2\pi}{\ell_j}n_j, \quad n_j \in \mathbb{Z}. \tag{1.72}$$

3 With the definition of the Fourier transform, Eq. (1.7), we have: $f(\mathbf{r}) = \int_{\mathbb{R}^3}\frac{d^3k}{(2\pi)^3}\tilde{f}(\mathbf{k})e^{i\mathbf{k}\cdot\mathbf{r}} \stackrel{!}{=} \int_{\mathbb{R}^3}\frac{d^3k}{(2\pi)^3}\tilde{f}(\mathbf{k})e^{i\mathbf{k}\cdot\mathbf{r}+i\mathbf{k}\cdot\mathbf{e}_j\ell_j} = f(\mathbf{r}+\ell_j\mathbf{e}_j), \Rightarrow e^{i\mathbf{k}\cdot\mathbf{e}_j\ell_j} \stackrel{!}{=} 1$

Here, ℓ_j is the period of the periodic boundary condition in the j^{th} direction. Then, all Fourier integrals over $\mathbf{k}$ space reduce to sums,

$$\int_{\mathbb{R}^3} \frac{d^3k}{(2\pi)^3} f(\mathbf{k}) \longrightarrow \frac{1}{V} \sum_{\mathbf{k}} f(\mathbf{k}). \tag{1.73}$$

The sum on the right hand side is over the discrete values of $\mathbf{k}$ as in Eq. (1.72).

The Hamiltonian, Eq. (1.69), of the free electromagnetic field is then given by

$$\hat{H}_f = \sum_{\mathbf{k},s} \hbar\omega_k \hat{a}^\dagger_{\mathbf{k},s} \hat{a}_{\mathbf{k},s}, \tag{1.74}$$

with

$$\hat{a}_{\mathbf{k},s} = \sqrt{\frac{1}{V}}\, \hat{a}_{\varepsilon_s}(\mathbf{k}). \tag{1.75}$$

Now, the matrix elements of the annihilation and creation operators have no physical dimension and they fulfil the commutation relation

$$\left[\hat{a}_{\mathbf{k},s} \hat{a}^\dagger_{\mathbf{k}',s'}\right] = \delta_{\mathbf{k},\mathbf{k}'} \delta_{s,s'}. \tag{1.76}$$

Besides, we note that in Eq. (1.74), we have omitted the constant, infinite *vacuum energy*.

The Fourier transform of the transverse vector potential with periodic boundary conditions reads

$$\hat{A}_{\mathbf{k}} = \sum_{s=1}^{2} \sqrt{\frac{\hbar V}{2\varepsilon_0 \omega_k}} \varepsilon_s(\mathbf{k}) \left(\hat{a}^\dagger_{\mathbf{k},s} + \hat{a}_{\mathbf{k},s}\right) \tag{1.77}$$

Eventually, in real space the transverse vector potential is given by

$$\hat{A}(\mathbf{r}) = \sum_{\mathbf{k},s} \mathcal{A}_k \varepsilon_s(\mathbf{k}) \left(\hat{a}^\dagger_{\mathbf{k},s} + \hat{a}_{\mathbf{k},s}\right) e^{i\mathbf{k}\cdot\mathbf{r}}, \tag{1.78}$$

with

$$\mathcal{A}_k = \sqrt{\frac{\hbar}{2\varepsilon_0 V \omega_k}} \tag{1.79}$$

and $\mathbf{k}$ given by Eq. (1.72).

On the one hand, the Hamiltonian in Eqs. (1.70) and (1.74) mark the end of this section of the quantisation of the electromagnetic fields plus charges; on the other hand, this Hamiltonian is the starting point for the derivation of the Dicke model and generalisations thereof which is discussed in the next section.

1.2 DERIVATION OF (GENERALISED) DICKE MODELS

In the last section, the Hamiltonian of a collection of charges interacting with the electromagnetic field was derived. In general, these charges can be any particles with an electrical charge: elementary particles like leptons or quarks, or composite particles like protons or ions. We concentrate on atoms, or more precisely, on electrons bound to a nucleus; the charge of the nucleus is not considered. The position of the atoms is fixed inside a resonator, or cavity. For this quasi zero dimensional system, the exponential in the transverse vector potential of Eq. (1.78) is not significant and $\mathbf{A}$ reduces to

$$\hat{A}(\mathbf{r}) = \sum_{\mathbf{k},s} \mathcal{A}_k \boldsymbol{\varepsilon}_s(\mathbf{k}) \left(\hat{a}^\dagger_{\mathbf{k},s} + \hat{a}_{\mathbf{k},s}\right), \tag{1.80}$$

where $\mathcal{A}_k$ is still given by the expression of Eq. (1.79) and V is the volume of the resonator. The values of $\mathbf{k}$ are still discrete as in Eq. (1.72) and real polarisation vectors $\boldsymbol{\varepsilon}_s(\mathbf{k})$ are considered only.

Each of the $\mathcal{N}$ identical atoms has $\mathcal{N}_e$ electrons. Hence, the Hamiltonian of Eqs. (1.74) and (1.70) reads

$$\begin{aligned}\hat{H} = \sum_{i=1}^{\mathcal{N}} \Bigg(\frac{1}{2m} \sum_{j=1}^{\mathcal{N}_e} \left[\hat{\mathbf{p}}_{i,j} - q\,\hat{\mathbf{A}}(\hat{\mathbf{r}}_{i,j})\right]^2 \\ + \hat{V}_C\left(\{\hat{\mathbf{r}}_{i,1}, \ldots, \hat{\mathbf{r}}_{i,\mathcal{N}_e}\}\right)\Bigg) + \sum_{\mathbf{k},s} \hbar\omega_k\, \hat{a}^\dagger_{\mathbf{k},s}\, \hat{a}_{\mathbf{k},s}.\end{aligned} \tag{1.81}$$

Here, m, q, $\hat{\mathbf{p}}_{i,j}$ and $\hat{\mathbf{r}}_{i,j}$ are the mass, the charge, the kinetic momentum and the position of the j^{th} electron of i^{th} atom, respectively, and $\hat{V}_C$ is the Coulomb energy of all electrons with respect to their respective nuclei [see Eqs. (1.38), (1.44)].

The Hamiltonian, Eq. (1.81), can be written as

$$\hat{H} = \sum_{i=1}^{\mathcal{N}} \left(\hat{h}_i^{(0)} + \hat{h}_i^{(1)}\right) + \sum_{\mathbf{k},s} \hbar\omega_k\, \hat{a}^\dagger_{\mathbf{k},s}\, \hat{a}_{\mathbf{k},s}, \tag{1.82}$$

with

$$\hat{h}_i^{(0)} = \sum_{j=1}^{\mathcal{N}_e} \frac{\hat{\mathbf{p}}_{i,j}^2}{2m} + \hat{V}_C\left(\{\hat{\mathbf{r}}_{i,1}, \ldots, \hat{\mathbf{r}}_{i,\mathcal{N}_e}\}\right) = \sum_n E_n\, |n\rangle^i\langle n| \tag{1.83}$$

and

$$\hat{h}_i^{(1)} = -\frac{q}{m} \sum_{j=1}^{\mathcal{N}_e} \hat{\mathbf{p}}_{i,j} \cdot \sum_{\mathbf{k},s} \boldsymbol{\varepsilon}_s(\mathbf{k}) \mathcal{A}_k \left(\hat{a}^\dagger_{\mathbf{k},s} + \hat{a}_{\mathbf{k},s}\right) \tag{1.84}$$

$$+ \frac{q^2}{2m} \sum_{j=1}^{\mathcal{N}_e} \sum_{\substack{\mathbf{k},s \\ \mathbf{k}',s'}} \boldsymbol{\varepsilon}_s \cdot \boldsymbol{\varepsilon}_{s'} \mathcal{A}_k \mathcal{A}_{k'} \left(\hat{a}^\dagger_{\mathbf{k},s} + \hat{a}_{\mathbf{k},s}\right)\left(\hat{a}^\dagger_{\mathbf{k}',s'} + \hat{a}_{\mathbf{k}',s'}\right). \tag{1.85}$$

Here, the eigensystem $\{E_n, |n\rangle^i\}$ of the free system — that is the kinetic energy of the $\mathcal{N}_e$ electrons of the i^{th} atom, plus the Coulomb energy of the $\mathcal{N}_e$ electrons with its respective nuclei — has been introduced. The energies E_n are the same for every atom.

Next, we proceed by expressing the kinetic momentum operator $\hat{\mathbf{p}}_{i,j}$ in this energy basis. First, we note that the identity

$$\hat{\mathbf{p}}_{i,j} = i\frac{m}{\hbar}\left[\hat{h}_i^{(0)}, \hat{\mathbf{r}}_{i,j}\right] \tag{1.86}$$

holds. If we then insert on both sides of this commutator a complete set of eigenstates of $\hat{h}_i^{(0)}$, the kinetic momentum can be written in a rather complicated form as

$$\hat{\mathbf{p}}_{i,j} = i\frac{m}{\hbar}\sum_{n,l}\left(E_n - E_l\right)\langle n|\hat{\mathbf{r}}_{i,j}|l\rangle\,|n\rangle^i\langle l|\,. \tag{1.87}$$

In addition, we introduce the coupling constants, also called coupling strengths,

$$g_{nl,k,s} = -i\sqrt{\mathcal{N}}\left(E_n - E_l\right)\mathcal{A}_k\boldsymbol{\varepsilon}_s(\mathbf{k})\cdot\mathbf{d}_{nl}/\hbar, \tag{1.88}$$

with the matrix element

$$\mathbf{d}_{nl} = q\sum_{j=1}^{\mathcal{N}_e}\langle n|\hat{\mathbf{r}}_{ij}|l\rangle\,, \tag{1.89}$$

of the dipole operator $\hat{\mathbf{d}}$, cf. (A.3). The dipole matrix elements $\mathbf{d}_{nl}$ are identical for all atoms. The factor $\sqrt{\mathcal{N}}$ together with the factor $\sqrt{1/V}$ in the definition of $\mathcal{A}_k$, Eq. (1.79), results in coupling constants $g_{nl,k,s}$ which scale with the number density of the atoms. Hence in the thermodynamic limit[4], the coupling constants are fixed.

Generally, the coupling constants are complex numbers. The complex conjugates of the coupling constants are given by

$$g^*_{nl,k,s} = +i\sqrt{\mathcal{N}}\left(E_n - E_l\right)\mathcal{A}_k\boldsymbol{\varepsilon}_s(\mathbf{k})\cdot\mathbf{d}_{ln}/\hbar = g_{ln,k,s}. \tag{1.90}$$

Furthermore, we define the collective operators

$$\hat{A}_n^l = \sum_{i=1}^{\mathcal{N}}|n\rangle^i\langle l| \tag{1.91}$$

and the diamagnetic parameter

$$\kappa = \sqrt{\frac{q^2\mathcal{N}\mathcal{N}_e\hbar}{4m\varepsilon_0 V}}. \tag{1.92}$$

4 In the thermodynamic limit, the limits $\mathcal{N}\to\infty$, $V\to\infty$ with $\mathcal{N}/V = \text{const.}$ is considered, see 1.3.3

With these definitions, the Hamiltonian of Eq. (1.82) assumes the form

$$\begin{aligned}\hat{H} &= \sum_n E_n \hat{A}_n{}^n + \sum_{k,s} \hbar\omega_k \, \hat{a}^\dagger_{k,s} \, \hat{a}_{k,s} \\ &+ \sum_{k,s} \sum_{n>l} \left(\frac{g_{nl,k,s}}{\sqrt{\mathcal{N}}} \hat{A}_n{}^l + \frac{g^*_{nl,k,s}}{\sqrt{\mathcal{N}}} \hat{A}_l{}^n \right) \left(\hat{a}^\dagger_{k,s} + \hat{a}_{k,s} \right) \\ &+ \sum_{k,k'} \sum_{s,s'} \frac{\kappa^2}{\sqrt{\omega_k \omega_{k'}}} \, \varepsilon_s(k) \cdot \varepsilon_{s'}(k') \left(\hat{a}^\dagger_{k,s} + \hat{a}_{k,s} \right) \left(\hat{a}^\dagger_{k,s'} + \hat{a}^\dagger_{k,s'} \right).\end{aligned} \tag{1.93}$$

All four terms of this Hamiltonian have a physical interpretation: the first two terms give the energy of the uncoupled atoms and electromagnetic field, respectively. The third term is the so-called dipole interaction of the atoms with the electromagnetic field. It shuffles energy between these two degrees of freedom. At last, the fourth term is the so-called diamagnetic term. The name *diamagnetic* term is due to the fact that this term contains a term quadratic in the vector potential $\mathbf{A}$. This results in an increase of energy of the system when A increases. Thus a state with non-zero A is energetically unfavourable. In fact, in solid-state and molecular physics this term is responsible for the phenomenon of diamagnetism. The diamagnetic term is discarded in most applications of the Dicke model, since it is assumed negligible. However, we will see that this is not the case, if the strength of the dipole interaction is increased.

1.2.1 *Special Case I: The Dicke Model*

The Hamiltonian, Eq. (1.93), is the most general Dicke-like Hamiltonian. It describes the interaction of atoms with an arbitrary number of energy levels with the electromagnetic modes of a resonator. The most important specialisation of it is the original *Dicke Hamiltonian*. Here, two states of the atoms and one mode of the electromagnetic field are considered only. The quantum number n can take the values 1 and 2, and k and s are fixed and can be omitted for notational convenience. By an appropriate definition of the phase of the eigenstates $|n\rangle$ of the atomic Hamiltonian $\hat{h}_i^{(0)}$, the sole coupling constant g can be chosen real. Finally, the diamagnetic term is completely dropped. Then, the Hamiltonian (1.93) reads

$$\hat{H} = E_1 \hat{A}_1{}^1 + E_2 \hat{A}_2{}^2 + \hbar\omega \hat{a}^\dagger \hat{a} + \frac{g}{\sqrt{\mathcal{N}}} \left(\hat{a}^\dagger + \hat{a} \right) \left(\hat{A}_2{}^1 + \hat{A}_1{}^2 \right) \tag{1.94}$$

Usually, for this system consisting of two-level atoms, one introduces collective spin operators

$$\hat{J}_z = \frac{1}{2} \left(\hat{A}_2{}^2 - \hat{A}_1{}^1 \right), \quad \hat{J}_+ = \hat{A}_1{}^2, \quad \hat{J}_- = \hat{A}_2{}^1 \tag{1.95}$$

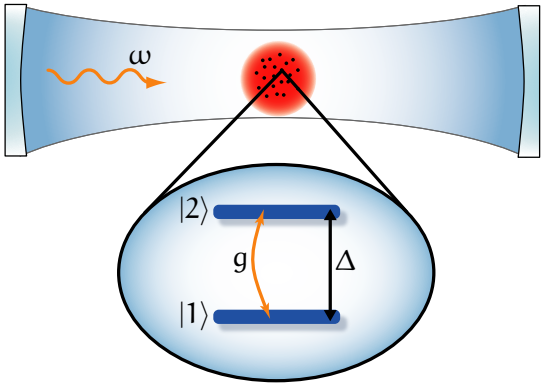

Figure 1.1: The Dicke model: A cloud of atoms interacts with one electromagnetic mode of a resonator. Both, atoms and resonator make up the whole (closed) system. No additional driving of the resonator or the atoms is present. The atoms are described by two-level systems, with energy separation Δ. The mode of the resonator with frequency ω induces transitions between these two states $|1\rangle$ and $|2\rangle$. The corresponding coupling strength is given by g.

obeying the commutation relations for angular momentum operators; except for a possible factor $\hbar$, depending on the definition of the commutation relations of the collective spin operators. For details about this, see Sec. A.2 in the Appendix. In terms of these collective spin operators, the representation

$$\hat{H} = \Delta \hat{J}_z + \hbar\omega\, \hat{a}^\dagger \hat{a} + \frac{g}{\sqrt{\mathcal{N}}}\left(\hat{a}^\dagger + \hat{a}\right)\left(\hat{J}_+ + \hat{J}_-\right) \tag{1.96}$$

of the well-known Dicke Hamiltonian is obtained (Dicke, 1954; Arimondo, 1996; Emary and Brandes, 2003a; Garraway, 2011). Note that a constant term proportional to the particle number operator $\hat{\mathcal{N}} = \hat{A}_1{}^1 + \hat{A}_2{}^2$ was dropped, to obtain the Dicke Hamiltonian, Eq. (1.96), from the Hamiltonian of Eq. (1.94). The parameter Δ is given by the difference of the two energy levels, $\Delta = E_2 - E_1$. The setup of the Dicke model is visualised in Fig. 1.1.

1.2.2 *Special Case II: The Lambda-Model*

We obtain a model with less stringent simplifications as in the Dicke model of the Hamiltonian of Eq. (1.93), if we include more energy levels or more modes of the resonator. We consider both, i. e. one extra energy level and one extra mode of the resonator.

We allow for transitions between the three energy levels in the so-called Lambda-configuration (Λ-configuration), where the two energetically lower lying single-particle eigenstates $|1\rangle$ and $|2\rangle$, the ground-state manifold, are coupled to the energetically highest single-particle eigenstate $|3\rangle$, the excited state, only. Thus, the coupling $g_{12,k,s}$ is zero. This can be achieved either by choosing both polarisations ε_s

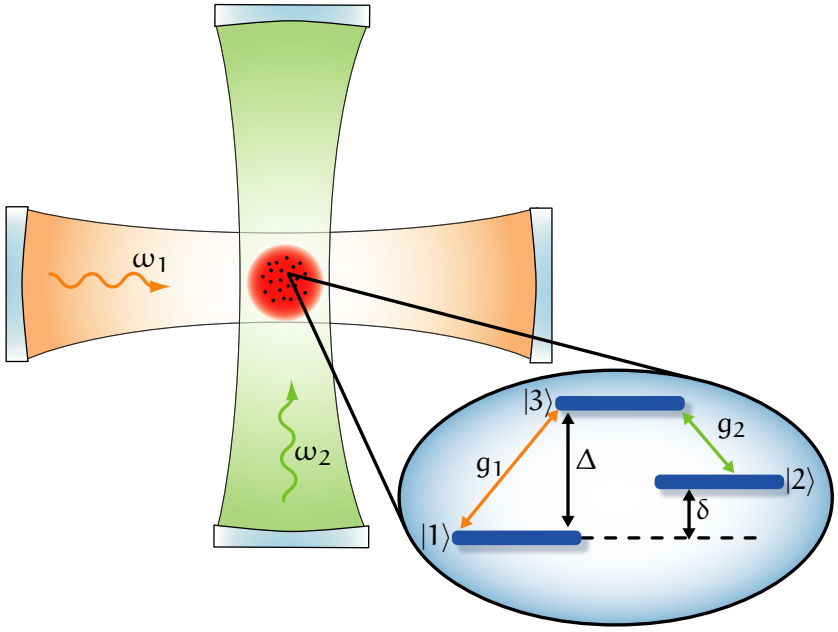

Figure 1.2: Lambda-model: A cloud of atoms interacts with two electromagnetic modes of a resonator. The atoms are described by three-level systems in Lambda-configuration, with energy separations Δ between the single-particle states $|1\rangle$ and $|3\rangle$, and δ between $|1\rangle$ and $|2\rangle$. The modes of the resonator with frequencies ω_1 and ω_2 induce transitions between the states $|1\rangle$ and $|3\rangle$, and $|2\rangle$ and $|3\rangle$, respectively. The corresponding coupling strengths are given by g_1 and g_2, respectively.

perpendicular to $\mathbf{d}_{12}$, or by even having $\mathbf{d}_{12} = 0$. This may be due to symmetry. The Lambda-model is illustrated in Fig. 1.2.

The two modes of the electromagnetic field with the quantum numbers $(\mathbf{k}, s)$ and $(\mathbf{k}', s')$ are abbreviated with 1 and 2, respectively. Both modes can induce both possible transitions $|1\rangle \longleftrightarrow |3\rangle$ and $|2\rangle \longleftrightarrow |3\rangle$. This results in four coupling constants. As in the Dicke model of the previous section, we can choose these four coupling constants real,

$$g_1 := g_{31,1} = c_{31}\sqrt{\frac{1}{\omega_1}}\,|\varepsilon_1 \cdot \mathbf{d}_{31}| \tag{1.97}$$

$$g_{31,2} = c_{31}\sqrt{\frac{1}{\omega_2}}\,|\varepsilon_2 \cdot \mathbf{d}_{31}|, \tag{1.98}$$

$$g_{32,1} = c_{32}\sqrt{\frac{1}{\omega_1}}\,|\varepsilon_1 \cdot \mathbf{d}_{32}| \tag{1.99}$$

$$g_2 := g_{32,2} = c_{32}\sqrt{\frac{1}{\omega_2}}\,|\varepsilon_2 \cdot \mathbf{d}_{32}|, \tag{1.100}$$

with $c_{3n} = (E_3 - E_n)\sqrt{\frac{\hbar\mathcal{N}}{2\varepsilon_0 V}}/\hbar$ [see the definition of the coupling constants in Eq. (1.88)]. With the definitions

$$\chi_1 = \sqrt{\frac{\omega_1}{\omega_2}}\frac{|\boldsymbol{\varepsilon}_2 \cdot \mathbf{d}_{31}|}{|\boldsymbol{\varepsilon}_1 \cdot \mathbf{d}_{31}|} \text{ and } \chi_2 = \sqrt{\frac{\omega_2}{\omega_1}}\frac{|\boldsymbol{\varepsilon}_1 \cdot \mathbf{d}_{32}|}{|\boldsymbol{\varepsilon}_2 \cdot \mathbf{d}_{32}|}, \tag{1.101}$$

the two coupling constants in Eqs. (1.98) and (1.99) can be written as

$$g_{31,2} = \chi_1 g_1 \text{ and } g_{32,1} = \chi_2 g_2. \tag{1.102}$$

Eventually, the Hamiltonian of the Lambda-model reads

$$\begin{aligned}\hat{H} = &\sum_{n=1}^{3} E_n \hat{A}_n^{\,n} + \sum_{n=1}^{2} \hbar\omega_n \hat{a}_n^\dagger \hat{a}_n \\ &+ \frac{g_1}{\sqrt{\mathcal{N}}}\left(\hat{A}_3^{\,1} + \hat{A}_1^{\,3}\right)\left[\hat{a}_1^\dagger + \hat{a}_1 + \chi_1\left(\hat{a}_2^\dagger + \hat{a}_2\right)\right] \\ &+ \frac{g_2}{\sqrt{\mathcal{N}}}\left(\hat{A}_3^{\,2} + \hat{A}_2^{\,3}\right)\left[\hat{a}_2^\dagger + \hat{a}_2 + \chi_2\left(\hat{a}_1^\dagger + \hat{a}_1\right)\right] \\ &+ \sum_{n=1}^{2} \frac{\kappa^2}{\omega_n}\left(\hat{a}_n^\dagger + \hat{a}_n\right)^2 + 2\frac{\boldsymbol{\varepsilon}_1 \cdot \boldsymbol{\varepsilon}_2 \kappa^2}{\sqrt{\omega_1\omega_2}}\left(\hat{a}_1^\dagger + \hat{a}_1\right)\left(\hat{a}_2^\dagger + \hat{a}_2\right).\end{aligned} \tag{1.103}$$

The properties of this Hamiltonian, including the diamagnetic term, are studied in Ch. 3.

For a simplified version of this Hamiltonian, we neglect the diamagnetic terms proportional to κ, and allow transitions in the two branches of the Lambda-configuration by one mode of the electromagnetic field, respectively, only. Then, the Hamiltonian simplifies to

$$\begin{aligned}\hat{H} = &\sum_{n=1}^{3} E_n \hat{A}_n^{\,n} + \sum_{n=1}^{2} \hbar\omega_n \hat{a}_n^\dagger \hat{a}_n \\ &+ \frac{g_1}{\sqrt{\mathcal{N}}}\left(\hat{A}_3^{\,1} + \hat{A}_1^{\,3}\right)\left(\hat{a}_1^\dagger + \hat{a}_1\right) + \frac{g_2}{\sqrt{\mathcal{N}}}\left(\hat{A}_3^{\,2} + \hat{A}_2^{\,3}\right)\left(\hat{a}_2^\dagger + \hat{a}_2\right).\end{aligned} \tag{1.104}$$

The properties of this Hamiltonian are studied in detail in Ch. 2.

In conclusion, in the previous two sections, we have derived the classical Langrangian and Hamiltonian in the Coulomb gauge. The latter was quantised in a canonical way, by introducing, eventually, creation and annihilation operators. To adapt the finite range of every experiment in the laboratory, we have applied periodic boundary conditions. However, these become exact in the thermodynamic limit. In order to derive the Hamiltonian of the generalised Dicke models, the dipole approximation was made, i. e. the transverse vector potential does not depend on the exact position of the atoms in the resonator. This is justified as long as the wavelength of the mode of the resonator is large compared to the extent of the atomic cloud. Finally, we have restricted the number of atomic single-particle energy levels to two

for the Dicke model, and to three for the generalised Dicke model in Lambda-configuration.

In the following section, we discuss the properties of the original Dicke model and give a review of Dicke superradiance and the superradiant phase transition.

1.3 THE DICKE MODEL & SUPERRADIANCE

1.3.1 *Properties of the Dicke Model*

The Dicke model of quantum optics and its collective properties were first studied by Robert Henry Dicke (DICKE, 1954). The Hamiltonian of this model is given by

$$\hat{H} = \Delta \sum_{n=1}^{\mathcal{N}} \hat{s}_z^{(n)} + \hbar\omega \hat{a}^\dagger \hat{a} + \frac{g}{\sqrt{\mathcal{N}}} \sum_{n=1}^{\mathcal{N}} \left(\hat{a}^\dagger + \hat{a}\right)\left(\hat{s}_+^{(n)} + \hat{s}_-^{(n)}\right). \quad (1.105)$$

It can be microscopically derived for atomic systems (cf. Sec. 1.2). Here, the bosonic operators $\hat{a}$ represent one mode of a resonator and the $\mathcal{N}$ atoms are represented by two-level systems which are described by the spin-1/2 operators $\hat{s}_j^{(n)}$, $j \in \{x, y, z, +, -\}$, $n \in \{1, \ldots, \mathcal{N}\}$, respectively, which fulfil the commutation relations for angular momentum operators,

$$\left[\hat{s}_j^{(n)}, \hat{s}_k^{(m)}\right] = \delta_{n,m} i\hbar \sum_{\ell=1}^{3} \varepsilon_{j,k,\ell}\, \hat{s}_\ell^{(n)}. \quad (1.106)$$

Here, $\varepsilon_{j,k,\ell}$ is the Levi-Civita symbol[5]. Since they act on different Hilbert spaces, operators of different atoms (n, m) always commute. Therefore, in the following, we will consider commutators with operators of the same atom only. If it is clear from the context, the label n for the atoms will be even omitted in the following.

Based on these commutation relation, the commutation relations for the so-called raising $(+)$ and lowering $(-)$ operators,

$$\hat{s}_\pm = \hat{s}_x \pm i\hat{s}_y \quad (1.107)$$

can be derived,

$$\left[\hat{s}_z, \hat{s}_\pm\right] = \pm\hbar\hat{s}_\pm, \quad \left[\hat{s}_+, \hat{s}_-\right] = 2\hbar\hat{s}_z. \quad (1.108)$$

On the one hand, the separation of the atoms is small compared to the wavelength of the mode of the resonator. On the other hand, the overlap of the wave functions of the single atoms has to be small such that the particle symmetry can be omitted. In addition, this means

5 With $\varepsilon_{1,2,3} = 1$ as well as for an even number of permutations of the indices, e. g. $\varepsilon_{2,3,1}$; for an odd number of permutations of the indices the symbol gives -1, e. g. $\varepsilon_{2,1,3} = -1$. If two indices are equal, the symbol gives 0.

that the actual position of the atoms is irrelevant and the coordinates of the atoms can be ignored.

We remark that there is no direct interaction between the atoms, i. e. there is no collision term present in the Hamiltonian. However, due to the coupling to the resonator field, the atoms interact indirectly with each other; in fact this is a long range interaction.

The Hamiltonian of the Dicke model is a many-body generalisation of the Rabi model (Rabi, 1937; Larson, 2007; Braak, 2011). And, as the Rabi model in the rotating-wave approximation has its counterpart in the Jaynes–Cummings model (Jaynes and Cummings, 1963; Meystre, 1992; Shore and Knight, 1993; Larson, 2007), the corresponding rotating-wave approximated Dicke model is given by the Tavis–Cummings model (Tavis and Cummings, 1968, 1969).

COLLECTIVE SPIN OPERATORS The form of the Dicke Hamiltonian suggests the introduction of so-called *collective* spin operators,

$$\hat{J}_j = \sum_{n=1}^{N} \hat{s}_j^{(n)}, \quad j \in \{x, y, z, +.-\}. \tag{1.109}$$

In terms of the collective spin operators, the Hamiltonian of Eq. (1.96) is obtained. These operators affect all atoms in the same manner, i. e. *collectively*.

In order to derive the commutation relations for the collective spin operators, we use the commutation relation of the spin-$1/2$ operators, Eq. (1.106). Then we obtain

$$\left[\hat{J}_j, \hat{J}_k\right] = \sum_{n,m=1}^{N} \left[\hat{s}_j^{(n)}, \hat{s}_k^{(m)}\right] = i\hbar \sum_{n=1}^{N} \sum_{\ell=1}^{3} \varepsilon_{j,k,\ell}\, \hat{s}_\ell^{(n)} = i\hbar \sum_{\ell=1}^{3} \varepsilon_{j,k,\ell}\, \hat{J}_\ell. \tag{1.110}$$

Hence, since the collective spin operators fulfil the commutation relations of angular momentum, they are, as the name suggests, angular momentum operators as well.

In conclusion, the Dicke model describes the interaction of collective (large) spins via a bosonic mode. As we pointed out earlier, this is a long range interaction, which gives a glimpse on the connexion of the Dicke model with the Lipkin–Meshkov–Glick model (Lipkin, Meshkov, and Glick, 1965; Meshkov, Glick, and Lipkin, 1965; Glick, Lipkin, and Meshkov, 1965) and its phase transition (Ribeiro, Vidal, and Mosseri, 2008).

STATES OF THE DICKE MODEL In general the states of the Hamiltonian of the Dicke model can be expanded by products of states of the individual atoms,

$$|m_1, m_2, \ldots, m_N\rangle, \tag{1.111}$$

where m_n gives the eigenvalues of the $\hat{s}_z$ operator of the n^{th} atom. To be specific, consider

$$|\uparrow\uparrow\downarrow\uparrow\downarrow\rangle\,, \tag{1.112}$$

a five-atom state with three atoms in the upper and two atoms in the lower energy level. These states are eigenstates of the collective $\hat{J}_z$ operator, which measures the difference of the number of atoms in the upper and the lower state. The corresponding eigenvalue of $\hat{J}_z$ is denoted by M. It is either integer (even number of atoms) or half-integer (odd number of atoms); however, in both cases the difference of two eigenvalues is always integer.

Now consider the Hamiltonian of the Dicke model in the limit of $g \to 0$. Then the Hamiltonian commutes both with $\hat{J}^2 = \sum_{k=1}^{3} \hat{J}_k^2$ and with $\hat{J}_z$. Neglecting the part of the resonator in the state vectors at the moment, we can thus construct simultaneous eigenstates $|r, M\rangle$ of $\hat{J}^2$, $\hat{J}_z$, and $\hat{H}$. These eigenstates fulfil

$$\hat{J}^2\,|r, M\rangle = r(r+1)\,|r, M\rangle \tag{1.113}$$

and

$$\hat{J}_z\,|r, M\rangle = M\,|r, M\rangle\,. \tag{1.114}$$

From Dicke (1954) stems the term *cooperation number* for the quantum number r. It follows from the commutation relations of the angular momentum operators, that the modulus of M is bounded by r (Sakurai, 1994). In addition, the maximal value of M is given by $N/2$, i. e. if all atoms occupy the upper energy level. This corresponds to the maximal possible value of the collective spin which we denote by J. In conclusion, the inequality

$$|M| \leqslant r \leqslant \frac{N}{2} =: J \tag{1.115}$$

holds. Hence, for a specific value of r, there are $2r+1$ states $|r, M\rangle$. The $N+1$ states with $r = \frac{N}{2}$ (maximal cooperativity) are called *Dicke states* (Emary and Brandes, 2003a). Among the Dicke states are the states where all N spins point in a single direction, e. g. the state $|r = \frac{N}{2}, M = -\frac{N}{2}\rangle = |\downarrow\downarrow \ldots \downarrow\rangle$.

Given a value for M, there are in general many distributions of atoms which result in the same value for M. To be specific, the states $|\uparrow\uparrow\downarrow\rangle$ and $|\downarrow\uparrow\uparrow\rangle$ give both the value $M = 1/2$. Hence, first of all, the states $|r, M\rangle$ are in general highly degenerate and the degeneracy is given by [permutations of multisets (Abramowitz and Stegun, 1972; Bronstein et al., 2001)]

$$d_M = \binom{N}{\frac{N}{2}+M, \frac{N}{2}-M} = \frac{N!}{(\frac{N}{2}+M)!(\frac{N}{2}-M)!}, \tag{1.116}$$

where $\binom{a}{b,c}$ is the multinomial coefficient. Secondly, to distinguish between states with same values of r and M, the permutation of atoms have to be specified. Alternatively, symmetry-adapted states can be used (Arecchi et al., 1972). The latter are conveniently characterised by means of Young tableaux (Scharf, 1970; Sakurai, 1994). This goes as follows. We denote the states of a single spin by a box, $\square$, and the states of N spins by N boxes, $\square \otimes \square \otimes \ldots \otimes \square$. As an example consider the simplest case, i. e. the case $N = 2$. Then the many-body states reduce to two sets of states,

$$\square \otimes \square = \begin{array}{|c|}\hline \\ \hline \\ \hline \end{array} \oplus \square\square . \tag{1.117}$$

Remember that each box corresponds to a single spin. The Young tableaux on the right-hand side of Eq. (1.117) are read as follows: *(i)* Vertically stacked boxes correspond to anti-symmetrised states, *(ii)* horizontally written boxes correspond to symmetrised states, *(iii)* horizontally and vertically placed boxes correspond to mixed symmetry (not present in the example). So in the above example, the Young tableau $\begin{array}{|c|}\hline \\ \hline \\ \hline \end{array}$ corresponds to the single anti-symmetric (singlet) state

$$|r = 0, M = 0\rangle = \frac{1}{\sqrt{2}}\big(|\uparrow\downarrow\rangle - |\downarrow\uparrow\rangle\big). \tag{1.118}$$

In addition, the second Young tableau $\square\square$ corresponds to the three symmetric (triplet) states

$$|r = 1, M = 1\rangle = |\uparrow\uparrow\rangle\,, \tag{1.119}$$

$$|r = 1, M = 0\rangle = \frac{1}{\sqrt{2}}\big(|\uparrow\downarrow\rangle + |\downarrow\uparrow\rangle\big), \tag{1.120}$$

$$|r = 1, M = -1\rangle = |\downarrow\downarrow\rangle\,. \tag{1.121}$$

The same construction can be done for arbitrary number N of spins. However, this becomes cumbersome for increasing N.

One last note concerning the Young tableaux: as was explicitly shown in the above example, the totally symmetric Young tableaux with horizontally placed boxes only, contain the states where all spins point in a single direction. For this reason, this Young tableau represents the Dicke states.

SELECTION RULES Up to now, we have considered the Hamiltonian of the Dicke model without the atom-light coupling, i. e. $g = 0$. For finite values of g, the coupling term $\frac{g}{\sqrt{N}}(\hat{a}^\dagger + \hat{a})(\hat{J}_+ + \hat{J}_-)$ induces transitions between the eigenstates $|r, M\rangle$ [see Eq. (A.42)],

$$\hat{J}_\pm |r, M\rangle \propto |r, M \pm 1\rangle\,. \tag{1.122}$$

These transitions are accompanied with either a creation or annihilation of one photon in the mode of the resonator.

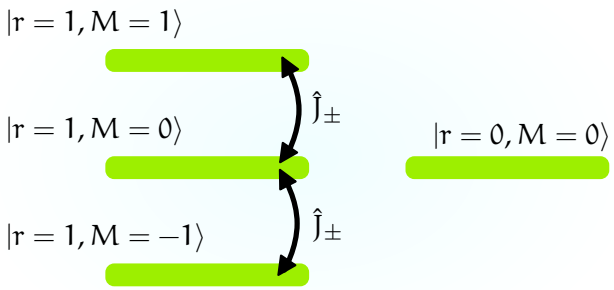

Figure 1.3: Transitions between states in the two-atom Dicke model. On the left are the triplet states; on the right is the single singlet state [see Eqs. (1.118) - (1.121)]. The Dicke Hamiltonian induces transitions (arrows) via the collective operators $\hat{J}_\pm$ among the states with equal quantum number r.

The collective operator $\hat{J}^2$ is still conserved and correspondingly r is still a *good* quantum number. Contrary, the operator $\hat{J}_z$ does not commute with the Hamiltonian. Consequently the selection rules

$$\Delta r = 0, \quad \Delta M = \pm 1 \tag{1.123}$$

hold. Thus, having a state vector with a certain eigenvalue of $\hat{J}^2$, the state vector will remain in the sector of the Hilbert space with this eigenvalue. This is depicted in Fig. 1.3 for the two-atom case from Eqs. (1.118)-(1.121).

One last remark: if the Hamiltonian contains terms with no collective spin operators, e. g. operators which act on a single spin only, then $\hat{J}^2$ as well does not commute with the Hamiltonian of the Dicke model anymore, r is no good quantum number, and transitions between states with different values of r and different Young tableaux i. e. different symmetries are possible. This would correspond to *non-vertical* transitions in Fig. 1.3.

Tied with the Dicke model is the phenomenon of superradiance. There are two instances of superradiance. One appears for systems with a finite number of atoms which are initially excited and are coupled to a resonator in a vacuum state. The other instance of superradiance appears as a thermodynamic or quantum phase for a infinite number of atoms in the regime of large atom-field coupling g. Whereas the second instance is of main interest in this thesis, we will briefly discuss the first instance for the sake of completeness in the next subsection.

1.3.2 *Dicke Superradiance*

Consider a system of $\mathcal{N}$ two-level atoms in a state with all atoms in their respective excited state (a Dicke state),

$$|r = J, M = J\rangle = |\uparrow\uparrow \ldots \uparrow\rangle\,. \tag{1.124}$$

Remember, we have set $J = \mathcal{N}/2$. Now, think of putting the atoms inside a resonator which is in a vacuum state, i. e. there are no photons present. Now let this state evolve in time under the dynamics of the Hamiltonian of the Dicke model, Eq. (1.96). Due to the coupling term $g\hat{a}^\dagger(\hat{J}_+ + \hat{J}_-)$ in the Hamiltonian, the atomic state will couple with the vacuum state of the resonator and eventually transfer excitations to the resonator. To be concrete, the rate $I_r(M)$ of spontaneous emission from the state $|r, M\rangle$ to the energetically lower lying state $|r, M-1\rangle$ is proportional to the matrix element (Sakurai, 1967) [see Eq. (A.42)]

$$|\langle r, M-1|\hat{J}_-|r, M\rangle|^2 = (r - M + 1)(r + M). \tag{1.125}$$

For a single atom ($r = M = 1/2$), this matrix element is one. Consequently, $I_r(M)$ is given by

$$I_r(M) = (r - M + 1)(r + M)I_0, \tag{1.126}$$

where I_0 is the spontaneous emission rate for a single atom in the resonator.

The state $|r = J, M = J\rangle$ will thus descend the *ladder* of Dicke states $|r = J, M = J\rangle \to |r = J, M = J-1\rangle \to \ldots \to |r = J, M = -J+1\rangle \to |r = J, M = -J\rangle$ and radiate with the rate $I_{\mathcal{N}/2}(M)$. This rate is largest for values of M around zero. If the number $\mathcal{N}$ of atoms is large, the rate of spontaneous emission is approximately given by

$$I_{\mathcal{N}/2}(M \ll \mathcal{N}) = \frac{\mathcal{N}^2}{4} I_0. \tag{1.127}$$

So in the course of time, the emitted radiation in the resonator is proportional to the squared of the number of radiators (atoms) in the volume. This is in stark contrast to the case if the $\mathcal{N}$ atoms would radiate independently with different phases, i. e. incoherently. Then the emitted radiation is given by $\mathcal{N}$ times the radiation of a single atom. Contrary to that, here, the emission rate is proportional to $\mathcal{N}^2$ which corresponds to the case that all atoms radiate in phase, i. e. coherently. This observation led Dicke (1954) to the term *superradiant*,

> "*For want of a better term, a gas which is radiating strongly because of coherence will be called super-radiant*".

In experiment, Dicke superradiance is observed as a flash with intensity $\mathcal{N}^2$ and width $1/\mathcal{N}$ (Gross and Haroche, 1982). Dicke superradiance has been observed in many different physical system, for

example in atomic gases (Skribanowitz et al., 1973; Gross, Fabre, et al., 1976; Gross, Raimond, and Haroche, 1978; Röhlsberger et al., 2010; Goban et al., 2015), quantum dots (Scheibner et al., 2007), circuit QED (Mlynek et al., 2014), or semiconductors (Laurent et al., 2015).

We note that there are also exist so-called subradiant states (Dicke, 1954; Scully, 2015; Guerin, Araújo, and Kaiser, 2016). These are highly correlated states as well, but are characterised by a low cooperation number and show suppressed radiation rates. The singlet state of the two-atom system above is an example of a subradiant state. The atoms still radiate coherently but with mutual opposite phases.

To conclude, Dicke superradiance is a collective quantum mechanical phenomenon, since in the beginning the photonic mode of the resonator can be in a vacuum state and quantum fluctuations trigger transitions from the state $|r = J, M = J\rangle$ down the ladder of Dicke states. This would be impossible without the quantum vacuum fluctuations. Hence, there is no Dicke superradiance for a classical system without an electromagnetic field. So, Dicke superradiance is the extension of spontaneous emission of a single atom to many atoms, like lasing is the generalisation of stimulated emission of one atom to many atoms. This statement makes clear that Dicke superradiance and lasing share the same background, but are based on two different physical mechanisms. In addition, the rates for stimulated emission of superradiant states are *normal* (Dicke, 1954).

1.3.3 *The Hepp–Lieb Superradiant Phase Transition*

The striking phenomenon of Dicke superradiance occurs for a large but finite number $\mathcal{N}$ of atoms. In a seminal paper, Hepp and Lieb (1973b) have studied the thermodynamic properties of the Hamiltonian of the Tavis–Cummings model, i. e. the Dicke model in a rotating-wave approximation. They have computed the free energy and thermodynamic expectation values of intensive observables in the thermodynamic limit, i. e. for $\mathcal{N} \to \infty$, $V \to \infty$, with $\rho = \mathcal{N}/V = \text{const.}$, and found a phase transition from a *normal* to a so-called *superradiant* phase. Here, the superradiant phase is characterised by a macroscopic excitation of both the atoms and the mode of the resonator, and a spontaneous polarisation of the atoms. Macroscopic means that the corresponding thermodynamic expectation value is extensive, i. e. it scales with the number of atoms in the system. On the other hand, in the normal phase, on average, all atoms are in the ground state and no photon is excited in the mode of the resonator.

The superradiant phase is realised for high coupling strengths and low temperatures. More precisely, the phase boundary between the two phases is given explicitly by the relation[6]

$$g(T) = \frac{\sqrt{\hbar\omega\,\Delta}}{2}\sqrt{\frac{1}{\tanh[\frac{1}{2}\Delta/(k_B T)]}}\,, \tag{1.128}$$

where g, ω, and Δ are defined as in Secs. 1.2.1, 1.3.1, k_B is Boltzmann's constant, and T is the temperature of the system.

Shortly after the paper of Hepp and Lieb (1973b), Wang and Hioe (1973) analysed the thermodynamics of the Dicke model in the rotating-wave approximation as well. They considered the canonical partition sum and used Glauber's coherent states to evaluate the resonator part of the partition sum. Due to the fact that only collective spin operators enter the Hamiltonian of the Dicke model, they obtained the remaining atomic part of the partition function by a simple diagonalisation of a two-by-two matrix. In the end, Wang and Hioe reproduced the findings of Hepp and Lieb for the superradiant phase transition.

Already a few years before the paper of Hepp and Lieb (1973b), Mallory (1969) observed that for high coupling strengths, states with a larger number of excitations in the mode of the resonator, are lower in energy. In addition, Scharf (1970) analysed the spectrum of the Hamiltonian of the Dicke model and computed asymptotic expressions for the eigenvalues for large atom number. In his paper Scharf shortly notes that for large couplings strengths, the ground-state energy can become negative and a phase transition can occur.

The superradiant phase appears for the Dicke model in the rotating-wave approximation for large values of the coupling strength. However, the rotating-wave approximation becomes worse for large values of the coupling strength (Agarwal, 1971; Walls, 1972; Knight and Allen, 1973), i. e. the Tavis–Cummings model should be a bad description for the system in the superradiant phase. Thus, Hepp and Lieb (1973a) on the one hand extended their previous paper, and Hioe (1973) and Carmichael, Gardiner, and Walls (1973) extended the calculation of Wang and Hioe (1973). They all considered the full Hamiltonian of the Dicke model without the rotating-wave approximation and obtained qualitatively the same results as before. The only difference lies in the fact that the phase boundary is shifted by a factor of 2.

The discovery of the superradiant phase transition in the Dicke model triggered a myriad of following publications ranging from dissipative pumped Dicke models (Hepp and Lieb, 1973c; Dembiński and Kossakowski, 1974) which combine lasing with superradiance, coupling to phonons (Thompson, 1975) leading to an enhancement

6 In fact, this is the result for the *Dicke model* and not for the Tavis–Cummings model. However, the result of Hepp and Lieb (1973b) is identical except for the factor $1/2$ outside the square root.

of the number of excitations in the mode of the resonator and a first-order superradiant phase transition, to studies of the original Dicke model by other methods like *gap equations* (Vertogen and De Vries, 1974) or the Holstein–Primakoff transformation to study the superradiant quantum phase transition (Emary and Brandes, 2003a).

Newer trends concern the Berry (Liberti, Plastina, and Piperno, 2006), or geometric phase (Chen, Li, and Liang, 2006) as an indicator for the superradiant quantum phase transition, or the extension of ground-state quantum phase transitions to phase transitions in the excited states (Brandes, 2013). Furthermore, there is also interest in dynamical properties of the phase transition (Bastidas et al., 2012), how the character of the phase and the point of the phase transition changes when dissipation for the atoms or the resonator mode is taken into account (Kopylov, Emary, and Brandes, 2013; Bhaseen et al., 2012; Keeling, Bhaseen, and Simons, 2010; Genway et al., 2014), or how the phase transition can be controlled by time-delayed feedback (Kopylov, Emary, Schöll, et al., 2015).

1.3.3.1 *Thermal Phase Transitions*

Thermodynamic phases of matter are characterised by certain properties like particle density, order, or elasticity. The solid phase of water for example has a high particle density, is highly ordered, and hardly elastic. Contrary, the gaseous phase of water is characterised by a low particle density, no order at all, and a high elasticity. Each phase retains these properties upon small changes of parameters like temperature or pressure, respectively. However, for large modifications of the parameters, eventually, one of the phases will become unstable whereas the other phase becomes stable. This is the point where the phase transition occurs. The stability of the phases is quantified by the thermodynamic potentials, like the internal energy, the free energy, or Gibbs free energy. Consider, for example, the free energy,

$$F(T, V, \mathcal{N}) = E(T, V, \mathcal{N}) - TS. \tag{1.129}$$

Here, E is the internal energy and S is the entropy of the system. The phase with the lowest free energy is stable, whereas the other phase is unstable. For parameter values at the phase transition, the thermodynamic potential is non-analytic. In general, this non-analyticity is in theory realised in systems in the thermodynamic limit only.

The Hepp–Lieb superradiant phase transition is a so-called second-order or continuous phase transition. The order of phase transitions is determined by the degree of the non-analyticity of the thermodynamic potential (Goldenfeld, 2010; Jaeger, 1998). For a n^{th}-order phase transition, the first $n-1$ partial derivatives of F are continuous, whereas the n^{th} derivative shows a discontinuity. In practice, only first and higher-order phase transitions are discriminated. Therefore, the latter are comprised as *continuous* phase transitions.

Examples for first-order phase transitions are the melting of ice to water or the formation of a Bose–Einstein condensate in an ideal Bose gas (GRIFFIN, SNOKE, and STRINGARI, 1995, Sec. 3); examples of second-order phase transition are the paramagnetic–ferromagnetic phase transition in the Ising model (HUANG, 1964, Sec. 17.3), the phase transition from the fluid to the gaseous phase at the critical point in the van der Waals model, and of course the superradiant phase transition in the Dicke model.

During first-order phase transition, energy, the so-called latent heat, is exchanged between the system and its environment but the temperature of the system remains the same. Considering the example of the ice-water phase transition, the latent heat is consumed to break up the inter-molecular binding forces.

On the other hand, second-order or continuous phase transitions are typically characterised by the breakdown of some symmetry in the systems during the process of the phase transition. Consider for example the Ising model. In the paramagnetic phase, the mean magnetisation is zero, i. e. no preferred direction for the Ising spins is present. In contrast, in the ferromagnetic phase, all spins point along the same direction although the Hamiltonian of the systems does not prefer this specific direction. This is also the essence of spontaneous symmetry breaking.

The simple expression of Eq. (1.129) for the free energy already gives an intuitive mathematical explanation why phase transitions occur. For a system to be in thermal equilibrium, the free energy needs to be minimal. In view of Eq. (1.129), this can be achieved either by minimising the internal energy E or by maximising the entropy S. Thus we have a competition between energy and entropy. For low temperatures, the entropy term can be neglected and the state of the system is characterised by a minimal E. In most physical systems this is realised by states with some kind of order. On the other hand, for high temperatures, the entropy term in Eq. (1.129) dominates and high-entropy states define the system. States of high entropy have a disordered character. Hence, the first observation is that for intermediate temperatures, there must be some kind of transition from the ordered to the disordered state of the system. This transition can become manifest in the thermodynamic limit via a phase transition. The second observation is that high-temperature phases have disordered character and low-temperature phases have ordered character. Consider for instance the paramagnetic-ferromagnetic phase transition in the Ising model. In the high-temperature paramagnetic phase, each spin points in an individual direction. Contrary, in the low-temperature ferromagnetic phase, all spins point along the same direction and are thus perfectly ordered.

1.3.3.2 *Quantum Phase Transitions*

In the limit $T \to 0$ the internal energy E and the free energy F are identical, cf. Eq. (1.129). Hence upon minimisation of the free energy, the free energy is given by the ground-state energy of the system and is thus solely determined by quantum properties. Different phases of matter can still exist at zero temperature and are realised by different parameters α of the underlying Hamiltonian $\hat{H}(\alpha)$.

Examples of Quantum phase transitions are the Mott insulator-superfluid phase transition in the Bose–Hubbard model (Fisher et al., 1989; Greiner et al., 2002), the quantum Ising model (Sachdev, 1999), or, as we will see shortly, the superradiant phase transition in the Dicke model (Emary and Brandes, 2003a).

Quantum phase transitions are an intense field of research. On the one hand, the ground state of certain quantum many-body system, i. e. the phase, can be either a tool or a resource for quantum computation (Nielsen and Chuang, 2002) and quantum simulation (Jaksch, Bruder, et al., 1998; Jaksch and Zoller, 2005; Lewenstein et al., 2007). In addition, quantum many-body physics and its dynamics can help to understand thermalisation (Altland and Haake, 2012).

1.3.3.3 *The Hepp–Lieb Quantum Phase Transition in the Dicke Model*

The zero-temperature quantum phase transition in the generalised Dicke model is of predominant importance for this thesis. For this reason, this section is devoted to give a review of the quantum phase transition in the original Dicke model.

First start with a short reprise of the Dicke model. The Hamiltonian written in terms of the collective spin is given by (cf. Sec. 1.3.1)

$$\hat{H} = \Delta \hat{J}_z + \hbar\omega \, \hat{a}^\dagger \hat{a} + \frac{g}{\sqrt{N}} (\hat{a}^\dagger + \hat{a})(\hat{J}_+ + \hat{J}_-). \tag{1.130}$$

Before we analyse the Hamiltonian in detail, we consider two limiting cases: namely the extreme cases of large, $g \gg \Delta, \hbar\omega$, and small, $g \ll \Delta, \hbar\omega$, coupling strengths g.

For small g, the two terms $\Delta \hat{J}_z$ and $\omega \, \hat{a}^\dagger \hat{a}$ dominate in the Hamiltonian (1.130). Thus the eigenstates of the system are product states of the eigenstates of both the operators $\hat{J}_z$ and $\hat{a}^\dagger \hat{a}$, i. e. a product of Dicke and Fock states. The state with lowest energy is then the product state where the mode of the resonator is in its vacuum state and the collective spin is in a Dicke state with $M = -J$. Hence for small coupling strength g, all atoms are in their respective ground state and no photon is excited in the resonator. This is visualised in the top panel of Fig. 1.4. In the following, this will be called the *normal phase*.

In the other limit, for large coupling strengths g, the coupling term $g(\hat{a}^\dagger + \hat{a})(\hat{J}_+ + \hat{J}_-)$ dominates. Using Eq. (A.32) for the collective spin operators and represent the $\hat{a}$ and $\hat{a}^\dagger$ operators in terms of the position operator $\hat{x}$ of the mode oscillator (Glauber, 1963), the coupling

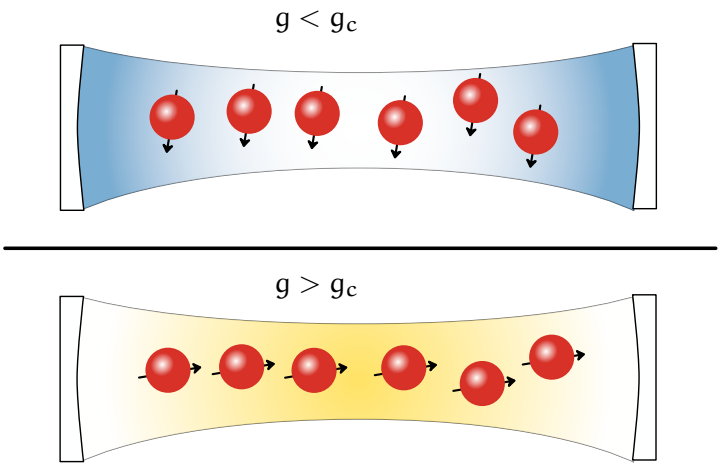

Figure 1.4: State of the Dicke model for $g < g_c$ (top panel) and for $g > g_c$ (bottom panel). For small couplings, all atoms occupy their respective ground state. The two-level atoms are represented by spin-1/2 systems. Thus all spins point downwards in the normal phase. In contrast for the superradiant phase where the coupling constant g is large, the atoms are spontaneously polarised, i. e. the spins point in x direction. In addition, the mode of the resonator is macroscopically excited, which is indicated by the yellow shading.

term can be written in the form $g\,\hat{x}\,\hat{J}_x$. Thus in this limit, the eigenstates of the Hamiltonian, Eq. (1.130), of the Dicke model are product states of eigenstates of the position operator for oscillator and Dicke states in the $\hat{J}_x$ basis, respectively. The product state with the lowest energy corresponds to a product state with a displaced oscillator and a state for the collective spin with $\langle \hat{J}_z \rangle = 0$ and $\langle \hat{J}_x \rangle = \pm J = \pm \mathcal{N}/2$. Thus for large couplings, the atoms are spontaneously and macroscopically polarised and the mode of the resonator is in a coherent state (Glauber, 1963; Sakurai, 1994). This is visualised in the bottom panel of Fig. 1.4. This phase is called the *superradiant phase*.

We see that the two limits of small and large coupling strengths support completely different ground states. On the one hand there is an excitation-less ground state; on the other hand, the ground state has macroscopic excitations both in the atomic and in the resonator degrees of freedom. In principle there could be a smooth crossover from the one to the other ground state upon changing the coupling strength g. However, we will see that this is not the case and at a certain value g_c, a phase transition sets in.

For arbitrary coupling strength and finite atom number, no exact analytical solution, i. e. determination of the eigensystem, has been found so far. Moreover the model is non-integrable (Emary and Brandes, 2003a). Since we are interested in the phase transition and its properties, we will consider the thermodynamic limit $\mathcal{N} \to \infty$ only. There are different methods to analyse the Hamiltonian of the Dicke

model in this limit, e. g. setting up semi-classical equations of motion (Bhaseen et al., 2012; Kopylov, Emary, Schöll, et al., 2015; Bakemeier, Alvermann, and Fehske, 2012, 2013), or study the semi-classical energy landscape (Engelhardt et al., 2015). In this thesis, we employ a method which is based upon the Holstein–Primakoff transformation (Emary and Brandes, 2003a,b),

$$\hat{J}_z = \hat{b}^\dagger \hat{b} - \frac{\mathcal{N}}{2}, \quad \hat{J}_+ = \hat{b}^\dagger \sqrt{\mathcal{N} - \hat{b}^\dagger \hat{b}}, \quad \hat{J}_- = \sqrt{\mathcal{N} - \hat{b}^\dagger \hat{b}}\, \hat{b}. \tag{1.131}$$

The operators $\hat{b}^\dagger$, $\hat{b}$ are bosonic creation and annihilation operators and fulfil the canonical commutation relation

$$[\hat{b}, \hat{b}^\dagger] = 1. \tag{1.132}$$

A review of the Holstein–Primakoff transformation and its generalisation is given in Appendix A.3. In the end, all approaches are equivalent and are essentially different sides of a coin of a mean-field theory.

Additionally, the bosonic operators both for the spin, $\hat{b}$, and for the mode of the resonator, $\hat{a}$, are displaced via a displacement operator (Glauber, 1963) by the, in general complex, displacements Ψ and φ, respectively,

$$\hat{b} = \hat{d} + \sqrt{\mathcal{N}}\Psi, \quad \hat{a} = \hat{c} + \sqrt{\mathcal{N}}\varphi. \tag{1.133}$$

The fluctuation operators $\hat{c}$ and $\hat{d}$ fulfil $\langle \hat{c} \rangle = \langle \hat{d} \rangle = 0$. For every state in the Hilbert space with at most $\mathcal{N}$ atoms, it holds that $\langle \hat{b} \rangle / \sqrt{\mathcal{N}} \leqslant 1$. Hence the above scaling with $\sqrt{\mathcal{N}}$ guarantees $|\Psi| \leqslant 1$. In addition, we define the real quantity

$$\psi = \sqrt{1 - \Psi^* \Psi}. \tag{1.134}$$

By expanding the square root in Eqs. (1.131) in powers of $\sqrt{\mathcal{N}}$, the Hamiltonian, Eq. (1.130), of the Dicke model can be written in the form

$$\hat{H} = \mathcal{N} \hat{h}^{(0)} + \mathcal{N}^{1/2} \hat{h}^{(1)} + \mathcal{N}^0 \hat{h}^{(2)} + \mathcal{N}^{-1/2} \hat{h}^{(3)} + \ldots, \tag{1.135}$$

where the terms in the Hamiltonian have been sorted in powers of $\mathcal{N}^{1/2}$. All terms proportional to $\mathcal{N}^{-1/2}$ and lower can be neglected in the thermodynamic limit. The individual Hamiltonians $\hat{h}^{(\ell)}$ are given by

$$\hat{h}^{(0)} = \Delta \Psi^* \Psi - \frac{\Delta}{2} + \hbar\omega \varphi^* \varphi + g(\varphi^* + \varphi)(\Psi^* + \Psi)\psi, \tag{1.136}$$

$$\begin{aligned} \hat{h}^{(1)} = {} & \Delta(\Psi \hat{d}^\dagger + \Psi^* \hat{d}) + \hbar\omega(\varphi \hat{c}^\dagger + \varphi^* \hat{c}) \\ & + g(\hat{c}^\dagger + \hat{c})(\Psi^* + \Psi)\psi + g(\varphi^* + \varphi)(\hat{d}^\dagger + \hat{d})\psi \\ & - \frac{g}{2}(\varphi^* + \varphi)(\Psi^* + \Psi)(\Psi \hat{d}^\dagger + \Psi^* \hat{d})/\psi, \end{aligned} \tag{1.137}$$

and

$$\begin{aligned}\hat{h}^{(2)} &= \Delta\hat{d}^\dagger\hat{d} + \hbar\omega\hat{c}^\dagger\hat{c} + g(\hat{c}^\dagger + \hat{c})(\hat{d}^\dagger + \hat{d})\psi \\ &- \frac{g}{2}(\hat{c}^\dagger + \hat{c})(\Psi^* + \Psi)(\Psi\hat{d}^\dagger + \Psi^*\hat{d})/\psi \\ &- \frac{g}{2}(\varphi^* + \varphi)(\hat{d}^\dagger + \hat{d})(\Psi\hat{d}^\dagger + \Psi^*\hat{d})/\psi \\ &- \frac{g}{2}(\varphi^* + \varphi)(\Psi^* + \Psi)\hat{d}^\dagger\hat{d}/\psi \\ &+ \frac{1}{8}g(\varphi^* + \varphi)(\Psi^* + \Psi)(\Psi\hat{d}^\dagger + \Psi^*\hat{d})^2/\psi^3.\end{aligned} \tag{1.138}$$

On closer inspection, we see that the prefactors of the operators $\hat{d}$, $\hat{d}^\dagger$, $\hat{c}$, and $\hat{c}^\dagger$ in $\hat{h}^{(1)}$ are obtained by differentiating $\hat{h}^{(0)}$ with respect to Ψ, Ψ^*, φ, and φ^*, respectively. The same observation can be made, when comparing the coefficients appearing in $\hat{h}^{(2)}$ and $\hat{h}^{(1)}$. This property is a consequence of the affine displacement of the creation and annihilation operators and the Taylor expansion of the square root originating from the Holstein–Primakoff transformation.

From Eq. (1.133) it is clear that a possible phase of the displacements Ψ and φ can be defined in the operators $\hat{b}$ and $\hat{a}$, respectively and, finally, get absorbed in the states. Consequently, the displacements Ψ and φ can be chosen real. Then the Hamiltonians from above are written as,

$$\hat{h}^{(0)} = \Delta\Psi^2 - \frac{\Delta}{2} + \hbar\omega\varphi^2 + 4g\varphi\Psi\psi, \tag{1.139}$$

$$\begin{aligned}\hat{h}^{(1)} &= \Delta\Psi(\hat{d}^\dagger + \hat{d}) + \hbar\omega\varphi(\hat{c}^\dagger + \hat{c}) + 2g\Psi\psi(\hat{c}^\dagger + \hat{c}) \\ &+ 2g\varphi\psi(\hat{d}^\dagger + \hat{d}) - 2g\varphi\Psi^2(\hat{d}^\dagger + \hat{d})/\psi,\end{aligned} \tag{1.140}$$

$$\begin{aligned}\hat{h}^{(2)} &= \Delta\hat{d}^\dagger\hat{d} + \hbar\omega\hat{c}^\dagger\hat{c} + g\psi(\hat{c}^\dagger + \hat{c})(\hat{d}^\dagger + \hat{d}) \\ &- g\Psi^2(\hat{c}^\dagger + \hat{c})(\hat{d}^\dagger + \hat{d})/\psi - g\varphi\Psi(\hat{d}^\dagger + \hat{d})^2/\psi \\ &- 2g\varphi\Psi\,\hat{d}^\dagger\hat{d}/\psi + \frac{1}{2}g\varphi\Psi^2(\hat{d}^\dagger + \hat{d})^2/\psi^3\end{aligned} \tag{1.141}$$

We see that the Hamiltonian of the Dicke model separates into an operator-free contribution, $\hat{h}^{(0)}$, a part $\hat{h}^{(1)}$ linear in the operators, and a part $\hat{h}^{(2)}$ bi-linear in the operators. The Hamiltonian $\hat{h}^{(0)}$ enters with a prefactor $\mathcal{N}$ in the Hamiltonian, Eq. (1.135). Hence, in the thermodynamic limit, it gives the main contribution to the energy of the system and represents the ground-state energy of the system. The term $\hat{h}^{(1)}$ will drop out, as we will see in the following. Finally, the term $\hat{h}^{(2)}$ represents low-energy excitations above the ground state.

In Sec. 1.3.3.1, we have seen that for zero temperature, the energy of the system is identical to the free energy. Furthermore, the free energy needs to be minimal in thermal equilibrium. Therefore, the displacements Ψ and φ have to be chosen such that the expectation value of the Hamiltonian becomes minimal. Since we consider the thermody-

namic limit only, this minimisation is equivalent to minimising the ground-state energy $\hat{h}^{(0)}$. In conclusion, the equations

$$\frac{\partial \hat{h}^{(0)}}{\partial \varphi} = 0 \tag{1.142}$$

and

$$\frac{\partial \hat{h}^{(0)}}{\partial \Psi} = 0 \tag{1.143}$$

have to be fulfilled. Inserting the expression of $\hat{h}^{(0)}$ from Eq. (1.139), results in the requirements,

$$\hbar\omega\varphi + 2g\Psi\psi = 0 \tag{1.144}$$

and

$$\Delta\Psi + 2g\varphi(\psi - \Psi^2/\psi) = 0, \tag{1.145}$$

or rather, when combining both equations,

$$\Psi\left[1 - \left(\frac{g}{g_c}\right)^2 (1 + 2\Psi^2)\right] = 0. \tag{1.146}$$

Here we have defined the critical coupling strength

$$g_c = \frac{\sqrt{\hbar\omega\Delta}}{2}, \tag{1.147}$$

whose meaning becomes clear shortly.

The Eq. (1.146) has two solutions:

(*i*) one trivial solution with

$$\Psi_n = 0 \quad \text{and} \quad \varphi_n = 0, \tag{1.148}$$

and

(*ii*) one non-trivial solution with

$$\Psi_s = \pm\sqrt{\frac{1}{2}\left[1 - \left(\frac{g_c}{g}\right)^2\right]} \quad \text{and} \quad \varphi_s = \mp\frac{g}{\hbar\omega}\sqrt{1 - \left(\frac{g_c}{g}\right)^4}. \tag{1.149}$$

Up to now we only know that these two solutions correspond to extrema of the ground-state energy. To test for minima, we analyse the Hessian matrix of $\hat{h}^{(0)}$,

$$\mathbf{H} = \begin{pmatrix} \frac{\partial^2 \hat{h}^{(0)}}{\partial \Psi^2} & \frac{\partial^2 \hat{h}^{(0)}}{\partial \Psi \partial \varphi} \\ \frac{\partial^2 \hat{h}^{(0)}}{\partial \varphi \partial \Psi} & \frac{\partial^2 \hat{h}^{(0)}}{\partial \varphi^2} \end{pmatrix} = \begin{pmatrix} 2\Delta + 4g\frac{\varphi\Psi(2\Psi^2-3)}{\psi^3} & 4g\frac{1-2\Psi^2}{\psi} \\ 4g\frac{1-2\Psi^2}{\psi} & 2\hbar\omega \end{pmatrix}, \tag{1.150}$$

from which one distinguishes minima from maxima by the sign of its determinant; a positive sign corresponds to a minimum and a

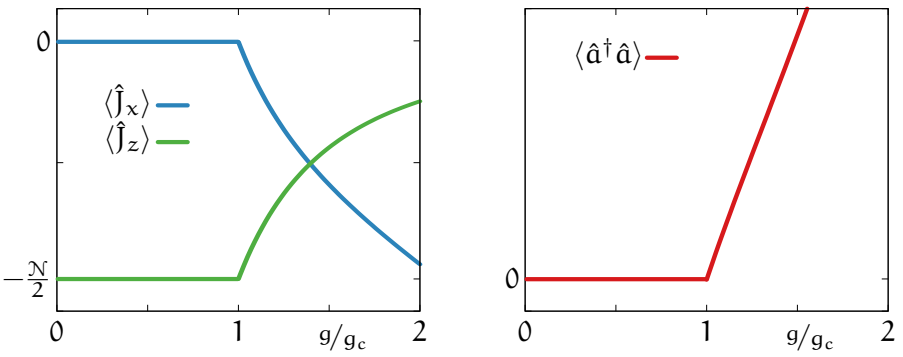

Figure 1.5: Ground-state expectation values of the collective spin operators $\hat{J}_x$ and $\hat{J}_z$, and the occupation $\hat{a}^\dagger \hat{a}$ of the resonator mode as functions of g/g_c. The units of $\langle \hat{a}^\dagger \hat{a} \rangle$ are arbitrary.

negative sign to a maximum. Inserting the above solutions, (1.148) and (1.149), yields

$$\mathrm{Det}\big[\mathbf{H}(\Psi_n, \varphi_n)\big] = -g^2 + g_c^2 \tag{1.151}$$

and

$$\mathrm{Det}\big[\mathbf{H}(\Psi_s, \varphi_s)\big] = 2(g^2 - g_c^2). \tag{1.152}$$

So we see that for $g < g_c$ solution *(i)* minimises the free energy, whereas for $g > g_c$ the second solution *(ii)* provides a minimal free energy. Hence, for $g < g_c$, solution (i) describes the physical state of the system and for $g > g_c$, solution *(ii)* does.

To see the physical meaning of both solutions, we look at ground-state expectation values of the observables $\hat{a}^\dagger \hat{a}$, $\hat{J}_z$, and $\hat{J}_x$. All three can be written in terms of the displacements φ and Ψ as follows,

$$\langle \hat{a}^\dagger \hat{a} \rangle = \mathcal{N}\varphi^2, \quad \langle \hat{J}_z \rangle = \mathcal{N}\big(\Psi^2 - 1/2\big), \quad \langle \hat{J}_x \rangle = \mathcal{N}\Psi\sqrt{1-\Psi^2}. \tag{1.153}$$

Inserting the two solutions, (1.148) and (1.149), we obtain

$$\langle \hat{a}^\dagger \hat{a} \rangle_n = 0, \quad \langle \hat{J}_z \rangle_n = -\frac{\mathcal{N}}{2}, \text{and } \langle \hat{J}_x \rangle_n = 0 \tag{1.154}$$

for the first solution, and

$$\langle \hat{a}^\dagger \hat{a} \rangle_s = \mathcal{N}\left(\frac{g}{\hbar\omega}\right)^2 \left[1 - \left(\frac{g_c}{g}\right)^4\right], \langle \hat{J}_z \rangle_s = -\frac{\mathcal{N}}{2}\left(\frac{g_c}{g}\right)^2, \tag{1.155}$$

$$\langle \hat{J}_x \rangle_s = \pm\frac{\mathcal{N}}{2}\sqrt{1 - \left(\frac{g_c}{g}\right)^4} \tag{1.156}$$

for the second solution.

The indices correspond to the ones of the solution of Eqs. (1.148), (1.149). The latter solution shows a macroscopic[7] occupation of the

7 Macroscopic, since the expectation values scale with the particle number $\mathcal{N}$

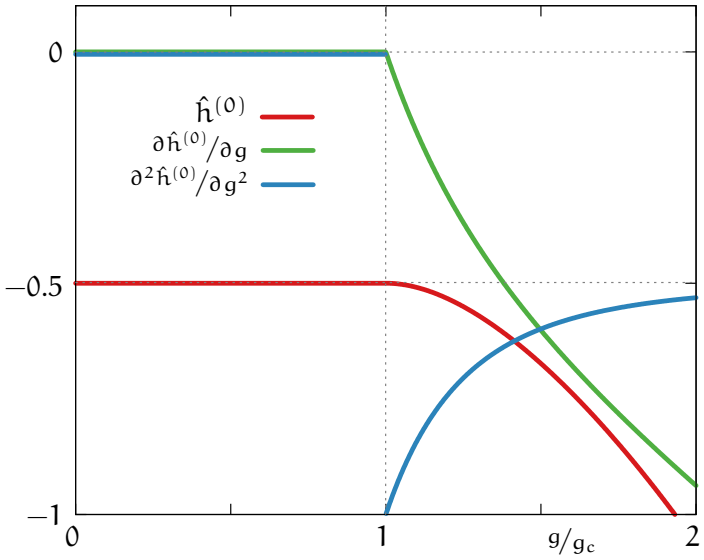

Figure 1.6: Ground-state energy $\hat{h}^{(0)}$ and its first, $\partial\hat{h}^{(0)}/\partial g$, and second, $\partial^2\hat{h}^{(0)}/\partial g^2$, derivative as functions of g/g_c in arbitrary units and with $\Delta = 1$. The ground-state energy itself and its first derivative are continuous, whereas its second derivative shows a discontinuity at $g = g_c$.

mode of the resonator, a macroscopic excitation of the atoms, and a spontaneous polarisation of the atoms in spin-x direction. Due to this spontaneous occupation of the resonator mode and spontaneous polarisation of the atoms, this solution, or phase, is called *superradiant* phase. On the other hand, the first solution with no excitations for both the resonator and the atoms and no polarisation of the atoms is called *normal* phase.

In Fig. 1.5, the ground-state expectation values for all three observables, $\hat{J}_x$, $\hat{J}_z$, and $\hat{a}^\dagger\hat{a}$ are shown. We clearly see a non-analyticity at $g = g_c$, i. e. a quantum phase transition. The order can be deduced from the free energy, i. e. the ground-state energy. The latter is given by inserting the displacements Ψ and φ into $\hat{h}^{(0)}$, which yields,

$$\hat{h}^{(0)} = \begin{cases} -\frac{\Delta}{2} & , \quad g < g_c \\ -\frac{\Delta}{4}\left[\left(g/g_c\right)^2 + \left(g_c/g\right)^2\right] & , \quad g > g_c. \end{cases} \tag{1.157}$$

First and second derivative with respect to g of $\hat{h}^{(0)}$ are given by

$$\frac{\partial\hat{h}^{(0)}}{\partial g} = \begin{cases} 0 & , \quad g < g_c \\ -\frac{\Delta}{2}\frac{1}{g_c}\left[g/g_c - \left(g_c/g\right)^3\right] & , \quad g > g_c \end{cases} \tag{1.158}$$

$$\frac{\partial^2\hat{h}^{(0)}}{\partial g^2} = \begin{cases} 0 & , \quad g < g_c \\ -\frac{\Delta}{2}\frac{1}{g_c^2}\left[1 + 3\left(g_c/g\right)^4\right] & , \quad g > g_c. \end{cases} \tag{1.159}$$

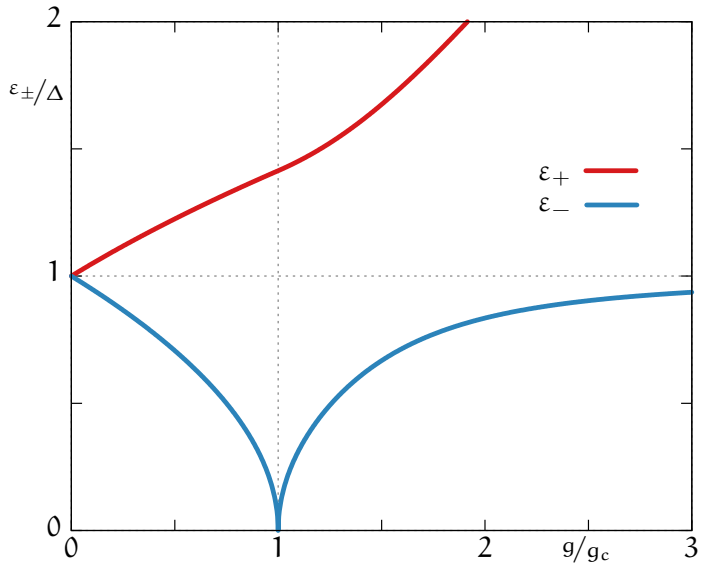

Figure 1.7: Low-energy excitation energies $\varepsilon_\pm$ as functions of g/g_c on resonance $\Delta = \hbar\omega$. Both dispersions are continuous and one dispersion vanishes at the point of the phase transition, $g = g_c$.

The ground-state energy and its first and second derivative are shown in Fig. 1.6. One sees that the ground-state energy itself and its first derivative are continuous for all coupling strengths g. However, the second derivative of $\hat{h}^{(0)}$ shows a discontinuity at the critical coupling strength g_c. Hence, at the critical coupling strength g_c the system undergoes a quantum phase transition of second order, i. e. a continuous quantum phase transition.

From the analysis of the ground-state energy $\hat{h}^{(0)}$, we have derived various properties of the superradiant phase transition. What additional information can be gained from the other terms, $\hat{h}^{(1)}$ and $\hat{h}^{(2)}$ of the Hamiltonian? First, $\hat{h}^{(1)}$ becomes identically zero, upon inserting the solutions for the displacements Ψ and φ. Second, $\hat{h}^{(2)}$ is bilinear in the creation and annihilation operators of the atoms and the mode of the resonator. Using a Bogoliubov and a canonical transformation (Emary and Brandes, 2003a), $\hat{h}^{(2)}$ can be cast in the form

$$\hat{h}^{(2)} = \varepsilon_+ \hat{e}_+^\dagger \hat{e}_+ + \varepsilon_- \hat{e}_-^\dagger \hat{e}_-, \tag{1.160}$$

where $\hat{e}_\pm^\dagger$ and $\hat{e}_\pm$ are creation and annihilation operators as well; see Sec. A.4.1 of the appendix for details. The bosonic operators are given by linear combinations of the operators $\hat{c}$ and $\hat{a}$ (Emary and Brandes, 2003a). They correspond to low-energy excitations above the ground state with energies $\varepsilon_\pm$. The energies $\varepsilon_\pm$ are shown in Fig. 1.7. Both excitation energies are continuous and the excitation energy ε_- vanishes on the phase transition at the critical coupling strength g_c. This is a general feature of continuous phase transitions, since in the

thermodynamic limit, the first excited state and the ground state approach arbitrarily close at the critical coupling strength g_c.

To conclude, we have analysed the superradiant quantum phase transition in the Dicke model with help of the Holstein–Primakoff transformation via a mean-field theory - the displacements Ψ and φ are mean-fields. All collective expectation values can be deduced from these mean-fields. In addition, the excitation energies of the bosonised system can be calculated as well. In Ch. 2, we will extend this procedure to analyse the generalised Dicke model with three-level systems interacting with two resonator modes. The calculation is in principle the same, but more involved.

1.3.4 *What is the Connection between Dicke Superradiance and the Hepp–Lieb Superradiant Phase Transition?*

We have two seemingly different phenomena, Dicke superradiance and the Hepp–Lieb superradiant phase transition. Now the question arises: why do they both share the name *superradiance*?

First, both phenomena originate from the same model - the Dicke model - and both superradiant effects are collective by nature. In addition, Dicke superradiance sets in for high densities of the atomic gas. In the Dicke model, the coupling strength g between atoms and the modes of the resonator is proportional to atomic density. Therefore, high values of g or high densities, respectively result in a superradiant phase transition as well.

Furthermore, for Dicke superradiance, the superradiant states are Dicke states with small values for the quantum number M and, in addition, are eigenstates of the collective $\hat{J}_z$ operator. However, the superradiant ground state in the superradiant phase for high coupling strengths g is no Dicke state, i. e. an eigenstate of the $\hat{J}_z$ operator[8]. Contrary, the superradiant ground state, for large g, is an eigenstate of the $\hat{J}_x$ operator. Identical is the expectation value for the $\hat{J}_z$ operator; it is zero in the superradiant phase for large g as well [cf. Eq. (1.155) and Fig. 1.5].

Another point is that in superradiant phase transitions, the mode of the resonator is a part of the system itself; thus it represents no external drive to the atoms, i. e. no energy is pumped into the system. As in Dicke superradiance, the field of the mode of the resonator facilitates spontaneous transitions between levels of the atoms. For this reason, we have the name superradiance. If we had a driven system, i. e. energy would be pumped into the atoms, then emission and absorption would be induced, and the dynamics would not solely be determined by spontaneous processes.

8 In fact, in the thermodynamic limit, this statement has to be relaxed, since then $\hat{J}_x$ and $\hat{J}_z$ commute.

1.4 THE SUPERRADIANT PHASE TRANSITION IN EXPERIMENT

As mentioned in Sec. 1.3.2, Dicke superradiance has been experimentally realised in various systems ranging from atomic to solid-state physics. Unfortunately, the same cannot been said for the Hepp–Lieb superradiant phase transition.

Soon after the discovery of the superradiant phase transition in the Dicke model, Rzażewski, Wódkiewicz, and Żakowicz (1975) showed that the phase transition is merely an artefact of the approximations done to the original light-matter Hamiltonian, Eq. (1.70). They argue that for real atoms, the coupling strength g, Eq. (1.88), and the diamagnetic parameter κ, Eq. (1.92), cannot be tuned independently. In particular, κ cannot be set to zero, i. e. the diamagnetic term proportional to $\boldsymbol{A}^2$ cannot be neglected. They considered the Hamiltonian of the Dicke model but with the diamagnetic term, $\kappa\big(\hat{a} + \hat{a}\big)^2$, included. Using the same techniques to calculate the partition sum of this extended Hamiltonian as Wang and Hioe (1973), they derived a new condition for the existence of a non-trivial, i. e. superradiant phase. However, by application of the exact Thomas–Reiche–Kuhn sum rule for atomic systems (see Sec. A.1), Rzażewski, Wódkiewicz, and Żakowicz (1975) showed that this condition is never satisfied and thus the normal phase is always stable and no superradiant phase is possible for real atomic systems. This fact is called no-go theorem.

Although there was some controversy (Gilmore, 1976; Orszag, 1977) whether or not the phase transition persists if the diamagnetic term is included, these objections were clarified by several publications (Rzażewski, Wódkiewicz, and Żakowicz, 1976; Rzażewski and Wódkiewicz, 1976; Knight, Aharonov, and Hsieh, 1978; Bialynicki-Birula and Rzążewski, 1979; Slyusarev and Yankelevich, 1979) and the no-go theorem for the Dicke model of atomic systems is undoubtedly valid.

With the advent of new quantum systems like superconducting electrical circuits (Blais et al., 2004), there was renewed interest in the study of superradiant quantum phase transitions (Chen, Chen, and Liang, 2007; Lambert et al., 2009; Nataf and Ciuti, 2010a,b). In fact, Nataf and Ciuti (2010a) considered a collection of artificial atoms, Cooper pair boxes, capacitively coupled to a transmission line resonator. They derived a Hamiltonian which has the same form as the Hamiltonian for real atoms, with a diamagnetic term included as well. However, in contrast to the $\boldsymbol{A}^2$ term of real atoms, here, the diamagnetic contribution can be made arbitrarily small and thus the no-go theorem is circumvented and the superradiant phase transition becomes possible for these artificial atomic systems. There was a controversy, though, if the effective model of Blais et al. (2004) and Nataf and Ciuti (2010a) correctly describes the underlying micro-

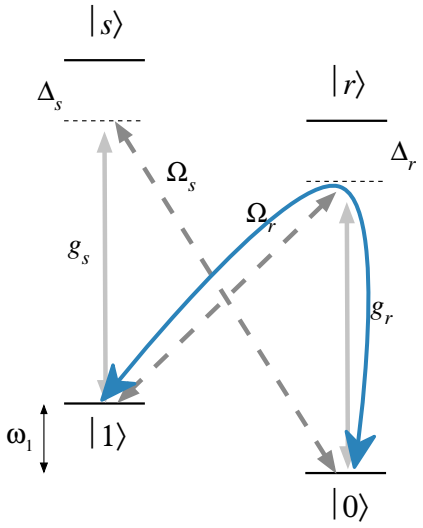

Figure 1.8: Proposed atomic level scheme of DIMER et al. (2007) to generate an effective Dicke Hamiltonian. The single-particle ground states $|0\rangle$ and $|1\rangle$ are coupled off-resonant to the excited states $|r\rangle$ and $|s\rangle$ via two lasers (with Rabi frequencies Ω_r and Ω_s, respectively) and a quantised mode of a resonator (with coupling strengths g_r and g_s). For instance, the blue, curved, double-headed arrow marks the transition which, after adiabatically eliminating the excited states, results in the term $(\hat{a}^\dagger \hat{J}_- + \hat{a}\hat{J}_+)$ of the effective Dicke Hamiltonian. Figure taken and adapted from DIMER et al. (2007).

scopic model correctly (VIEHMANN, DELFT, and MARQUARDT, 2011; CIUTI and NATAF, 2012; VIEHMANN, DELFT, and MARQUARDT, 2012).

Another route to realise the superradiant quantum phase transition is to create a physical system which is effectively described by a Dicke-type Hamiltonian. DIMER et al. (2007) proposed a theoretical scheme where four-level atoms interact simultaneously with one quantised light mode of a resonator and two classical electromagnetic fields of a pair of lasers, see Fig. 1.8. The two ground states are indirectly coupled via one of the lasers, one of the excited levels, and the mode of the resonator. On adiabatically eliminating both atomic excited states, the system is described by an effective Dicke Hamiltonian. The parameters entering this effective Hamiltonian are solely determined by the frequencies and intensities of the lasers and the resonator mode. The diamagnetic term seems to be irrelevant in this proposal.

Recently, BADEN et al. (2014) experimentally realised these cavity-assisted Raman transitions using two hyperfine ground states of ^{87}Rb atoms. They could easily tune the energies of the resonator mode and the spin, and observe the superradiant phase transition via the photon output of the resonator. Concerning the Lambda-model of this thesis, the outlook of BADEN et al. (2014) sounds very promising:

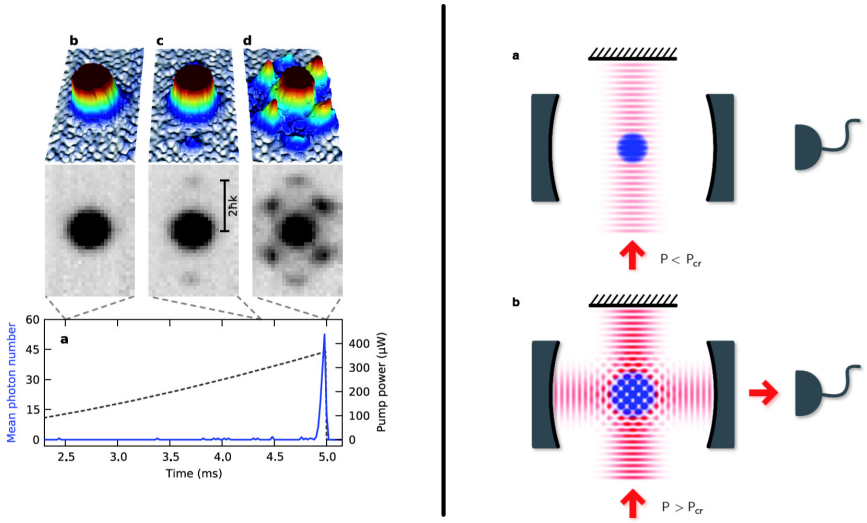

Figure 1.9: (*Left panel*): Experimental data from Baumann, Guerlin, et al. (2010), showing the formation of a self-organisation of a trapped Bose–Einstein condensate. The above two density plots give the momentum modes of the Bose–Einstein condensate in a time-of-flight image. The lower diagram shows the mean number of photons in the resonator on increasing the pump strength, i. e. increasing the coupling strength in the effective Dicke model. In the self-organising phase, i. e. the superradiant phase, higher momentum modes become macroscopically populated (upper two images) and the mean photon number shows a sharp peak (lower curve). (*Right panel*): Sketch of the spatial density distribution of the Bose–Einstein condensate, below (upper image) and above (lower image) the critical pump power P_{cr}. Above P_{cr} the atoms self-organise on a chequerboard pattern. Figures taken from Baumann, Guerlin, et al. (2010).

they note that their experimental setup could be easily extended to (effective) multi-level atoms and additional modes of the resonator.

In a similar scheme, the motional degrees of freedom of a Bose–Einstein condensate are coupled to a mode of a resonator and a pump laser (Nagy et al., 2010). In this proposal the effective two-level system is spanned by the ground state of the Bose–Einstein condensate and states with an additional photon momentum. The energy spacing of the two-level system is given by the detuning of pump laser and resonator mode frequency, whereas the coupling strength between the effective two-level systems and the resonator mode is proportional to the intensity of the pump laser. In a seminal work Baumann, Guerlin, et al. (2010) and Baumann, Mottl, et al. (2011) demonstrate for the first time the superradiant quantum phase transition of the Dicke model in experiment. They monitor the output of the resonator field and are thus able to see the phase transition in situ, see left panel of Fig. 1.9. The superradiant phase transition manifests itself in a chequerboard pattern of the Bose–Einstein condensate, see right

panel of Fig. 1.9. So, although the superradiant phase transition cannot be tested directly for atomic systems, the simulation or emulation of atomic systems allows for the experimental analysis of the Dicke model.

1.5 OUTLINE OF THIS THESIS

This introduction gave the basis for the rest of this thesis. The Dicke model in its original and its generalised form was derived microscopically. Of course, the Hamiltonian of the Dicke model can always be studied independently of any microscopic physical system like atoms interacting with light. But, for the existence of the superradiant phase in atomic systems and the validity of the no-go theorem in particular, the definition of the parameters in the Hamiltonian of the Dicke model in terms of the microscopic constants is crucial.

The rest of this thesis addresses the properties of a generalised Dicke model, the Lambda-model. In Ch. 2, we study the phases and phase transitions of the Lambda-model without the diamagnetic term. This chapter is not restricted to atomic system. Then, in Ch. 3, we will analyse how the phases and the phase transition of the Lambda-model is altered if the diamagnetic term is included. Intrinsically, this chapter directs its focus on atomic systems. Both chapters treat the quantum zero-temperature superradiant phase transition only. Contrary, in Ch. 4, we analyse how this quantum phase transition for the Lambda-model without diamagnetic term extends for finite temperatures. Ch. 5 summarises the results of this thesis and gives an outlook for following work.

2

PHASE TRANSITIONS AND DARK-STATE PHYSICS IN TWO-COLOUR SUPERRADIANCE

This Chapter is mostly based on the publication:

Hayn, Mathias, Clive Emary, and Tobias Brandes (2011): *Phase transitions and dark-state physics in two-color superradiance*, Phys. Rev. A **84**, p. 053856. doi: 10.1103/PhysRevA.84.053856.

2.1 INTRODUCTION

Superradiance is a collective phenomenon originating from atomic physics. There, it is regarded as a collective spontaneous emission process of a dense ensemble of radiating atoms (Gross and Haroche, 1982). The atoms interact indirectly via a light field. The first microscopic description of this phenomenon was given by Dicke (1954).

In the context of phase transitions, a collection of two-level systems coupled linearly to one bosonic mode undergoes a second-order phase transition from a normal to a superradiant phase at a certain critical coupling strength. This phase transition has been investigated theoretically a long time ago by Hepp and Lieb (1973b,a) and also by Wang and Hioe (1973). However, there is no experimental realisation in atomic systems to date. There were theoretical proposals to produce this phase transition in artificial quantum systems like *circuit* or *cavity quantum electrodynamic* (QED) systems (Chen, Chen, and Liang, 2007; Dimer et al., 2007; Lambert et al., 2009). Though, there exist no-go theorems for atomic, cavity, and circuit QED systems which theoretically preclude the normal–superradiant phase transition (Rzażewski, Wódkiewicz, and Żakowicz, 1975; Nataf and Ciuti, 2010a; Viehmann, Delft, and Marquardt, 2011).

Recently, experimental progress was achieved in this field by the group of Esslinger, who coupled a Bose–Einstein condensate to a single mode of an open optical cavity (Baumann, Guerlin, et al., 2010). The unitary dynamics of this system is described by an effective Dicke Hamiltonian (Baumann, Guerlin, et al., 2010; Nagy et al., 2010). Experimentally, the normal–superradiant phase transition is observed by measuring the mean intra-cavity photon number.

Inspired by this experimental realisation of an effective Hamiltonian of the Dicke model, we theoretically investigate an extension of the Dicke model; namely three-level systems in Lambda-configuration are considered. These are coupled to two independent bosonic modes. We are interested in how the phase transition is changed in this configuration. In addition, coherent population trapping (Arimondo, 1996),

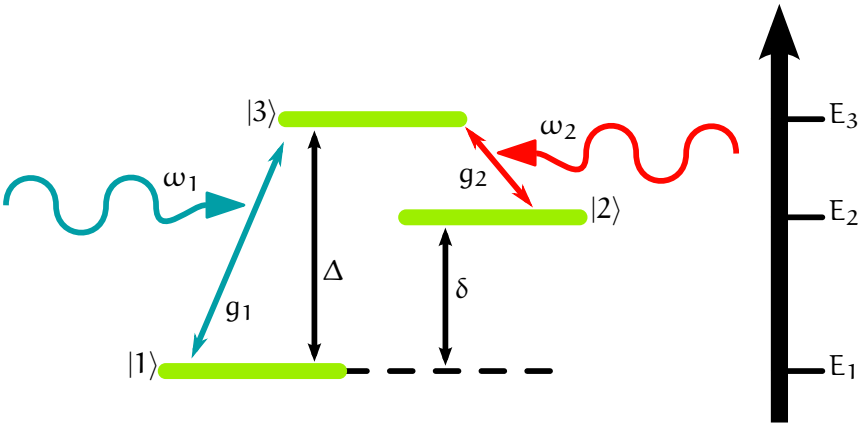

Figure 2.1: Level structure of the Lambda-configuration. One particle has two single-particle ground states $|1\rangle$, $|2\rangle$ and one excited state $|3\rangle$. The excited state is coupled to the two ground states via two independent bosonic modes with in general different frequencies ω_1, ω_2 and coupling strengths g_1, g_2.

dark states and the STIRAP scheme (Bergmann, Theuer, and Shore, 1998) are associated with this kind of system in the single-particle and semi-classical case. We therefore study to what extent dark-state physics plays a role in our quantum many-body setting.

This chapter is organised as follows: At the beginning, in Sec. 2.2, we introduce the model, give a detailed description of the Hamiltonian and discuss the symmetries of the model. Subsequently in Sec. 2.3, we describe the Holstein–Primakoff transformation for multi-level systems and derive an effective Hamiltonian in the thermodynamic limit. We diagonalise this effective Hamiltonian and give explicit expressions for the ground-state energy and the excitation energies. Section 2.4 addresses the phase transition: The zero-temperature phase diagram is mapped out and analysed. In Sec 2.4.2, we discuss properties of the appearing dark state. Finally, Sec. 2.5 closes with some conclusions.

2.2 THE MODEL

We consider a quantum mechanical system consisting of $\mathcal{N}$ distinguishable particles and two independent bosonic modes. Each particle i possess three energy levels $|1\rangle^{(i)}$, $|2\rangle^{(i)}$, and $|3\rangle^{(i)}$ with energies $E_1 \leqslant E_2 \leqslant E_3$, respectively. For later analysis we define, $\Delta = E_3 - E_1$, $\delta = E_2 - E_1$, with $\Delta \geqslant \delta \geqslant 0$. The level scheme is in so-called *Lambda*-configuration. Each of the two lowest energy levels couple to the

highest energy level via one of the bosonic modes, respectively (see Fig. 2.1). The Hamiltonian has the form (cf. Sec. 1.2.2)

$$\hat{H} = \sum_{n=1}^{3} E_n \hat{A}_n^{\,n} + \sum_{n=1}^{2} \Big[\hbar\omega_n \, \hat{a}_n^\dagger \, \hat{a}_n + \frac{g_n}{\sqrt{\mathcal{N}}} (\hat{a}_n^\dagger + \hat{a}_n) \left(\hat{A}_n^{\,3} + \hat{A}_3^{\,n} \right) \Big]. \quad (2.1)$$

Here, $\hat{A}_r^{\,s}$ are defined by

$$\hat{A}_r^{\,s} = \sum_{i=1}^{\mathcal{N}} |r\rangle^{(i)}\langle s|, \quad r, s = 1, 2, 3, \quad (2.2)$$

and represent collective particle operators. See Sec. A.2 of the appendix for details.

The diagonal operators $\hat{A}_n^{\,n}$ measure the occupation of the n^{th} energy level, i.e. how many of the $\mathcal{N}$ particles are in the single-particle energy state $|n\rangle$. This illustrates the first term in the Hamiltonian (2.1). The second term gives the energy of the two bosonic modes, each one having the frequency ω_1 and ω_2, respectively. The operators $\hat{a}_n^\dagger$ and $\hat{a}_n$ create and annihilate a boson in the n^{th} mode. They fulfil canonical commutator relations, $[\hat{a}_n, \hat{a}_m^\dagger] = \delta_{n,m}$ and $[\hat{a}_n, \hat{a}_m] = 0$. Lastly, the third term in the Hamiltonian, (2.1), represents the interaction of the particles with the two bosonic modes. Here, g_n are the corresponding coupling constants. This model was derived in Sec. 1.2.2.

We call the first ($|1\rangle$) and the third ($|3\rangle$) energy levels of the particle system together with the first bosonic mode *blue branch*, since $\Delta \geqslant \delta$ is assumed. Correspondingly, we call the second ($|2\rangle$) and the third ($|3\rangle$) energy level of the particle system together with the second bosonic mode *red branch* (see Fig. 2.1).

2.2.1 *Symmetries and Phase Transition*

Our model is a generalisation of the Dicke model (Dicke, 1954; Emary and Brandes, 2003a), where particles with only two energy levels are considered, and the two states are coupled via one bosonic mode. In the thermodynamic limit, the Dicke model exhibits a non-analytic behaviour in physical observables as a function of the coupling strength g. Thus, the Dicke model exhibits a quantum phase transition, which is continuous, i.e. of second order and separates two phases: a *normal phase* and a so-called *superradiant phase*. The superradiant phase has a ground state with spontaneously broken symmetry. A similar behaviour is anticipated in the extended model.

In analogy to the Dicke model, here exist two symmetry operators

$$\hat{\Pi}_n = \exp\Big\{ -i\pi \big(-\hat{A}_n^{\,n} + \hat{a}_n^\dagger \, \hat{a}_n \big) \Big\}, \qquad n = 1, 2, \quad (2.3)$$

which commute with the Hamiltonian, Eq. (2.1). These operators have the physical meaning of *parity operators* and have eigenvalues ± 1. The operator $\hat{\eta}_n = -\hat{A}_n^{\,n} + \hat{a}_n^\dagger \hat{a}_n$ in the exponent of the parity operator, Eq. (2.3), is related to the number of excitations in the blue ($n = 1$) or in the red ($n = 2$) branch of the Lambda-system and the number of excitations in the corresponding n^{th} bosonic mode, respectively. The operator $\hat{\eta}_n$ itself is not conserved, i.e. $[\hat{\eta}_n, \hat{H}] \neq 0$. This is consistent with the Dicke model (Emary and Brandes, 2003a).

In the rotating-wave approximation, the operators $\hat{\eta}_n$ become conserved quantities. Conservation of the two parities means that the Hilbert space decomposes into four irreducible subspaces. It is the parity which is spontaneously broken in the superradiant phase of the Dicke model. Thus, we expect that at least *one* of the parities is also spontaneously broken in our model.

2.2.2 *Collective Operators*

Using the definition (2.2) of the operators $\hat{A}_r^{\,s}$, one can show that the two sets of traceless operators $\{\frac{1}{2}(\hat{A}_3^{\,3} - \hat{A}_n^{\,n}), \hat{A}_n^{\,3}, \hat{A}_3^{\,n}\}$, $n = 1, 2$ fulfil the angular momentum algebra, respectively, i.e. they are generators of the special unitary group SU(2) and can be understood as angular momentum operators. See Sec. A.2 of the appendix for details. In addition, the operators $\hat{A}_r^{\,s}$ fulfil the algebra of generators of the unitary group U(3) (Okubo, 1975; Klein and Marshalek, 1991)

$$\left[\hat{A}_r^{\,s}, \hat{A}_n^{\,m}\right] = \delta_{s,n}\, \hat{A}_r^{\,m} - \delta_{r,m}\, \hat{A}_n^{\,s} \tag{2.4}$$

and are, according to that, generators of the group U(3). It is known, that the generators of the group U(N) can be represented by either N or by $N - 1$ independent bosons (Okubo, 1975; Klein and Marshalek, 1991). The first choice corresponds to the *Schwinger boson* representation (Schwinger, 1952; Okubo, 1975; Sakurai, 1994), the latter choice to the *Holstein–Primakoff* transformation of the generators (Okubo, 1975; Holstein and Primakoff, 1940; Klein and Marshalek, 1991).

2.3 METHODS

The Dicke model was introduced in 1954 (Dicke, 1954). To date there exists no exact analytical solution to this model for a finite number $\mathcal{N}$ of particles. However, the Dicke Hamiltonian can be exactly diagonalised in the thermodynamic limit (Emary and Brandes, 2003a), i.e. $\mathcal{N} \to \infty$. This can be achieved by using the already mentioned Holstein–Primakoff transformation. We apply a generalised version of the Holstein–Primakoff transformation to diagonalise the Hamiltonian (2.1) of the Lambda-system. The following calculation is a gener-

alisation of the computations done in Sec. 1.3.3.3 and in (EMARY and BRANDES, 2003a).

2.3.1 *The Generalised Holstein–Primakoff Transformation*

In this thesis we discuss in particular the Lambda-system which has $N = 3$ single-particle states. Though, we will formulate the following argument for a general number N of single-particle states. The number of particles is denoted by $\mathcal{N}$, whereas the number of single-particle states is denoted by N.

The generalised Holstein–Primakoff transformation maps the generators $\hat{A}_r{}^s$ of the group U(N) onto a combination of creation and annihilation operators $\hat{b}_r^\dagger, \hat{b}_r$ of $N-1$ independent bosons. Hence, the operators $\hat{b}_r^\dagger$ and $\hat{b}_r$ fulfil canonical commutator relations, $[\hat{b}_r, \hat{b}_s^\dagger] = \delta_{r,s}$, $[\hat{b}_r, \hat{b}_s] = 0$. These bosons we will refer to as Holstein–Primakoff bosons (HP bosons for brevity). One of the N states of the single-particle system is called the *reference state*, which we denote with $|m\rangle$. The meaning of the state $|m\rangle$ and which of the N states can be used as a reference state will be elucidated later. Then, the generalised Holstein–Primakoff transformation is given by (KLEIN and MARSHALEK, 1991)

$$\left.\begin{aligned} \hat{A}_r{}^s &= \hat{b}_r^\dagger\, \hat{b}_s, \\ \hat{A}_r{}^m &= \hat{b}_r^\dagger\, \hat{\Theta}_m(\mathcal{N}), \\ \hat{A}_m{}^s &= \hat{\Theta}_m(\mathcal{N})\, \hat{b}_s, \\ \hat{A}_m{}^m &= \hat{\Theta}_m(\mathcal{N})^2, \end{aligned}\right\} \; r, s \neq m \tag{2.5}$$

with

$$\hat{\Theta}_m(\mathcal{N}) = \sqrt{\mathcal{N} - \sum_{r\neq m} \hat{b}_r^\dagger\, \hat{b}_r}\ . \tag{2.6}$$

There are at most $\mathcal{N}$ HP bosons per mode, i.e. the expectation value satisfies $\langle \hat{b}_r^\dagger\, \hat{b}_r \rangle \leqslant \mathcal{N}$, $r \neq m$, due to the operator $\hat{\Theta}_m(\mathcal{N})$ and the fact that $\hat{b}_r$ acting on a state with zero HP bosons in the r^{th} mode equals to zero. In addition, the number of HP bosons in all $N-1$ modes does not exceed $\mathcal{N}$, i.e. $\sum_{r\neq m} \langle \hat{b}_r^\dagger\, \hat{b}_r \rangle \leqslant \mathcal{N}$.

We now apply the generalised Holstein–Primakoff transformation, Eq. (2.5), to the Hamiltonian (2.1) with e.g. $|1\rangle$ as the reference state ($m = 1$) and obtain

$$\begin{aligned} \hat{H}_{m=1} = E_1\, \mathcal{N} + \delta\, \hat{b}_2^\dagger\, \hat{b}_2 + \Delta\, \hat{b}_3^\dagger\, \hat{b}_3 + \sum_{n=1}^{2} \hbar\omega_n\, \hat{a}_n^\dagger\, \hat{a}_n \\ + \frac{g_1}{\sqrt{\mathcal{N}}}(\hat{a}_1^\dagger + \hat{a}_1)\, \left(\hat{b}_3^\dagger\, \hat{\Theta}_1(\mathcal{N}) + \hat{\Theta}_1(\mathcal{N})\, \hat{b}_3\right) \\ + \frac{g_2}{\sqrt{\mathcal{N}}}(\hat{a}_2^\dagger + \hat{a}_2)\, (\hat{b}_3^\dagger\, \hat{b}_2 + \hat{b}_2^\dagger\, \hat{b}_3). \end{aligned} \tag{2.7}$$

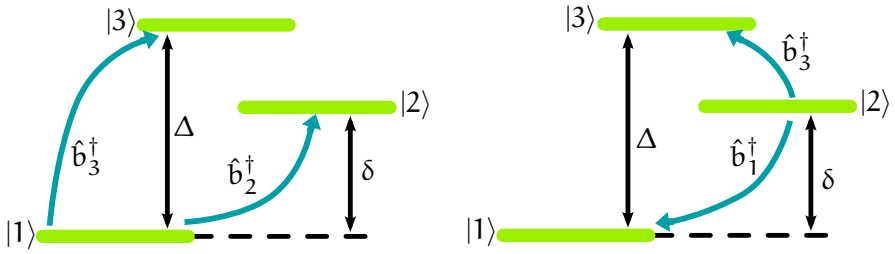

Figure 2.2: Physical interpretation of the bosons introduced via the generalised Holstein–Primakoff transformation (2.5): the two bosonic operators $\hat{b}_r^\dagger$, with $r \neq m$, can be understood as collectively exciting the particles from the reference state $|m\rangle$ (*left*: $m = 1$, *right*: $m = 2$) to the state $|r\rangle$. The analogue holds for the annihilation operators $\hat{b}_r$.

The first line is the free part of the Hamiltonian, from which one can infer the meaning of the HP bosons: The number of HP bosons in the mode with frequency δ is given by the operator $\hat{b}_2^\dagger \hat{b}_2$. This means that $\hat{b}_2^\dagger$ is related to the creation of excitations with energy δ, which is the energy separation of the single-particle energy levels $|1\rangle$ and $|2\rangle$. Thus, the operator $\hat{b}_2^\dagger$ can be understood as collectively exciting the particles from the first energy level to the second one. This is visualised in Fig. 2.2. An analogous reasoning can be given for the other HP boson corresponding to the operator $\hat{b}_3$.

2.3.2 *The Thermodynamic Limit*

The expectation value of the HP boson operators $\hat{b}_r$ is zero for a finite number $\mathcal{N}$ of particles. In contrast, in the thermodynamic limit, the expectation value of this operator can be finite, and is then macroscopic. Given that the occupations $\langle \hat{A}_n^n \rangle$ and $\langle \hat{a}_n^\dagger \hat{a}_n \rangle$ should scale with the particle number $\mathcal{N}$, we make the ansatz

$$\hat{b}_r = \sqrt{\mathcal{N}}\, \Psi_r + \hat{d}_r, \quad r \neq m, \tag{2.8a}$$

$$\hat{a}_n = \sqrt{\mathcal{N}}\, \varphi_n + \hat{c}_n, \quad n = 1, 2, \tag{2.8b}$$

in the thermodynamic limit. Here $\sqrt{\mathcal{N}}\, \Psi_r$ and $\sqrt{\mathcal{N}}\, \varphi_n$ are the ground-state expectation values of $\hat{b}_r$ and $\hat{a}_n$, respectively. This means that the ground-state expectation value of the bosonic operators $\hat{d}_r$ and $\hat{c}_n$ is zero and, consequently, these operators can be interpreted as quantum fluctuations. Furthermore, they fulfil canonical commutator relations and their matrix elements are of the order of $\mathcal{N}^0$. The parameters Ψ_r and φ_n can be chosen real and range from zero to one, which ensures $\langle \hat{b}_r^\dagger \hat{b}_r \rangle \leqslant \mathcal{N}$. Another viewpoint is that the operators $\hat{d}_r$ and $\hat{c}_n$ can be generated from $\hat{b}_r$ and $\hat{a}_n$, respectively, by a canonical transformation and can be considered as displaced bosonic modes (Emary and Brandes, 2003a).

Using the ansatz (2.8), we find that the ground-state occupations of the particles and of the bosonic modes are given by

$$\langle \hat{A}_r{}^r \rangle = \mathcal{N}\Psi_r^2 + \langle \hat{d}_r^\dagger \hat{d}_r \rangle, \qquad r \neq m, \tag{2.9}$$

$$\langle \hat{A}_m{}^m \rangle = \mathcal{N}\psi_m^2 - \sum_{r\neq m} \langle \hat{d}_r^\dagger \hat{d}_r \rangle, \tag{2.10}$$

$$\langle \hat{a}_n^\dagger \hat{a}_n \rangle = \mathcal{N}\varphi_n^2 + \langle \hat{c}_n^\dagger \hat{c}_n \rangle, \qquad n = 1,2, \tag{2.11}$$

with the abbreviation

$$\psi_m^2 = 1 - \sum_{r\neq m} \Psi_r^2. \tag{2.12}$$

Inserting the ansatz of Eq. (2.8) into the operator $\hat{\Theta}_m(\mathcal{N})$, Eq. (2.6), of the Holstein–Primakoff transformation, Eq. (2.5), we obtain

$$\hat{\Theta}_m(\mathcal{N}) = \sqrt{\mathcal{N}\psi_m^2 - \sum_{r\neq m} \left[\hat{d}_r^\dagger \hat{d}_r + \sqrt{\mathcal{N}}\,\Psi_r \left(\hat{d}_r^\dagger + \hat{d}_r\right)\right]}\,. \tag{2.13}$$

Since we are working in the thermodynamic limit, we can asymptotically expand the square root in powers of $\sqrt{1/\mathcal{N}}$ and obtain up to the order $\mathcal{N}^{-1}$:

$$\begin{aligned}\hat{\Theta}_m(\mathcal{N}) \approx \sqrt{\mathcal{N}}\,\psi_m \Bigg\{ 1 &- \frac{1}{2\sqrt{\mathcal{N}}\,\psi_m^2} \sum_{r\neq m} \Psi_r \left(\hat{d}_r^\dagger + \hat{d}_r\right) \\ &- \frac{1}{2\mathcal{N}\psi_m^2} \sum_{r\neq m} \left[\hat{d}_r^\dagger \hat{d}_r + \sum_{s\neq m} \frac{\Psi_r \Psi_s}{4\psi_m^2} \left(\hat{d}_r^\dagger + \hat{d}_r\right)\left(\hat{d}_s^\dagger + \hat{d}_s\right)\right]\Bigg\}.\end{aligned} \tag{2.14}$$

In this expansion we have neglected terms of the order $\mathcal{N}^{-3/2}$ and higher, which do not contribute to the Hamiltonian (2.7) in the thermodynamic limit.

Finally, we insert the expression (2.14) for the operator $\hat{\Theta}_m(\mathcal{N})$ and the ansatz (2.8) into the Hamiltonian (2.7). In the thermodynamic limit, we can neglect terms with inverse powers of $\mathcal{N}$ and constants of the order $\mathcal{N}^0$. This eventually yields

$$\hat{H}_{m=1} = \mathcal{N}\hat{h}_{m=1}^{(0)} + \sqrt{\mathcal{N}}\,\hat{h}_{m=1}^{(1)} + \hat{h}_{m=1}^{(2)}, \tag{2.15}$$

with

$$\begin{aligned}\hat{h}_{m=1}^{(0)} = {} & E_1 + \delta\Psi_2^2 + \Delta\Psi_3^2 + \hbar\omega_1\,\varphi_1^2 + \hbar\omega_2\,\varphi_2^2 \\ & + 4\,g_1\,\varphi_1\,\psi_1\,\Psi_3 + 4\,g_2\,\varphi_2\,\Psi_2\,\Psi_3,\end{aligned} \tag{2.16}$$

and

$$\begin{aligned}\hat{h}_{m=1}^{(1)} = {} & \left(\hat{d}_2^\dagger + \hat{d}_2\right)\left[\delta\Psi_2 - 2\,g_1\,\varphi_1\,\Psi_2\,\Psi_3/\psi_1 + 2\,g_2\,\varphi_2\,\Psi_3\right] \\ & + \left(\hat{d}_3^\dagger + \hat{d}_3\right)\left[\Delta\Psi_3 + 2\,g_1\,\varphi_1\,\psi_1\left(1 - \Psi_3^2/\psi_1^2\right) + 2\,g_2\,\varphi_2\,\Psi_2\right] \\ & + \left(\hat{c}_1^\dagger + \hat{c}_1\right)\left(\hbar\omega_1\,\varphi_1 + 2\,g_1\,\psi_1\,\Psi_3\right)\Big] \\ & + \left(\hat{c}_2^\dagger + \hat{c}_2\right)\left(\hbar\omega_2\,\varphi_2 + 2\,g_2\,\Psi_2\,\Psi_3\right)\Big],\end{aligned} \tag{2.17}$$

and

$$\begin{aligned}\hat{h}^{(2)}_{m=1} &= \hat{d}_2^\dagger\,\hat{d}_2\left[\delta - 2\,g_1\,\varphi_1\,\Psi_3/\psi_1\right] \\ &+ \hat{d}_3^\dagger\,\hat{d}_3\left[\Delta - 2\,g_1\,\varphi_1\,\Psi_3/\psi_1\right] + \hbar\omega_1\,\hat{c}_1^\dagger\,\hat{c}_1 + \hbar\omega_2\,\hat{c}_2^\dagger\,\hat{c}_2 \\ &- \left(\hat{d}_2^\dagger + \hat{d}_2\right)^2 \frac{1}{2} g_1\,\varphi_1\,\Psi_2^2\,\Psi_3/\psi_1^3 \\ &- \left(\hat{d}_3^\dagger + \hat{d}_3\right)^2 g_1\,\varphi_1\,\Psi_3/\psi_1\left(1 + \tfrac{1}{2}\Psi_3^2/\psi_1^2\right) \\ &- \left(\hat{d}_2^\dagger + \hat{d}_2\right)\left(\hat{d}_3^\dagger + \hat{d}_3\right) g_1\,\varphi_1\,\Psi_2/\psi_1\left(1 + \Psi_3^2/\psi_1^2\right) \\ &+ \left(\hat{d}_3^\dagger\,\hat{d}_2 + \hat{d}_2^\dagger\,\hat{d}_3\right) 2\,g_2\,\varphi_2 \\ &- \left(\hat{c}_1^\dagger + \hat{c}_1\right)\left(\hat{d}_2^\dagger + \hat{d}_2\right) g_1\,\Psi_2\,\Psi_3/\psi_1 \\ &+ \left(\hat{c}_1^\dagger + \hat{c}_1\right)\left(\hat{d}_3^\dagger + \hat{d}_3\right) g_1\,\psi_1\left(1 - \Psi_3^2/\psi_1^2\right) \\ &+ \left(\hat{c}_2^\dagger + \hat{c}_2\right)\left(\hat{d}_2^\dagger + \hat{d}_2\right) g_2\,\Psi_3 \\ &+ \left(\hat{c}_2^\dagger + \hat{c}_2\right)\left(\hat{d}_3^\dagger + \hat{d}_3\right) g_2\,\Psi_2.\end{aligned} \tag{2.18}$$

The Hamiltonian $\hat{H}$ separates into three parts $\hat{h}^{(n)}$, each one scaling with $\mathcal{N}^{(2-n)/2}$ and containing products of n operators $\hat{d}_r$, $\hat{c}_i$.

2.3.3 *Ground-State Properties*

The ground-state energy $\hat{h}^{(0)}_m$ (2.16) of the Hamiltonian (2.15) is a function of the parameters φ_1, φ_2, Ψ_2 and Ψ_3. Next, we extremise the ground-state energy with respect to these parameters, i. e. we stipulate

$$\frac{\partial \hat{h}^{(0)}_{m=1}}{\partial \varphi_n} \stackrel{!}{=} 0, \quad n = 1, 2, \tag{2.19a}$$

$$\frac{\partial \hat{h}^{(0)}_{m=1}}{\partial \Psi_r} \stackrel{!}{=} 0, \quad r = 2, 3. \tag{2.19b}$$

In the case of ψ_1 being finite, this stipulation is equivalent to set the coefficients of the *linear* Hamiltonian $\hat{h}^{(1)}_{m=1}$ (2.17) equal to zero [cf. (Emary and Brandes, 2003a)].

The first set of Eqs. (2.19a) gives conditional equations for the parameters φ_n of the bosonic modes,

$$\varphi_1 = -2\frac{g_1}{\hbar\omega_1}\,\psi_1\,\Psi_3, \quad \varphi_2 = -2\frac{g_2}{\hbar\omega_2}\,\Psi_2\,\Psi_3, \tag{2.20}$$

which, when inserted into the second set of Eqs. (2.19b), gives conditional equations for the parameters Ψ_r of the HP-bosons,

$$\left[\delta + 4\left(\frac{g_1^2}{\hbar\omega_1} - \frac{g_2^2}{\hbar\omega_2}\right)\Psi_3^2\right]\Psi_2 = 0, \tag{2.21a}$$

$$\left[\Delta - 4\frac{g_1^2}{\hbar\omega_1}\left(1 - \Psi_2^2 - 2\Psi_3^2\right) - 4\frac{g_2^2}{\hbar\omega_2}\Psi_2^2\right]\Psi_3 = 0. \tag{2.21b}$$

These equations have several sets of solutions:

(*i*) NORMAL STATE. The trivial solution, $\Psi_2 = \Psi_3 = 0$, is attended by $\varphi_1 = \varphi_2 = 0$ [see Eq. (2.20)]. Since φ_n^2 measures the macroscopic ($\sim \mathcal{N}$) ground-state expectation value of the n^{th} bosonic mode [see Eq. (2.11)], this trivial solution describes the *normal state*, i. e.. no superradiant state of the system. In addition, the ground-state expectation value of the occupation of the n^{th} energy level, which is given by $\langle \hat{A}_n^n \rangle$, is macroscopic for $n = 1$ only [see Eqs. (2.9), (2.10)]. Thus, all particles occupy their respective single-particle ground state $|1\rangle$. The ground-state energy of the many-particle system is given by $\hat{h}^{(0)}_{\text{normal}} = E_1$. Finally, we note that the normal state is always a solution of the equations (2.20) and (2.21), irrespective of the couplings g_1 and g_2. However, analysing the Hessian matrix of $\hat{h}^{(0)}_{m=1}$, restricts[1] the range of the first coupling to

$$g_1 < \frac{\sqrt{\Delta\, \hbar\omega_1}}{2} \equiv g_{1,c}, \tag{2.22}$$

where we have defined a critical coupling strength $g_{1,c}$.

(*ii*) BLUE SUPERRADIANT STATE. Of course the Eqs. (2.21) give non-trivial solutions as well. The second solution is given by

$$\Psi_2 = 0, \qquad \Psi_3 = \pm\sqrt{\frac{1}{2}}\sqrt{1 - \left(\frac{g_{1,c}}{g_1}\right)^2}, \tag{2.23a}$$

$$\varphi_1 = \mp\frac{g_1}{\hbar\omega_1}\sqrt{1 - \left(\frac{g_{1,c}}{g_1}\right)^4}, \qquad \varphi_2 = 0. \tag{2.23b}$$

In contrast to the previous solution, this solution has a finite parameter φ_1 and for this reason a finite and macroscopic occupation $\langle \hat{a}_1^\dagger\, \hat{a}_1 \rangle$ of the first bosonic mode. This solution corresponds to a *superradiant* state of the system, where superradiance occurs in the blue branch of the Lambda-system. More precisely, we call this state a *blue superradiant state*. Furthermore, the first *and* the third single-particle energy level are macroscopically occupied.

If we insert the solution (2.23) into the ground-state energy (2.16) of the many-particle system, we obtain

$$\hat{h}^{(0)}_{\text{blue}} = E_1 - \frac{\Delta}{4}\left(\frac{g_1}{g_{1,c}}\right)^2\left[1 - \left(\frac{g_{1,c}}{g_1}\right)^2\right]^2. \tag{2.24}$$

Hence, the ground-state energy of the superradiant state is always smaller than the ground-state energy of the normal state. However, this solution is only valid for couplings $g_1 \geqslant g_{1,c}$, since for smaller couplings g_1 the non-zero parameters of the solution (2.23) become purely imaginary and, in addition, the Hessian matrix of $\hat{h}^{(0)}_{m=1}$ becomes indefinite.

1 Cf. the discussion for the Dicke model in Sec. 1.3.3.3, in particular the analysis from Eq. (1.150) on.

(*iii*) RED SUPERRADIANT STATE. There can be another set of parameters φ_n, Ψ_r which extremise the ground-state energy $\hat{h}^{(0)}_m$. This set cannot be deduced from the ground-state energy $\hat{h}^{(0)}_{m=1}$, Eq. (2.16), because it represents not a *local* but a *global* minimum of $\hat{h}^{(0)}_{m=1}$. Since $\hat{h}^{(0)}_{m=1}$ is defined on the unit ball $B_2 = \{(x,y) \in \mathbb{R}^2 \,|\, x^2 + y^2 \leqslant 1\}$, the global minimum lies on the boundary of B_2, that is $\Psi_2^2 + \Psi_3^2 = 1$ ($\psi_1 = 0$) holds. To obtain this global minimum one has to first of all set $\psi_1 = 0$ in Eq. (2.16) and omit all terms involving ψ_1 in Eq. (2.17). Secondly, one extremises the ground-state energy as before, but taking the constraint $\Psi_2^2 + \Psi_3^2 = 1$ into account. Eventually, we obtain

$$\Psi_2 = \pm\sqrt{\frac{1}{2}}\sqrt{1 + \left(\frac{g_{2,c_1}}{g_2}\right)^2}, \tag{2.25a}$$

$$\Psi_3 = \pm\sqrt{\frac{1}{2}}\sqrt{1 - \left(\frac{g_{2,c_1}}{g_2}\right)^2}, \tag{2.25b}$$

$$\varphi_1 = 0, \quad \varphi_2 = \mp\frac{g_2}{\hbar\omega_2}\sqrt{1 - \left(\frac{g_{2,c_1}}{g_2}\right)^4}, \tag{2.25c}$$

where we have introduced

$$g_{2,c_1} \equiv \frac{\sqrt{(\Delta - \delta)\,\hbar\omega_2}}{2} \tag{2.26}$$

a second critical coupling strength.

The occupation of the first single-particle energy level $|1\rangle$ is not macroscopic, i.e. it is negligible in the thermodynamic limit. Since $\varphi_1 = 0$ and φ_2 is finite, this state also corresponds to a superradiant state, whereat superradiance occurs in the red branch of the Lambda-system. We call this superradiant state a *red superradiant* state.

This red superradiant solution can also be found by direct extremisation of the ground-state energy $\hat{h}^{(0)}_{m=2}(\Psi_1, \Psi_3)$, i.e. if one considers the second level $|2\rangle$ as the reference state m of the Holstein–Primakoff transformation, Eq. (2.5). In general, one can say that using the Holstein–Primakoff transformation in the thermodynamic limit with the m^{th} state as the reference state, one can describe many-particle states in which the occupation of the m^{th} energy level of the single-particle system is finite. In order to describe the normal state, which is a state where *all* particles occupy their respective ground state $|1\rangle$, one has to take $|1\rangle$ as the reference state ($m = 1$). In contrast, to describe a state where no particle occupies its respective single-particle ground state $|1\rangle$, either $|2\rangle$ ($m = 2$) or $|3\rangle$ ($m = 3$) has to be chosen as the reference state.

At last, the ground-state energy of this red superradiant state is given by

$$\hat{h}^{(0)}_{\text{red}} = E_1 + \delta - \frac{1}{4}\left[\left(\sqrt{\Delta} + \sqrt{\delta}\right)\frac{g_2}{g_{2,c_2}} - \left(\sqrt{\Delta} - \sqrt{\delta}\right)\frac{g_{2,c_2}}{g_2}\right]^2, \tag{2.27}$$

where

$$g_{2,c_2} \equiv \frac{\left(\sqrt{\Delta}+\sqrt{\delta}\right)\sqrt{\hbar\omega_2}}{2} \tag{2.28}$$

is a third critical coupling strength.

UNPHYSICAL SOLUTION. There is also a solution of the Eqs. (2.21) which corresponds to a state where both branches of the Lambda-system are superradiant. However, this state is either not well defined for certain couplings g_1 and g_2 or it does *not* minimise the ground-state energy (2.16). In the latter case, this solution can be attributed to a point of inflection on the energy landscape $\hat{h}^{(0)}_{m=1}(\Psi_2, \Psi_3)$.

A further solution of the Eqs. (2.21) represents a dark state. This state is discussed in detail in Sec. 2.4.2.

2.3.4 *Excitation Energies*

So far, we have extremised the ground-state energy $\hat{h}^{(0)}$ of the Hamiltonian (2.15) in the thermodynamic limit. By this procedure, the linear part $\hat{h}^{(1)}$ is eliminated as well. The next step is to diagonalise the quadratic part $\hat{h}^{(2)}$. This can be achieved by means of a principle axis or *Bogoliubov* transformation (EMARY and BRANDES, 2003a). See Sec. A.4.2 of the appendix for details. The diagonalised Hamiltonian is then given by

$$\hat{h}^{(2)} = \sum_{n=1}^{4} \hbar\varepsilon_n \, \hat{e}_n^\dagger \, \hat{e}_n, \tag{2.29}$$

where $\hat{e}_n^\dagger(\hat{e}_n)$ create (annihilate) quasi-particles which refer to bosonic excitations, i.e. $\hat{e}_n^\dagger$ and $\hat{e}_n$ satisfy canonical commutator relations. The operators $\hat{e}_n^\dagger$, $\hat{e}_n$ and the excitation energies $\hbar\varepsilon_n$ have to be evaluated separately in the three different states. The determination of these quantities reduces to a diagonalisation of two-by-two matrices. The diagonalisation procedure yields four excitation energies, which are given in the appendix; see Eq. (A.156)-Eq. (A.162) of Sec. A.4.2.

2.4 PHASE TRANSITIONS

Comparing the ground-state energies of the states we found in the last section, we can derive the zero-temperature phase diagram. As mentioned before, the normal state is only stable for couplings $g_1 < g_{1,c}$ and its energy is independent of both coupling strengths g_1 and g_2. We also observed that the energy of the blue superradiant state is always less than the energy of the normal state. However, the blue superradiant state is stable for $g_1 \geqslant g_{1,c}$ only. In addition, by comparing the energies of the blue (2.24) and the red (2.27) superradiant state,

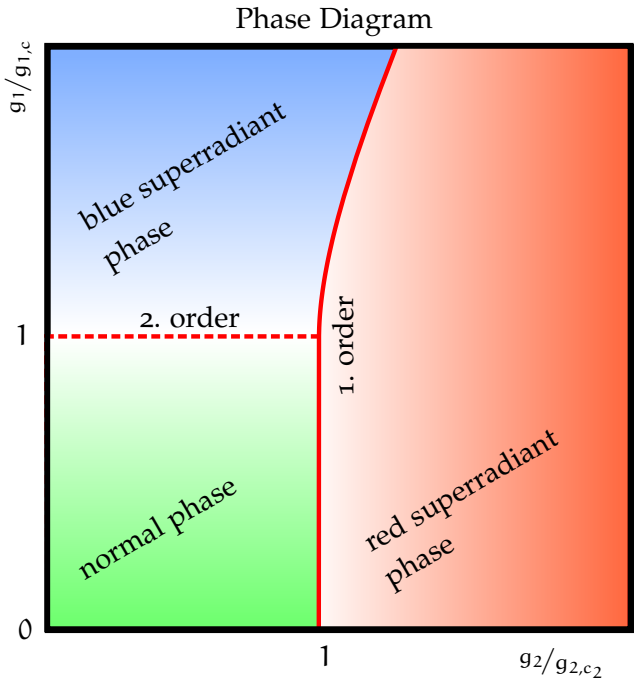

Figure 2.3: Phase diagram for $\Delta > \delta > 0$ showing the three different phases: the normal and the blue and red superradiant phase. The (symmetric) normal phase is defined by $\Psi_2 = \Psi_3 = \varphi_1 = \varphi_2 = 0$. In the (symmetry-broken) blue superradiant phase $\Psi_2 = 0, \Psi_3 \neq 0, \varphi_1 \neq 0$ and $\varphi_2 = 0$. Finally, in the (symmetry-broken) red superradiant phase $\Psi_2 \neq 0, \Psi_3 \neq 0, \varphi_1 = 0$ and $\varphi_2 \neq 0$ holds. The phase transition from the normal to the blue superradiant phase is of second order (red dashed line), whereas the phase transition from the normal to the red superradiant phase and between the two superradiant phases is of first order (red solid line). The normal *state* is meta-stable in the region of the red superradiant phase as long as $g_1 < g_{1,c}$.

we see that only for $g_2 \geqslant g_{2,c_2}$ the red superradiant state is stable. Furthermore, in this parameter regime its energy is always smaller than the energy of the normal state [see Eq. (2.27) with $g_2 = g_{2,c_2}$].

2.4.1 *The Phase Diagram*

From this discussion we derive the phase diagram which is shown in Fig. 2.3. It consists of three phases: one *normal phase* for couplings $g_1 < g_{1,c}$ and $g_2 < g_{2,c_2}$, one *blue superradiant phase* for couplings $g_1 \geqslant g_{1,c}$ and $g_2 \leqslant \bar{g}_{2,c}(g_1)$, and lastly one *red superradiant phase* for couplings $g_1 < \bar{g}_{1,c}(g_2)$ and $g_2 \geqslant g_{2,c_2}$. If both couplings are at criticality, $g_1 = g_{1,c}$ and $g_2 = g_{2,c_2}$, all three phases coexist, i.e. there is a *triple point* in the phase diagram. Here, $\bar{g}_{1,c}(g_2)$ and $\bar{g}_{2,c}(g_1)$ parameterise the same curve, which represents the phase boundary between the two superradiant phases (see Fig. 2.3). Both $\bar{g}_{1,c}(g_2)$ and $\bar{g}_{2,c}(g_1)$ are given by the condition that the energies of the blue (2.24) and the

red (2.27) superradiant state intersect, i.e. both can be obtained by setting the Eqs. (2.24) and (2.27) equal. For $\bar{g}_{1,c}(g_2)$ we obtain after several algebraic transformations

$$\bar{g}_{1,c}^2(g_2) = g_2^2 \frac{1}{2} \frac{\omega_1}{\omega_2} \Bigg\{ 1 + \left(\frac{g_{2,c_1}}{g_2}\right)^4 - \frac{\delta \hbar \omega_2}{2 g_2^2} + \left[1 + \left(\frac{g_{2,c_1}}{g_2}\right)^2\right] \sqrt{\left[1 - \left(\frac{g_{2,c_1}}{g_2}\right)^2\right]^2 - \frac{\delta \hbar \omega_2}{g_2^2}} \Bigg\}. \quad (2.30)$$

In the limit $\delta \to 0$, the phase boundary flattens to a straight line, $\lim_{\delta \to 0} \bar{g}_{1,c}(g_2) = \sqrt{\omega_1/\omega_2}\, g_2$.

The order of a phase transition is defined by the non-analytic behaviour of a thermodynamic potential (cf. Sec. 1.3.3.1). In the case of zero temperature, the ground-state energy represents a thermodynamic potential and hence its derivatives give the order of the phase transition. The ground-state energy of the normal state is E_1, irrespective of the couplings g_1 and g_2. Hence, all derivatives with respect to g_1 and g_2 vanish. Comparing this result with the first and second derivatives of the ground-state energy of the blue (2.24) and the red (2.27) superradiant state, we see that the phase transition from the normal phase to the blue (red) superradiant phase is of second (first) order. The ground-state energy is shown in Fig. 2.4.

In addition, the parameters Ψ_r ($r = 2, 3$) and φ_n ($n = 1, 2$) also give evidence for the phase transition and can be interpreted as *order parameters*. An order parameter is continuous for second-order phase transitions and discontinuous for first-order phase transitions (Goldenfeld, 2010). This behaviour is visible in Fig. 2.4. The order parameters are zero in the *symmetric* (normal) phase and are finite in the *symmetry-broken* (superradiant) phase. The corresponding symmetry is the parity symmetry (see Sec. 2.2). In the blue (red) superradiant phase, the parity symmetry corresponding to the parity operator $\hat{\Pi}_1$ ($\hat{\Pi}_2$) [see Eq. (2.3)] is broken, since e.g. in the blue superradiant phase for finite φ_1 the operator $\hat{c}_1^\dagger \hat{c}_1$ in the Hamiltonian (2.18) is not invariant under the symmetry transformation $\hat{\Pi}_1$: $\hat{\Pi}_1 \hat{c}_1^\dagger \hat{c}_1 \hat{\Pi}_1^\dagger = \hat{c}_1^\dagger \hat{c}_1 + \sqrt{\mathcal{N}}\, \varphi_1 (\hat{c}_1^\dagger + \hat{c}_1) + \mathcal{N} \varphi_1^2$.

Both, the phase transition and the order of the phase transition can also be deduced from the excitation energies. The excitation energies from the Eqs. (A.156)-(A.162) are shown in Fig. 2.5. At the phase transition at least one of the excitation energies either tends to zero or is discontinuous. The first case corresponds to a second-order, the latter case to a first-order phase transition. The second-order phase transition can be read off the excitation energy ε_4 which is zero for $g_1 = g_{1,c}$ and $g_2 < g_{2,c_2}$.

Finally, we note that the phase transition from the normal to the blue superradiant phase is in accordance with the superradiant phase transition in the Dicke model (Emary and Brandes, 2003a), i.e. it is

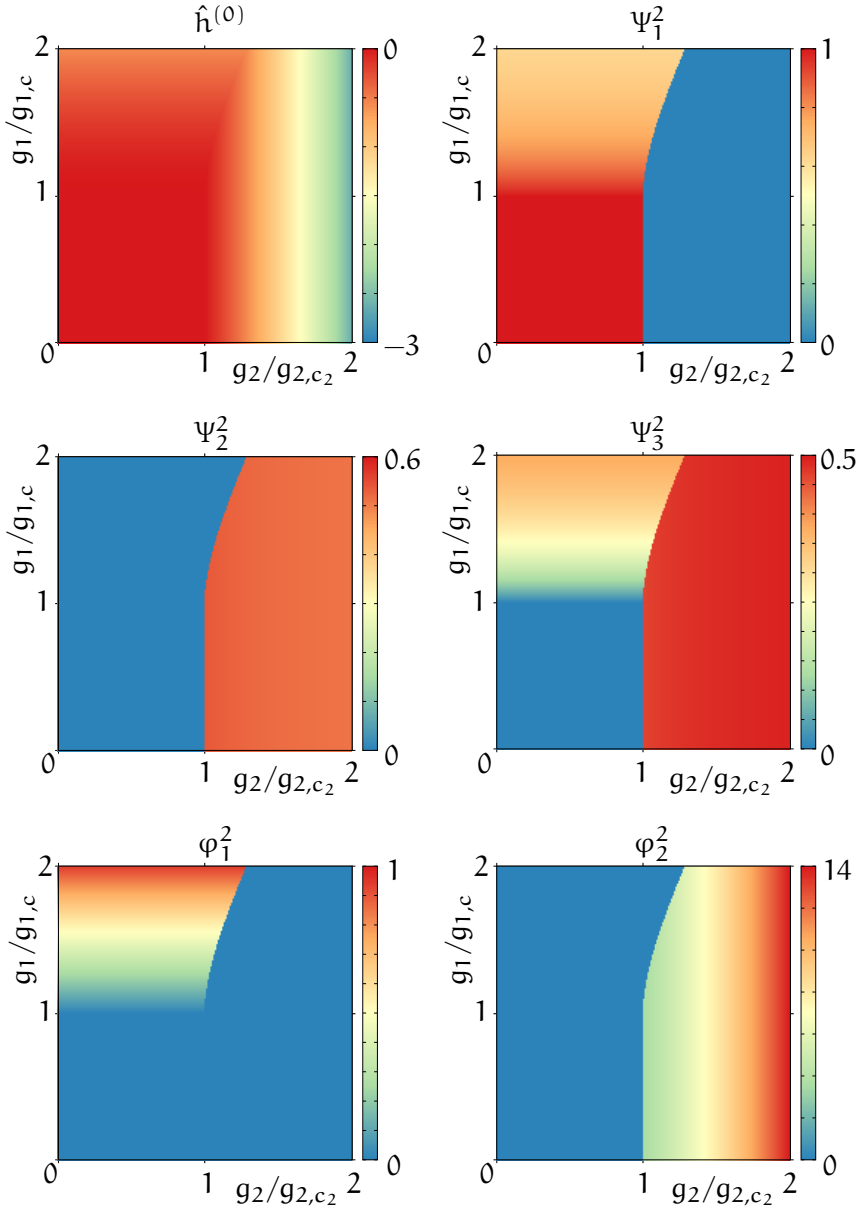

Figure 2.4: Ground-state energy $\hat{h}^{(0)}$, ground-state occupation φ_n^2 of the first ($n = 1$) and the second ($n = 2$) bosonic mode and the ground-state occupation Ψ_n^2 of the single-particle energy levels ($n = 1, 2, 3$). Numerical values: $\Delta = \hbar\omega_1 = 1$, $\delta = 0.75$, $\hbar\omega_2 = 0.25$ (on resonance).

of second order and one (the atomic) branch of the excitation energies tends to zero at the phase transition.

The discontinuity of the order parameters and the first derivative of the ground-state energy at the phase transition between the normal and the red superradiant phase scales with $\sqrt{\delta}$. Thus, this first-order phase transition becomes continuous in the limit $\delta \to 0$. However, the phase boundary between the two superradiant phases persists to be a first-order phase transition in this degenerate limit. This is also the case in the limit of large couplings, $g_1/g_{1,c}, g_2/g_{2,c_2} \to \infty$.

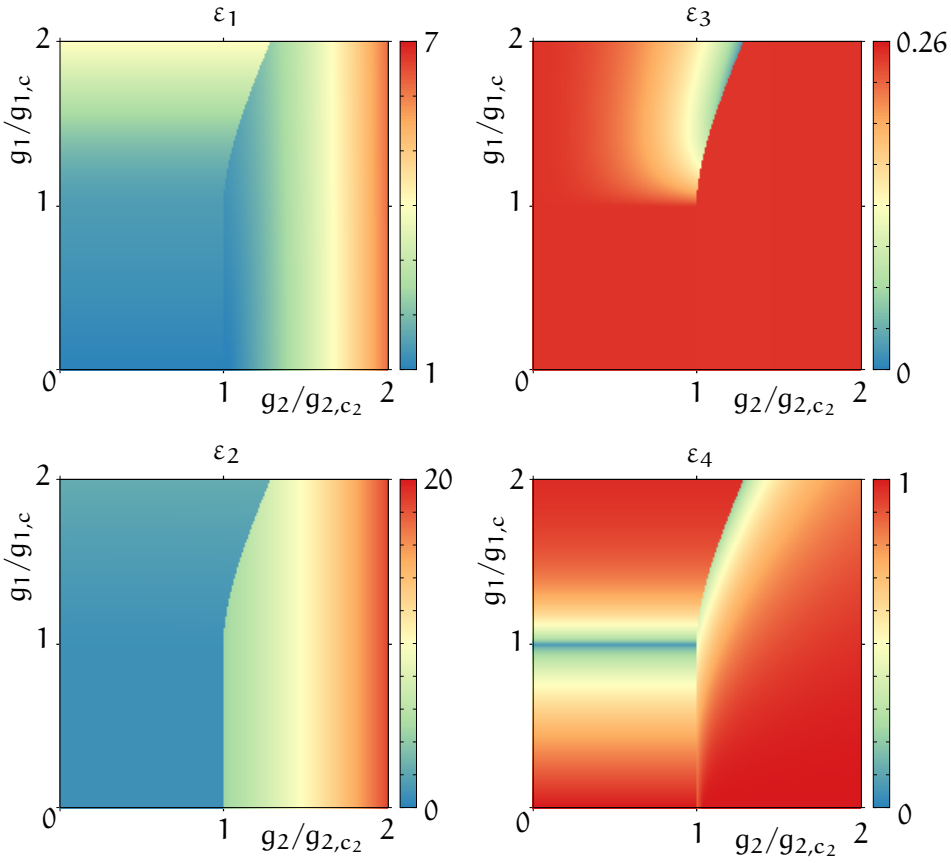

Figure 2.5: Excitation energies ε_n from Eqs. (A.156)-(A.162). Numerical values: $\Delta = \hbar\omega_1 = 1$, $\delta = 0.75$, $\hbar\omega_2 = 0.25$ (on resonance).

2.4.2 *Dark State*

Due to the interaction of a quantum system with its environment, decay processes within the quantum system occur. Eigenstates of the Hamiltonian which are unaffected by these decay processes are called dark states. In our model, a dark state is a many-body state which does not radiate, i. e. a state where the occupation in either of the bosonic modes is zero. This condition is satisfied if the two mean-fields φ_n are zero. From Eqs. (2.20) we see that the normal state, with $\Psi_2 = \Psi_3 = 0$, is a trivial dark state. In general, it suffices to set $\Psi_3 = 0$ for a dark state. Applying this condition to Eq. (2.21), we can identify a dark state for $\delta = 0$ only, i. e. for two energetically degenerate ground states. In the thermodynamic limit, the coherence of this dark state is given by $\langle \hat{A}_1^2 \rangle = \mathcal{N}\psi_1\Psi_2$, and is therefore finite apart from the two trivial cases $\psi_1 = 0$ or $\Psi_2 = 0$. The energy of the dark state is simply $\hat{h}^{(0)}_{\text{Dark}} = E_1$.

We obtain the excitation energies for the dark state by diagonalising $\hat{\mathrm{h}}^{(2)}_{m=1}$ from Eq. (2.18). For any given Ψ_2, these energies can be computed from the characteristic equation

$$\mathrm{Det}\begin{pmatrix} \Delta^2-\varepsilon^2 & 2\,g_1\,\psi_1\sqrt{\hbar\omega_1\,\Delta} & 2\,g_2\,\Psi_2\sqrt{\hbar\omega_2\,\Delta} \\ 2\,g_1\,\psi_1\sqrt{\hbar\omega_1\,\Delta} & (\hbar\omega_1)^2-\varepsilon^2 & 0 \\ 2\,g_2\,\Psi_2\sqrt{\hbar\omega_2\,\Delta} & 0 & (\hbar\omega_2)^2-\varepsilon^2 \end{pmatrix} = 0, \tag{2.31}$$

where $\mathrm{Det}\,M$ is the determinant of the matrix M. The characteristic equation is readily solved in the case of two-photon resonance ($\omega_1 = \omega_2 = \Delta/\hbar \equiv \omega$), yielding the energies

$$\varepsilon_1 = 0, \quad \varepsilon_2 = \hbar\omega, \tag{2.32}$$

$$\varepsilon_{3,4} = \sqrt{(\hbar\omega)^2 \pm 2\,\hbar\omega\sqrt{g_1^2\left(1-\Psi_2^2\right)+g_2^2\,\Psi_2^2}}\,, \tag{2.33}$$

where the additional zeroth mode ε_1 stems from the limit $\delta \to 0$.

The parameter Ψ_2 is arbitrary and can range from zero to one. For a given Ψ_2, we find by analysis of the Hessian matrix of $\hat{\mathrm{h}}^{(0)}_{m=1}$, that this dark state is meta-stable if the inequality

$$\left(g_1/g_{1,c}\right)^2\left(1-\Psi_2^2\right) \leqslant 1-\left(g_2/g_{2,c}\right)^2\Psi_2^2 \tag{2.34}$$

is satisfied. Otherwise this dark-state solution is unstable. In Eq. (2.34) we have introduced the critical coupling strength $g_{2,c} \equiv \sqrt{\hbar\omega_2\Delta}/2$.

We emphasise that the dark state exists for $\delta = 0$ only. By inspection of the inequality (2.34), we make the following statements: First, the dark state is stable for $g_1 < g_{1,c}$ *or* $g_2 < g_{2,c}$ only. Furthermore, if both coupling strengths fulfil $g_n < g_{n,c}$, i.e. in the normal phase, both ψ_1 and Ψ_2 can range from zero to one. On the other hand, if $g_2 > g_{2,c}$ and $g_1 < g_{1,c}$, then Ψ_2 is restricted to the interval $[0, \Psi_{2,\max}]$, where $\Psi_{2,\max} > 0$ is given by the inequality (2.34). Correspondingly ψ_1 is restricted to the interval $[\psi_{1,\min}, 1]$, with $\psi_{1,\min}$ given by $\sqrt{1-\Psi^2_{2,\max}}$. An analogue argument can be given for the case $g_1 > g_{1,c}$ and $g_2 < g_{2,c}$, where ψ_1 and Ψ_2 are interchanged.

For couplings $g_1 \gg g_{1,c}$ and $g_2 < g_{2,c}$, inequality (2.34) restricts the order parameters to $\psi_1 \approx 0$ and $\Psi_2 \approx 1$, i.e. only the second single-particle level is macroscopically occupied. On the other hand, for couplings $g_2 \gg g_{2,c}$ and $g_1 < g_{1,c}$ only the first single-particle level is macroscopically occupied, i.e. $\psi_1 \approx 1$ and $\Psi_2 \approx 0$. This *counter-intuitive* behaviour is reminiscent of the STIRAP scheme (Bergmann, Theuer, and Shore, 1998). In contrast to the STIRAP scheme, the actual values of the populations ψ_1 and Ψ_2 in this dark state are *not* defined by the coupling strengths g_1 and g_2, but rather by the preparation of the system. Thus, the system cannot be driven coherently

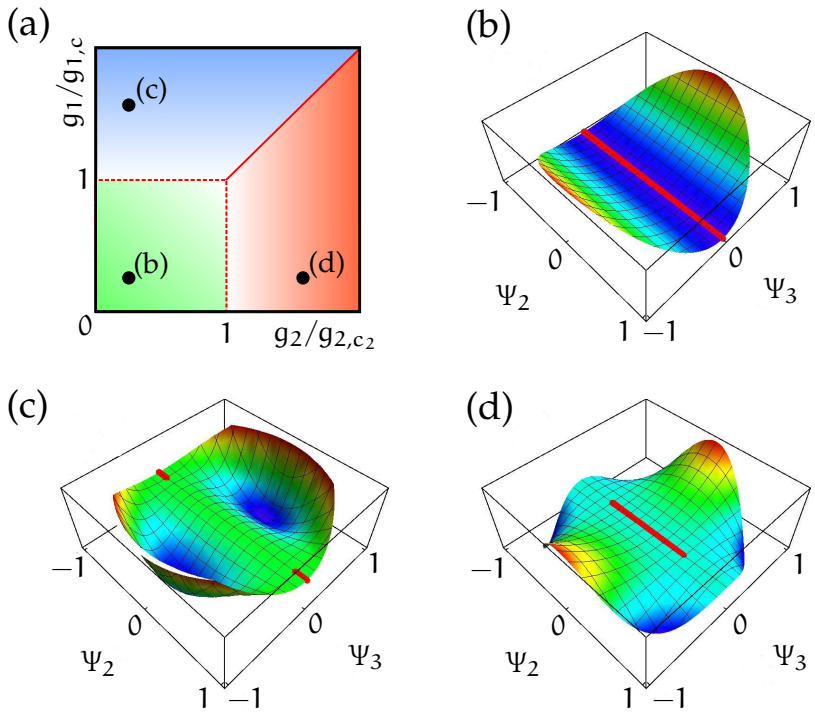

Figure 2.6: Phase diagram (a) as in Fig. 2.3 and ground-state energy surfaces $\hat{h}^{(0)}$ (b–d) in the degenerate ($\delta \to 0$) limit. In (a), the solid and the broken red lines denote first and second-order phase transitions, respectively. The red lines in (b–d) visualise the inequality (2.34), i.e. the line where the dark state with $\Psi_3 = 0$ is stable. However, as the red line is flat, fluctuations along the Ψ_2-direction transform stable states on the red line into unstable states outside the red line. Eventually, these states decay to superradiant states with $\Psi_3 \neq 0$.

from a state with all particles occupying the first single-particle energy level $|1\rangle$ to a state where all particles occupy the second single-particle energy level $|2\rangle$ just by changing the couplings.

In addition, we note that in this dark state the mode $\varepsilon_1 = 0$ in direction of Ψ_2 of the energy surface $\hat{h}^{(0)}(\Psi_2, \Psi_3)$ is trivially massless [see Eq. (2.32)]. Therefore, tiny fluctuations can easily excite this dark state along the direction of Ψ_2, making the state eventually unstable. This instability is visualized in Fig. 2.6

2.5 CONCLUSION

We have analysed an extension of the well-known Dicke model from two to three-level particles. By means of a Holstein–Primakoff transformation we have identified three stable states in the thermodynamic limit: a normal, a blue superradiant, and a red superradiant state. At zero temperature, these states correspond to three thermodynamic phases which we have arranged in a phase diagram. The phase transition between the normal and the blue superradiant phase is of sec-

ond order and all other phase transitions are of first order. We have also shown that a state with both superradiant states coexisting is not stable. A dark state with zero occupancy of the third single-particle level exists for $\delta = 0$ only. However, this dark state is not stable.

As in the original Dicke model, the same experimental difficulties arise in our extended Dicke model, i.e. reaching the critical coupling strength is challenging as well. Hence, using three-level atoms has no advantage over the use of two-level atoms.

However, we expect that similarly to the Dicke model and its realisation in the experiments of Baumann, Guerlin, et al. (2010), there should be experimental manageable systems which can theoretically be described by an effective Hamiltonian of the form presented here. In the case of the experiments of Baumann, Guerlin, et al. (2010), this might be achieved by coupling a Bose–Einstein condensate to an additional cavity mode. Furthermore, an even richer phase diagram with additional superradiant phases could be generated in such a system.

Considering a cold quantum gas in an optical lattice, a characteristic feature of our extended Dicke model especially in the degenerate limit, $\delta \to 0$, could appear. In this regard, we have an extension of a system proposed by Silver et al. (2010) in mind. There, it was shown that a two-band zero-hopping Bose–Hubbard model coupled to a cavity light field can be written as an effective Dicke model. If one superposes a superlattice of twice the wavelength of the original lattice, and couples the superlattice to two independent cavity light fields, this extended Bose–Hubbard model can be mapped to our extended Dicke model with $\delta = 0$. Since in experiment one has an extensive control over the parameters of cold quantum gases, the observation of superradiant phases should be feasible.

3

SUPERRADIANT PHASE TRANSITIONS AND THE DIAMAGNETIC TERM

This Chapter is mostly based on the publication:

Hayn, Mathias, Clive Emary, and Tobias Brandes (2012): *Superradiant phase transition in a model of three-level-Λ systems interacting with two bosonic modes*, Phys. Rev. A **86**, p. 063822. doi: 10.1103/PhysRevA.86.063822.

3.1 INTRODUCTION

Superradiant phase transitions in systems of atoms interacting with an electromagnetic field were first discussed theoretically by Hepp and Lieb (1973b,a), and Wang and Hioe (1973). The superradiant phase transition is characterised by a macroscopic and coherent excitation of both the atoms and the electromagnetic field modes. To date, superradiant phase transitions have been observed experimentally in artificial realisations of the seminal Dicke model (Dicke, 1954) in cold atoms (Baumann, Guerlin, et al., 2010), but not for real or for artificial atoms. The question which was debated forty years ago and which is under debate today again, is whether or not superradiant phase transitions are in principle possible in these systems (Rzażewski, Wódkiewicz, and Żakowicz, 1975; Nataf and Ciuti, 2010a; Viehmann, Delft, and Marquardt, 2011).

The system of an ensemble of atoms interacting with an electromagnetic field is often described by the Dicke model (Dicke, 1954). In this model, each individual atom is described by a two-level system and the electromagnetic field by a single mode of a resonator. For the generalised Dicke model with diamagnetic terms included [i. e. a Hopfield-like model (Hopfield, 1958)], there exists a no-go theorem (Rzażewski, Wódkiewicz, and Żakowicz, 1975; Nataf and Ciuti, 2010a; Viehmann, Delft, and Marquardt, 2011) which precludes the transition to a superradiant phase. This no-go theorem is a consequence of sum rules and of the appearance of a diamagnetic term in the microscopic Hamiltonian which is quadratic in the transverse vector potential $\mathbf{A}$. Thus no matter how low the temperature or how strong the coupling strength is, the superradiant phase transition does not exist in such models.

The no-go theorem has also been extended to multi-level Hopfield-like-models (Viehmann, Delft, and Marquardt, 2011). However, it has been commented (Ciuti and Nataf, 2012) that these kind of no-go theorems for multi-level systems do not apply to first-order

superradiant phase transitions and therefore new perspectives open up.

In this chapter we extend the abstract model of Ch. 2 by including a diamagnetic term and account for all boson-mediated transitions from the ground states to the excited state. We analyse and discuss the phases and phase transitions of this extended model and show that the system shows both a first and a second-order phase transition. We also discuss the symmetries of this model and show how they are related to the quantum phases of this system. Finally, we show that a no-go theorem in general does *not* hold for this model and a superradiant phase transition is in fact possible. However, due to the Thomas–Reiche–Kuhn sum rule, only the first-order phase transition survives. This is consistent with the results of Baksic, Nataf, and Ciuti (2013). There, three-level atoms were considered as well, and only a first-order superradiant phase transition was found.

3.2 THE MODEL

We consider a system consisting of $\mathcal{N}$ identical particles interacting with two modes of a bosonic field. The particles are described by three-level systems in Lambda-configuration, i.e. two in general non-degenerate ground states and one excited state with energies E_1, E_2, and E_3, and detunings $\delta = E_2 - E_1 \geqslant 0$ and $\Delta = E_3 - E_1 > 0$. The two bosonic modes have frequencies ω_1 and ω_2, respectively. In Fig. 1.2, the model is summarised graphically. The Hamiltonian is given by

$$\begin{aligned}\hat{H} = &\sum_{n=1}^{3} E_n \hat{A}_n^{\,n} + \sum_{n=1}^{2} \hbar\omega_n \hat{a}_n^\dagger \hat{a}_n \\ &+ \frac{g_1}{\sqrt{\mathcal{N}}}\left(\hat{A}_3^{\,1} + \hat{A}_1^{\,3}\right)\left[\hat{a}_1^\dagger + \hat{a}_1 + \chi_1\left(\hat{a}_2^\dagger + \hat{a}_2\right)\right] \\ &+ \frac{g_2}{\sqrt{\mathcal{N}}}\left(\hat{A}_3^{\,2} + \hat{A}_2^{\,3}\right)\left[\hat{a}_2^\dagger + \hat{a}_2 + \chi_2\left(\hat{a}_1^\dagger + \hat{a}_1\right)\right] \\ &+ \sum_{n=1}^{2} \frac{\kappa_n^2}{\omega_n}\left(\hat{a}_n^\dagger + \hat{a}_n\right)^2 + 2\frac{\kappa_3^2}{\sqrt{\omega_1\omega_2}}\left(\hat{a}_1^\dagger + \hat{a}_1\right)\left(\hat{a}_2^\dagger + \hat{a}_2\right). \quad (3.1)\end{aligned}$$

Here, $\hat{A}_n^{\,m}$ are collective atomic operators (see Sec. 1.2 and Sec. A.2) and $\hat{a}_n^\dagger$, $\hat{a}_n$ are the creation and annihilation operators of the n^{th} bosonic mode. The first two terms in Eq. (3.1) correspond to the energy of the free system of particles and the bosonic fields, respectively. The third and the fourth term proportional to the coupling constants g_1 and g_2 model the interaction between the particles and the bosonic fields. The dimensionless parameters χ_1 (χ_2) generate transitions from the first (second) ground state to the excited state induced by the second (first) bosonic mode. Eventually, the last terms scaling with κ_n represent a self interaction of the bosonic field.

Special cases of the Hamiltonian, Eq. (3.1), include (*i*) the model of Ch. 2 with $\chi_n = \kappa_n = 0$, and (*ii*) a model describing atoms interacting with two modes of an electromagnetic field with

$$g_n = \sqrt{\mathcal{N}}(E_3 - E_n)|\mathbf{d}_{3n} \cdot \boldsymbol{\varepsilon}_n| \mathcal{A}_n/\hbar, \tag{3.2}$$

$$\chi_n = \sqrt{\frac{\omega_n}{\omega_{n'}}} \frac{|\boldsymbol{\varepsilon}_{n'} \cdot \mathbf{d}_{3n}|}{|\boldsymbol{\varepsilon}_n \cdot \mathbf{d}_{3n}|} \quad (n' \neq n), \tag{3.3}$$

$$\kappa_1 = \kappa_2 = \kappa, \quad \kappa_3 = \sqrt{\boldsymbol{\varepsilon}_1 \cdot \boldsymbol{\varepsilon}_2}\kappa. \tag{3.4}$$

The derivation of this model and the detailed definition of the parameters is given in Sec. 1.2.2.

By virtue of the Thomas–Reiche–Kuhn sum rule, the couplings constants g_n are bounded. In our model, we have two important sum rules (the derivation can be found in Sec. A.1)

$$g_1 \leqslant \sqrt{\frac{\Delta}{\omega_1}}\,\kappa \equiv g_{1,\mathrm{TRK}} \quad \text{and} \quad g_2 \leqslant \sqrt{\frac{\Delta - \delta}{\omega_2}}\,\kappa \equiv g_{2,\mathrm{TRK}}. \tag{3.5}$$

Thus for given parameters, the light-matter coupling strengths g_1, g_2 for atomic systems cannot exceed $g_{1,\mathrm{TRK}}$, $g_{2,\mathrm{TRK}}$, respectively. This bound will be crucial in the next section where we discuss phase transitions of this model.

3.3 PHASE TRANSITIONS

In order to obtain the phase diagram of this system, we apply the techniques presented in Ch. 2. There, we have used the Holstein–Primakoff transformation (Holstein and Primakoff, 1940; Klein and Marshalek, 1991). This is a non-linear transformation, which maps the collective particle operators $\hat{A}_n^m$ onto bosonic creation and annihilation operators. The corresponding non-linear Hamiltonian can be linearised by introducing mean-fields both for the bosonic modes and for the creation and annihilation operators of the particles. Then, the Hamiltonian obtains the form

$$\hat{H} = \mathcal{N}\hat{h}^{(0)} + \sqrt{\mathcal{N}}\hat{h}^{(1)} + \hat{h}^{(2)} + \mathcal{O}(\mathcal{N}^{-1/2}), \tag{3.6}$$

where the order of $\mathcal{N}$ is explicitly given. Here, $\hat{h}^{(0)}$ corresponds to the ground-state energy, and $\hat{h}^{(2)}$ to the fluctuations around the ground state. In the thermodynamic limit, $\mathcal{N} \gg 1$, analysis of the ground-state energy $\hat{h}^{(0)}$ yields the relevant information for the phases, phase transitions, and phase diagram of the system. Explicitly, the ground-state energy is given by

$$\begin{aligned} E_0 := \hat{h}^{(0)} = \delta\Psi_2^2 + \Delta\Psi_3^2 + \left(\hbar\omega_1 + \frac{4\kappa_1^2}{\omega_1}\right)\varphi_1^2 + \left(\hbar\omega_2 + \frac{4\kappa_2^2}{\omega_2}\right)\varphi_2^2 \\ + 4g_1\psi_1\Psi_3(\varphi_1 + \chi_1\varphi_2) + 4g_2\Psi_2\Psi_3(\varphi_2 + \chi_2\varphi_1) \\ + 8\frac{\kappa_3^2}{\sqrt{\omega_1\omega_2}}\varphi_1\varphi_2. \end{aligned} \tag{3.7}$$

The real mean-fields φ_s (with $s = 1,2$), Ψ_n (with $n = 2,3$), and $\psi_1 = \sqrt{1-\Psi_2^2-\Psi_3^2}$ correspond to the two bosonic modes and the bosons introduced by the Holstein–Primakoff transformation, respectively (cf. Ch. 2). Finite values of the mean-fields give macroscopic populations of the bosonic modes or the three particle levels, i.e. if Ψ_3 (φ_1) is finite, then the third (first) energy level of the particles (bosonic mode) is macroscopically occupied. Particle number conservation implies $\Psi_2^2 + \Psi_3^2 \leqslant 1$.

We eliminate the two mean-fields φ_1 and φ_2 from E_0 by minimising E_0 with respect to these two mean-fields. Then, the ground-state energy is a function of the mean-fields Ψ_2 and Ψ_3 only: $E_0 = E_0(\Psi_2, \Psi_3)$. One can show that the normal state with $\Psi_2 = \Psi_3 = 0$ is always a critical point of E_0. However, it can still be a maximum, or, if it is a minimum, it can be a local minimum only. To check whether it is a minimum or a maximum, we analyse the Hessian of $E_0(\Psi_2 = 0, \Psi_3 = 0)$. This gives the inequality

$$g_1 \leqslant \sqrt{\frac{\Delta\hbar\omega_1}{4} \frac{\left(1+\frac{4\kappa_1^2}{\hbar\omega_1^2}\right)\left(1+\frac{4\kappa_2^2}{\hbar\omega_2^2}\right) - \frac{16\kappa_3^4}{\hbar^2\omega_1^2\omega_2^2}}{1+\frac{4\kappa_2^2}{\hbar\omega_2^2} + \frac{\omega_1}{\omega_2}\chi_1^2\left(1+\frac{4\kappa_1^2}{\hbar\omega_1^2}\right) - \frac{8\kappa_3^2}{\hbar\omega_2^2}\chi_1\sqrt{\frac{\omega_2}{\omega_1}}}} \equiv g_{1,c}. \tag{3.8}$$

As long as this inequality is fulfilled, the normal state minimises the ground-state energy.

Analysing the Hessian of $E_0(\Psi_2 = 0, \Psi_3 = 0)$, we can check whether or not the normal state minimises the ground-state energy. However, we do not see if it is a global minimum of E_0. To see this, we need to check all critical points of E_0. We do this by numerical minimisation of the ground-state energy E_0. Fig. 3.1 shows the order parameters Ψ_2 and Ψ_3 obtained by this numerical procedure. Regions with both $\Psi_2 = 0$ and $\Psi_3 = 0$ correspond to the normal phase, whereas the superradiant phase is characterised by regions with $\Psi_2 > 0$ or $\Psi_3 > 0$. As is clear from Fig. 3.1, the system supports a normal and a superradiant phase.

If two thermodynamic phases are separated by a second-order phase transition, the order parameter (which is given by the mean-fields) characterising this phase transition is continuous across the phase boundary. However, numerical analysis indicates that it is not a continuous phase transition along the entire phase boundary and at a certain point the order parameters, e.g. Ψ_2, become discontinuous. This behaviour is shown in Fig. 3.2. Then, the phase transition is of *first* order. Consequently, the phase boundary separating the normal from the superradiant phase consists of two segments which characterise a second (solid green line in Fig. 3.1) and a first (dashed green line in Fig. 3.1)-order phase transition, respectively. These two segments meet in a single point (red ring in Fig. 3.1). The location of this point

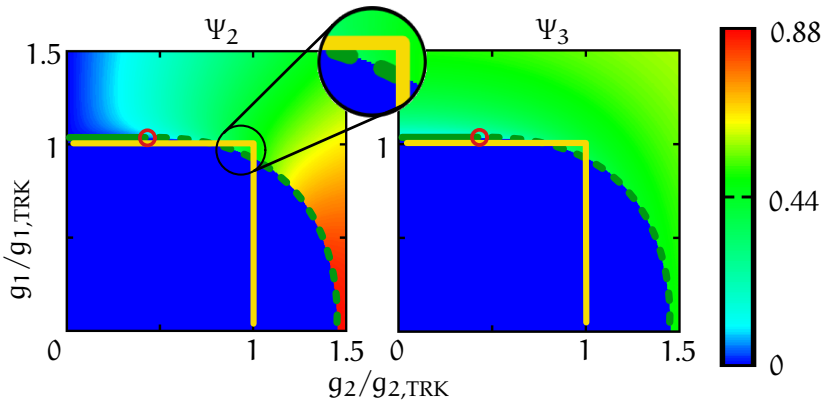

Figure 3.1: Mean-fields Ψ_2 and Ψ_3 for parameters $\delta = 0.1$, $\Delta = 1$, $\hbar\omega_1 = 0.5$, $\hbar\omega_2 = 0.6$, $\kappa_1 = \kappa_2 = 1$, $\kappa_3 = \sqrt{\varepsilon_1 \cdot \varepsilon_2}\kappa$, $\varepsilon_1 \cdot \varepsilon_2 = 0.5$, and $|\varepsilon_1 \cdot \mathbf{d}_{31}| = |\varepsilon_2 \cdot \mathbf{d}_{32}| = 1$. The green line gives the phase boundary and is separated into two segments: The solid (dashed) green line corresponds to a second (first)-order superradiant phase transition. The point where these two segments meet is marked with a red ring. The numerical value of g_1 for the boundary of the second-order phase transition is given by $1.03\, g_{1,\mathrm{TRK}}$ which coincides with the value obtained by an analytical analysis. The blue region below the green line in both diagrams represents the normal phase ($\psi_1 = 1$, $\Psi_2 = \Psi_3 = \varphi_1 = \varphi_2 = 0$). The complementary region corresponds to the superradiant phase where all mean-fields are finite. The accessible parameter region for atoms is indicated by the solid yellow box. The small inset clarifies that the superradiant phase is within this region. The couplings g_n are scaled with $g_{n,\mathrm{TRK}}$. These are the largest possible couplings for the analogous atomic model given by the Thomas–Reiche–Kuhn sum rule, Eq. (3.5). The diagrams for φ_1 and φ_2 look qualitatively the same as the diagram for Ψ_3. In addition, ψ_1 is obtained by using the relation $\psi_1 = \sqrt{1 - \Psi_2^2 - \Psi_3^2}$.

cannot be obtained by an analysis of stability of the normal phase. Likewise, we cannot derive an inequality analogous to Eq. (3.8) for g_2.

The continuous phase transition signals the breakdown of stability of the normal phase. Therefore, the phase boundary for the second-order phase transition is given by the value of g_1 where the inequality, Eq. (3.8), becomes an equation, i.e. for $g_1 = g_{1,c}$. Since $g_{1,c}$ does not depend on g_2, the phase boundary is a straight line. With the numerical values used to generate Fig. 3.1, $g_{1,c} = 1.03\, g_{1,\mathrm{TRK}}$ (dashed red line in Fig. 3.2), where $g_{1,\mathrm{TRK}}$ is given by Eq. (3.5). This is in perfect agreement with our numerical findings (see Fig. 3.1).

It is known (Viehmann, Delft, and Marquardt, 2011) that the critical coupling strength increases if the diamagnetic term proportional to κ increases. This becomes transparent, e.g., from the ground-state energy, Eq. (3.7), where the terms proportional to κ_1 (κ_2) are quadratic in φ_1 (φ_2) and thus increase the energy of the superradi-

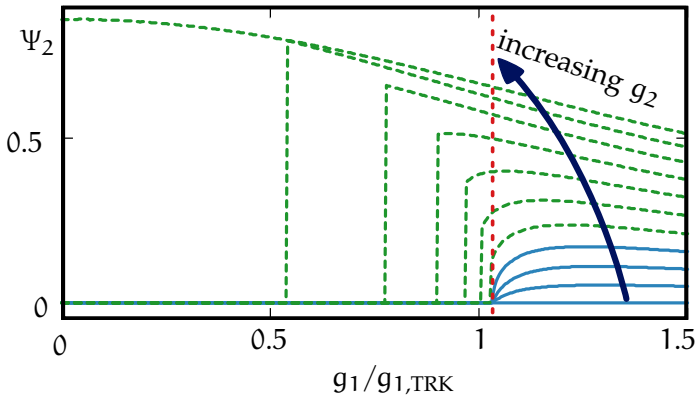

Figure 3.2: Mean-field Ψ_2 as a function of g_1 for different values of g_2, indicating the change of the order of the superradiant phase transition. The value of g_2 for each single line increases in direction of the arrow from 0 to 1.5 with an increment of 0.15. The other parameters are as in Fig. 3.1. In the range $0 \leqslant g_2 \leqslant 0.45$, Ψ_2 is continuous as a function of g_1 (solid blue lines), whereas for $g_2 \geqslant 0.6$, Ψ_2 is discontinuous (dashed green lines). The dashed red line marks the critical value for g_1 of Eq. (3.8) above which the normal phase is unstable and corresponds to the red ring in the top panel.

ant state. On the contrary, the parameters χ_n effectively give an additional contribution to the couplings g_n. Hence, larger parameters χ_n should lead to lower critical values of the coupling strengths. We have numerically computed the location of three points of the phase boundary for different values of $\kappa \equiv \kappa_1 = \kappa_2 = \kappa_3$ and $\chi \equiv \chi_1 = \chi_2$. This is shown in Fig. 3.3 and one clearly sees that an increase of κ leads to an increase of g_c as well, and that for large values of χ the critical coupling is lowered. We note that g_c as a function of χ decreases monotonically for $\kappa = 0$ only.

Concerning the atomic system, the couplings g_n are not arbitrary and cannot exceed a bound given by the Thomas–Reiche–Kuhn sum rule of Eqs. (3.5). These bounds are displayed by the solid yellow lines in Fig. 3.1. As can be seen in Fig. 3.1, this atomic system can in fact undergo a superradiant phase transition on the choice of the parameters. The numerical calculations show that this is a first-order phase transition. Indeed, combining the Thomas–Reiche–Kuhn sum rule for g_1, Eq. (3.5), with the stability criterion, Eq. (3.8), for the normal state, we see that in our model the normal state is stable for all $g_1 \leqslant g_{1,\mathrm{TRK}}$. Hence, concerning our model, the superradiant phase transition cannot be of second order. This is also in agreement with the results found for the single-mode model of Baksic, Nataf, and Ciuti (2013).

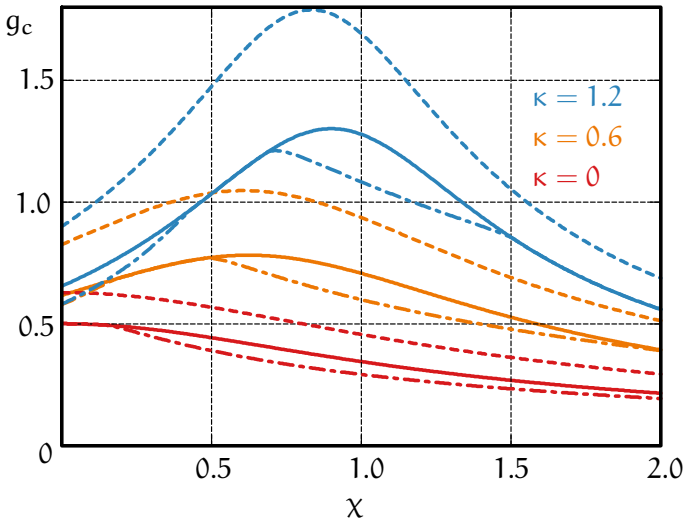

Figure 3.3: Critical coupling g_c at different points on the phase boundary as a function of $\chi \equiv \chi_1 = \chi_2$, and for different values of $\kappa \equiv \kappa_1 = \kappa_2 = \kappa_3$. The solid lines correspond to points on the phase boundary with $(g_1 = g_c, g_2 = 0)$, dashed lines to points with $(g_1 = 0, g_2 = g_c)$, and dashed dotted lines to points with $(g_1 = g_c, g_2 = g_c)$. The red lines correspond to $\kappa = 0$, the orange lines to $\kappa = 0.6$, and the blue lines to $\kappa = 1.2$. The remaining parameters are given by $\Delta = \hbar\omega_1 = 1$, $\delta = 0.1$, $\hbar\omega_2 = 0.9$.

3.4 SYMMETRIES

If one neglects the terms proportional to κ_n $(n = 1, 2, 3)$ and χ_n $(n = 1, 2)$, then the Hamiltonian, Eq. (3.1), commutes with the symmetry-operators $\hat{\Pi}'_n = \exp[-i\pi(-\hat{A}_n{}^n + \hat{a}_n^\dagger \hat{a}_n)]$, $(n = 1, 2)$. As was shown in Ch. 2, this gives rise to two superradiant states where a single bosonic mode is macroscopically occupied only (blue and red superradiant states), and either of the superradiant phases correspond to one broken symmetry. In contrast, including those terms, the symmetry operators do not commute with the Hamiltonian, Eq. (3.1), since

$$\hat{\Pi}'_n(\hat{a}_m^\dagger + \hat{a}_m)(\hat{a}_n^\dagger + \hat{a}_n)\hat{\Pi}'^\dagger_n = (\hat{a}_m^\dagger + \hat{a}_m)(\hat{a}_n^\dagger + \hat{a}_n) \times \begin{cases} -1 & : m \neq n, \\ +1 & : m = n. \end{cases} \tag{3.9}$$

Hence, the parities corresponding to the two branches of the Lambda-system are no conserved quantities anymore, since the term proportional to $(\hat{a}_1 + \hat{a}_1^\dagger)(\hat{a}_2 + \hat{a}_2^\dagger)$ *mixes* both bosonic modes. However, the operators

$$\hat{\Pi}_n = \exp\left[-i\pi\left(-\hat{A}_n{}^n + \hat{a}_1^\dagger \hat{a}_1 + \hat{a}_2^\dagger \hat{a}_2\right)\right] \quad (n = 1, 2) \tag{3.10}$$

do commute with the Hamiltonian, Eq. (3.1), and therefore this parity including both bosonic modes is conserved.

In the normal phase, both parities $\hat{\Pi}_1$, $\hat{\Pi}_2$ are conserved, whereas both parities are simultaneously broken in the superradiant phase. This loss of parity symmetry has a large impact on the phase diagram: in our numerical analysis, we obtain only one superradiant phase with both bosonic modes being macroscopically excited simultaneously (see Fig. 3.1). In addition, analytical calculations show that blue and red superradiant states are not stable. This is in contrast to the model without the terms proportional to κ_n and χ_n, where these superradiant states are the only superradiant phases and a state with both branches of the Lambda-system being simultaneously superradiant is not stable (cf. Ch. 2).

3.5 THE NO-GO THEOREM FOR SECOND-ORDER SUPERRADIANT PHASE TRANSITIONS

We consider the most general model of an ensemble of $\mathcal{N}$ multi-level atoms interacting with a *single* mode of a resonator. The Hamiltonian has the form

$$\hat{H} = \sum_{n=1}^{N} E_n \hat{A}_n^{\,n} + \hbar\omega \hat{a}^\dagger \hat{a} + \frac{\kappa^2}{\omega}(\hat{a}^\dagger + \hat{a})^2 + \sum_{n,m=1}^{N} \frac{1}{2}\frac{g_{n,m}}{\sqrt{N}}(\hat{A}_n^{\,m} + \hat{A}_m^{\,n})(\hat{a}^\dagger + \hat{a}). \quad (3.11)$$

Each of the $\mathcal{N}$ single atoms has N energy levels characterised by the non-degenerate energies $E_1 < E_2 < \ldots < E_N$. Populations of and transitions among the atomic energy levels are described by the collective operators $\hat{A}_n^{\,n}$ and $\hat{A}_n^{\,m}$, respectively. The frequency of the mode of the resonator is given by $\omega > 0$; the bosonic operator $\hat{a}^\dagger$ ($\hat{a}$) create (annihilate) a corresponding photon. The coupling of the transverse vector potential with the atoms is approximated by the dipole coupling, with coupling strength $g_{n,m} = g_{m,n}$, $g_{n,n} = 0$. The diamagnetic contribution is parameterised via the parameter κ. In deriving this Hamiltonian, we have neglected atom-atom and Coulomb interaction among different atoms.

The Thomas–Reiche–Kuhn sum rule [see Eq. (A.5)] of this model can be written in the form

$$\sum_{\substack{n=1 \\ n\neq m}}^{N} \frac{g_{n,m}^2}{E_{n,m}} \leqslant \frac{\kappa^2}{\omega}, \quad (3.12)$$

with $E_{n,m} = E_n - E_m$ and $m = 1, \ldots, N$. Note that in terms of oscillator strengths $f_{n,m} = \frac{g_{n,m}^2 \omega}{E_{m,n}\kappa^2}$, the Thomas–Reiche–Kuhn sum rule obtains the memorable form $\sum_n f_{n,m} = 1$.

Applying a Holstein–Primakoff transformation to the collective operators $\hat{A}_n^m$ and introducing mean-fields both for the atomic [Ψ_n, $(n = 2, \ldots, N)$] and for the photonic (φ) degrees of freedom, we obtain the ground-state energy per atom in the thermodynamic limit,

$$E_{GS} = E_1 + \sum_{n=2}^{N} E_{n,1}\Psi_n^2 + \left(\hbar\omega + 4\frac{\kappa^2}{\omega}\right)\varphi^2 + 2\varphi \sum_{n=2}^{N} \left(2g_{n,1}\sqrt{1 - \sum_{m=2}^{N} \Psi_m^2} + \sum_{m=2}^{N} g_{n,m}\Psi_m \right) \Psi_n. \quad (3.13)$$

Since we are only interested whether or not the normal state with $\Psi_n = \varphi = 0$ minimises the ground-state energy, Eq. (3.13), we expand the ground-state energy to second order in Ψ_n and φ. This yields

$$E_{GS} = E_1 + \sum_{n=2}^{N} E_{n,1}\Psi_n^2 + \left(\hbar\omega + 4\frac{\kappa^2}{\omega}\right)\varphi^2 + 4\sum_{n=2}^{\nu} g_{n,1}\Psi_n\varphi + \mathcal{O}(\Psi_n^3). \quad (3.14)$$

Because the ground-state energy has no terms linear in Ψ_n or φ, the normal state represents a critical point. In order to specify the type of the critical point, we calculate the Hessian of the ground-state energy, Eq. (3.14). We obtain

$$\frac{\partial^2 E_{GS}}{\partial\varphi^2} = 2\left(\hbar\omega + 4\frac{\kappa^2}{\omega}\right) + \mathcal{O}(\Psi_n^3), \quad (3.15)$$

$$\frac{\partial^2 E_{GS}}{\partial\Psi_m\,\partial\Psi_n} = 2E_{n,1}\delta_{n,m} + \mathcal{O}(\Psi_n), \quad (3.16)$$

and

$$\frac{\partial^2 E_{GS}}{\partial\varphi\,\partial\Psi_n} = 4g_{n,1} + \mathcal{O}(\Psi_n^2), \quad (3.17)$$

with $1 < n, m \leqslant N$. Hence, the Hessian for the normal state is given by

$$\mathbf{H}(E_{GS}, \Psi_n = 0, \varphi = 0) = 2\begin{pmatrix} \hbar\omega + 4\frac{\kappa^2}{\omega} & 2g_{2,1} & 2g_{3,1} & \ldots & 2g_{N-1,1} & 2g_{N,1} \\ 2g_{2,1} & E_{2,1} & 0 & \ldots & 0 & 0 \\ 2g_{3,1} & 0 & E_{3,1} & \ldots & 0 & 0 \\ \vdots & \vdots & \vdots & \ddots & \vdots & \vdots \\ 2g_{N-1,1} & 0 & 0 & \ldots & E_{N-1,1} & 0 \\ 2g_{N,1} & 0 & 0 & \ldots & 0 & E_{N,1} \end{pmatrix}. \quad (3.18)$$

Now we will proof that $\mathbf{H}$ is in fact positive definite which means that the critical point is a local minimum. Therefore, we compute the principal minors of $\mathbf{H}$. The k^{th} principal minor of a $n \times n$ matrix $\mathbf{M}$ is the determinant of the matrix where the first $n-k$ rows and columns of $\mathbf{M}$ are deleted. If all principal minors of a symmetric matrix are positive, then the matrix is positive definite. In the following we will show that all principal minors of $\mathbf{H}$ are positive.

One sees readily that the first $\nu - 1$ principal minors are positive since $E_{n,1}$ are positive by definition. Hence, we need to compute the ν^{th} principal minor which is the determinant of $\mathbf{H}$ itself. This is done by reducing $\mathbf{H}$ to a triangular matrix using elementary row operations. Eventually, this gives

$$\frac{1}{2}\mathrm{Det}\big[\mathbf{H}\big(E_{GS}, \Psi_n = 0, \varphi = 0\big)\big] = \begin{vmatrix} X & 0 & 0 & \dots & 0 & 0 \\ 2g_{2,1} & E_{2,1} & 0 & \dots & 0 & 0 \\ 2g_{3,1} & 0 & E_{3,1} & \dots & 0 & 0 \\ \vdots & \vdots & \vdots & \ddots & \vdots & \vdots \\ 2g_{\nu-1,1} & 0 & 0 & \dots & E_{\nu-1,1} & 0 \\ 2g_{\nu,1} & 0 & 0 & \dots & 0 & E_{\nu,1} \end{vmatrix}, \tag{3.19}$$

where $X = \hbar\omega + 4\frac{\kappa^2}{\omega} - 4\sum_{n=2}^{\nu} \frac{g_{n,1}^2}{E_{n,1}}$. Applying the Thomas–Reiche–Kuhn sum rule, Eq. (3.12), with $m = 1$, we obtain

$$X \geqslant \hbar\omega \tag{3.20}$$

which is always positive. Since the determinant of a triangular matrix is the product of its diagonal elements, the determinant of the Hessian for the normal state is positive. Hence we have shown that all principal minors are positive. Consequently, the Hessian is positive definite. This means that the normal state minimises the ground-state energy irrespective of the parameters of the Hamiltonian and no additional states, i.e. superradiant states, can evolve from the normal state continuously. Thus, no continuous, i.e. second-order, phase transitions are possible. However, this argument does not apply to first-order phase transitions and we can not say whether or not first-order phase transition can occur. In addition, a second-order superradiant phase transition originating from a superradiant phase which results from a first-order superradiant phase transition is also not covered by our analysis. We also note that a superradiant phase where a single one-particle energy level is macroscopically occupied only, can be excluded by a similar argument as presented above.

3.6 CONCLUSION

In this chapter, we have presented a generalised Dicke model of particles with three energy-levels in Lambda-configuration coupled to two bosonic modes where the microscopic Hamiltonian contains a diamagnetic term. We showed that this system exhibits a superradiant quantum phase transition in the thermodynamic limit. This phase transition can be both of first and of second order and we analytically derived the critical coupling strength for the second-order phase transition. Quantitatively, the whole phase diagram was obtained using numerical methods. Compared to the model without the diamagnetic term we have studied in Ch. 2, the phase diagram has one superradiant phase only. The loss of the second superradiant phase is directly connected to the diamagnetic term since it changes the parity symmetry of the Hamiltonian.

In addition, we mapped this abstract model to an atomic system interacting with two photonic modes of a resonator and showed by numerical calculations that the superradiant phase transition persists. We emphasise that the microscopic Hamiltonian includes diamagnetic contributions and that this model respects the Thomas–Reiche–Kuhn sum rule which gives bounds for the coupling strengths. This is in stark contrast to Hopfield-like-models, where the combination of the diamagnetic contribution and the sum rule suppresses the superradiant phase transition. Thus, compared to the Dicke-model with diamagnetic terms included and its generalisations (VIEHMANN, DELFT, and MARQUARDT, 2011), no no-go theorem exists in our model. However, we showed that the superradiant phase transition is of first order.

In experiments, our model would be realised by atoms, if they can be reduced to three-level systems in Lambda-configuration. In addition, the dipole matrix element $\mathbf{d}_{31}$ ($\mathbf{d}_{32}$) must not be orthogonal to the polarisation vector $\boldsymbol{\varepsilon}_2$ ($\boldsymbol{\varepsilon}_1$) of the two modes of the resonator.

In the paper of BAKSIC, NATAF, and CIUTI (2013) a similar model is discussed. They consider atoms in a general three-level-configuration, which are coupled to one mode of a resonator. Including a diamagnetic contribution in the Hamiltonian and respecting the Thomas–Reiche–Kuhn sum rule, they find a superradiant quantum phase transition. Thus, no no-go theorem exists in their model either. In particular for the Lambda-configuration, this phase transition is always of first order. This agrees with our results.

In addition, we have considered the most general model of multilevel atoms interacting with a *single* mode of a resonator which obey the Thomas–Reiche–Kuhn sum rule. We have shown that the normal state, the state where all atoms occupy their respective ground state and in the resonator no photon is excited, does always minimise the ground-state energy. Hence the normal phase is stable irrespective of

the parameters of the system and no second-order phase transition to superradiant phases are possible.

There is one point we want to remark: theoretically, the Dicke-model (i.e. a Hopfield-like-model without the diamagnetic term) supports a second-order phase transition (Hepp and Lieb, 1973b,a; Wang and Hioe, 1973; Carmichael, Gardiner, and Walls, 1973; Emary and Brandes, 2003a). The no-go theorem (Rzażewski, Wódkiewicz, and Żakowicz, 1975; Nataf and Ciuti, 2010a; Viehmann, Delft, and Marquardt, 2011) applies to these continuous phase transitions only. Hence, first-order phase transitions could in principle still provide a superradiant phase.

4

THERMODYNAMICS OF THE LAMBDA-MODEL

Parts of this Chapter appear in the publication:

HAYN, Mathias and Tobias BRANDES (2017): *Thermodynamics and superradiant phase transitions in a three-level Dicke model*, Phys. Rev. E **95**, p. 012153. DOI: 10.1103/PhysRevE.95.012153.

The finite-temperature phase transition in the Dicke model was first studied by HEPP and LIEB (1973b) and WANG and HIOE (1973). In fact, they considered the Tavis–Cummings model. i. e. the Dicke model in the rotating-wave approximation. Shortly after that, HEPP and LIEB (1973a), CARMICHAEL, GARDINER, and WALLS (1973), and HIOE (1973) relaxed this limitation and took the counter-rotating terms into account as well.

In this chapter, the finite-temperature phase transition of the Dicke model is addressed. We first give a review of the phase transition of the original Dicke model. Here the presentation follows the lines of WANG and HIOE (1973) and CARMICHAEL, GARDINER, and WALLS (1973). Then we study the finite-temperature phase transition in the Lambda-model.

4.1 FINITE-TEMPERATURE PHASE TRANSITION: DICKE MODEL

The Hamiltonian of the Dicke model is given by

$$\hat{H} = \Delta \hat{J}_z + \hbar\omega \hat{a}^\dagger \hat{a} + \frac{g}{\sqrt{N}}(\hat{a}^\dagger + \hat{a})(\hat{J}_+ + \hat{J}_-). \tag{4.1}$$

For the meaning of the terms and parameters, refer to the introduction, Sec. 1.2.1. The following calculation becomes more transparent, if we expand the collective spin operators $\hat{J}_n$ as (cf. Sec. 1.3.1)

$$\hat{J}_n = \sum_{k=1}^{N} \hat{s}_n^{(k)}, \qquad n \in \{x, y, z, +, -\}. \tag{4.2}$$

Here, $\hat{s}_n^{(k)}$ is the n^{th} component of the spin operator of the k^{th} particle, cf. (1.109) in Sec. 1.3.1. Using this expansion, the above Hamiltonian assumes the form

$$\hat{H} = \Delta \sum_{k=1}^{N} \hat{s}_z^{(k)} + \hbar\omega \hat{a}^\dagger \hat{a} + \frac{g}{\sqrt{N}}(\hat{a}^\dagger + \hat{a}) \sum_{k=1}^{N} \left(\hat{s}_+^{(k)} + \hat{s}_-^{(k)} \right). \tag{4.3}$$

All thermodynamic information of the equilibrium system is contained in the (canonical) partition sum (FEYNMAN, 1972)

$$Z = Z(N, T) = \mathrm{Tr}\{e^{-\beta \hat{H}}\}, \tag{4.4}$$

where the trace ranges over all degrees of freedom of the quantum system. Here, $\beta = 1/(k_B T)$ is the inverse temperature. In order to evaluate the trace, we have to choose a basis or rather a set of quantum numbers. It is understood that the basis must be complete or the set of operators has to form a complete set of commuting observables, respectively. A convenient choice for the spin degrees of freedom is a direct product of single-spin basis states $|m\rangle$; for the bosonic field we take Glauber's coherent states $|\alpha\rangle$ ($\alpha \in \mathbb{C}$) which are eigenstates of the annihilation operator (Glauber, 1963; Arecchi et al., 1972; Nussenzveig, 1973). Then the trace is evaluated as

$$\mathcal{Z} = \sum_{m_1=\pm 1} \cdots \sum_{m_{\mathcal{N}}=\pm 1} \int_{\mathbb{C}} \frac{d^2\alpha}{\pi} \langle m_1 \dots m_{\mathcal{N}}; \alpha | e^{-\beta \hat{H}} | m_1 \dots m_{\mathcal{N}}; \alpha \rangle \,. \tag{4.5}$$

The integration goes over the complex plane and $\int_{\mathbb{C}} d^2\alpha$ stands for $\int_{\mathbb{R}} d(\mathrm{Re}\{\alpha\}) \int_{\mathbb{R}} d(\mathrm{Im}\{\alpha\})$.

Since $|\alpha\rangle$ is an eigenket of the annihilation operator $\hat{a}$ with eigenvalue α, the bosonic part of the expectation values is easily calculated,

$$\mathcal{Z} = \int_{\mathbb{C}} \frac{d^2\alpha}{\pi} e^{-\beta \hbar \omega \alpha^* \alpha} \prod_{k=1}^{\mathcal{N}} \left[\sum_{m_k=\pm 1} \langle m_k | e^{-\beta \hat{h}^{(k)}(\alpha^*, \alpha)} | m_k \rangle \right], \tag{4.6}$$

with the single-particle Hamiltonian

$$\hat{h}^{(k)}(\alpha^*, \alpha) = \Delta \hat{s}_z^{(k)} + \frac{g}{\sqrt{\mathcal{N}}} \left(\alpha^* + \alpha \right) \left(\hat{s}_+^{(k)} + \hat{s}_-^{(k)} \right). \tag{4.7}$$

As the Dicke model describes an interacting system, the Hamiltonian consists of non-commuting parts. Therefore, the above factorisation of the exponential is in general not valid. However, everything is fine in the thermodynamic limit, $\mathcal{N} \to \infty$.

The sum in the squared brackets of Eq. (4.6) is a representation of the trace of the single-particle degrees of freedom. Moreover, the trace does not depend on the specific particle. Hence, the partition sum factorises and can be written as

$$\mathcal{Z} = \int_{\mathbb{C}} \frac{d^2\alpha}{\pi} e^{-\beta \hbar \omega \alpha^* \alpha} \, \mathrm{Tr}\left\{ e^{-\beta \hat{h}(\alpha^*, \alpha)} \right\}^{\mathcal{N}}. \tag{4.8}$$

The remaining single-particle trace is evaluated in the eigenbasis of the single-particle Hamiltonian

$$\hat{h}(\alpha^*, \alpha) = \begin{pmatrix} \frac{\Delta}{2} & \frac{g}{\sqrt{\mathcal{N}}} \left(\alpha^* + \alpha \right) \\ \frac{g}{\sqrt{\mathcal{N}}} \left(\alpha^* + \alpha \right) & -\frac{\Delta}{2} \end{pmatrix}, \tag{4.9}$$

where we have explicitly written out the matrices for the spin operators.

Then, the trace of the exponential operator in Eq. (4.8) is the sum of the exponentials of the eigenvalues of the operator. Thus, it suffices to know the eigenvalues of $\hat{h}(\alpha^*, \alpha)$; these are given by

$$\varepsilon_\pm = \pm\frac{\Delta}{2}\sqrt{1+\frac{4g^2}{\Delta^2\mathcal{N}}\left(\alpha^*+\alpha\right)^2}. \tag{4.10}$$

With this, we can sum up the particle-part of the partition sum,

$$\mathcal{Z} = \int_C \frac{d^2\alpha}{\pi}\, e^{-\beta\hbar\omega\alpha^*\alpha}\left[2\cosh\left(\frac{\beta\Delta}{2}\sqrt{1+\frac{4g^2}{\Delta^2\mathcal{N}}\left(\alpha^*+\alpha\right)^2}\right)\right]^{\mathcal{N}}. \tag{4.11}$$

The last step is to evaluate the bosonic part of the partition sum. This cannot be done exactly. But, instead of computing the integral numerically, we can approximate the integral for large $\mathcal{N}$ by Laplace's method (saddle point approximation) (Bender and Orszag, 1999; Jänich, 2001). First we decompose α in its real and imaginary part as

$$\alpha = x + ip,\ \alpha^* = x - ip, \tag{4.12}$$

$$\mathrm{Re}\{\alpha\} = x = \frac{1}{2}(\alpha+\alpha^*),\ \mathrm{Im}\{\alpha\} = p = \frac{1}{2i}(\alpha-\alpha^*), \tag{4.13}$$

$$d^2\alpha = dx\, dp. \tag{4.14}$$

In addition, we scale x and p with the number $\mathcal{N}$ of particles,

$$y = x/\sqrt{\mathcal{N}},\ z = p/\sqrt{\mathcal{N}}. \tag{4.15}$$

With these definitions, the partition sum can be written as

$$\mathcal{Z} = \frac{\mathcal{N}}{\pi}\int_{\mathbb{R}} dy \int_{\mathbb{R}} dz\, e^{-\mathcal{N}f(y,z)}, \tag{4.16}$$

where $f(y,z)$ in the exponential reads

$$f(y,z) = \beta\hbar\omega(y^2+z^2) - \ln\left[2\cosh\left(\frac{\beta\Delta}{2}\sqrt{1+16g^2y^2/\Delta^2}\right)\right]. \tag{4.17}$$

From the form of the integral in Eq. (4.16), it is clear that for large $\mathcal{N}$ the main contribution to the integral is given by the minima of $f(y,z)$. Larger values of $f(y,z)$ are exponential suppressed with respect to the values of the minima of $f(y,z)$. This is the essence of the *saddle point* or *Laplace's approximation*.

Since z enters only quadratically in $f(y,z)$, the minima are located on the z axis, i. e. $z = 0$. Minimisation with respect to y leads to the equation

$$0 = y\left[\left(\frac{g_c}{g}\right)^2\Omega(y) - \tanh\left[\frac{\beta\Delta}{2}\Omega(y)\right]\right], \tag{4.18}$$

with

$$\Omega(y) = \sqrt{1+\frac{4\hbar\omega}{\Delta}\left(\frac{g}{g_c}\right)^2 y^2} \tag{4.19}$$

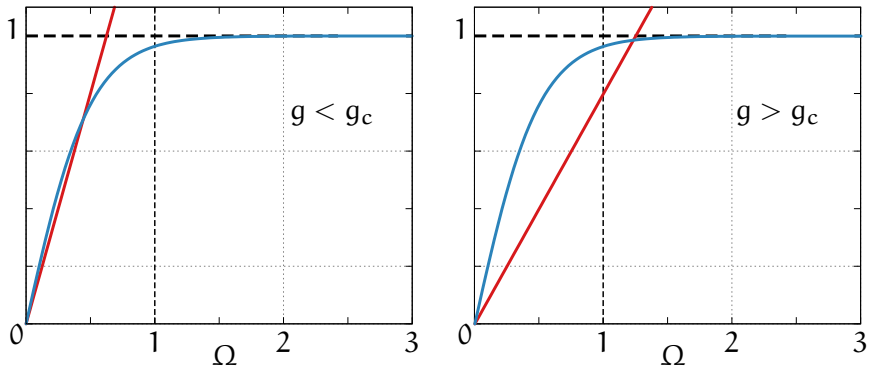

Figure 4.1: Graphical solution of Eq. (4.18) for $g < g_c$ (left) and $g > g_c$ (right) for fixed temperature and finite y. The red straight line corresponds to the first term, $(\frac{g_c}{g})^2\Omega(y)$, the other blue curved line corresponds to the tanh term of Eq. (4.18). Of physical relevance is the region $\Omega > 1$ only. Thus, no meaningful solution exists for $g < g_c$, whereas for $g > g_c$ exactly one solution exists.

and

$$g_c = \frac{\sqrt{\hbar\omega\Delta}}{2}. \tag{4.20}$$

Since $\tanh(x)$ is bounded by 1 and $\Omega(y) \geqslant 1$, Eq. (4.18) is solved for $g < g_c$ by $y = 0$ only, see left part of Fig. 4.1. Contrary for $g > g_c$, non-trivial solutions of Eq. (4.18) can exist, depending on the value of β, i. e. on the temperature T, see right part of Fig. 4.1. In the limit $\beta \gg \Delta$ the hyperbolic tangent is one. Thus for $g > g_c$ and large β, or small T, Eq. (4.18) always has two solutions. Since $\lim_{y\to\infty} f(y, z) \to +\infty$, the non-trivial solution corresponds to a global minimum and the solution $y = 0$ corresponds to a local maximum of f. Hence, the non-trivial solution defines the state of the system in this parameter regime.

We emphasise that if a non-trivial solution exists, than this solution is unique. This is because both, the hyperbolic tangent and its derivative, are monotonous functions.

To find the smallest value of β for which Eq. (4.18) still gives a non-trivial solution, we have to consider the point where the vertical thick dashed grid line in Fig. 4.1 intersects with the tangent hyperbolic, i. e. the smallest attainable value of the tangent hyperbolic. Hence, Eq. (4.18) with $\Omega = 1$ or $y = 0$ needs to be solved,

$$\frac{g}{g_c} = \frac{1}{\sqrt{\tanh\left(\frac{\beta\Delta}{2}\right)}}. \tag{4.21}$$

This curve defines the phase boundary $g_c(T)$ between the normal ($y = 0$) and the superradiant ($y \neq 0$) phase [cf. Eq. (1.128)]. The corresponding phase diagram is shown in Fig. 4.2.

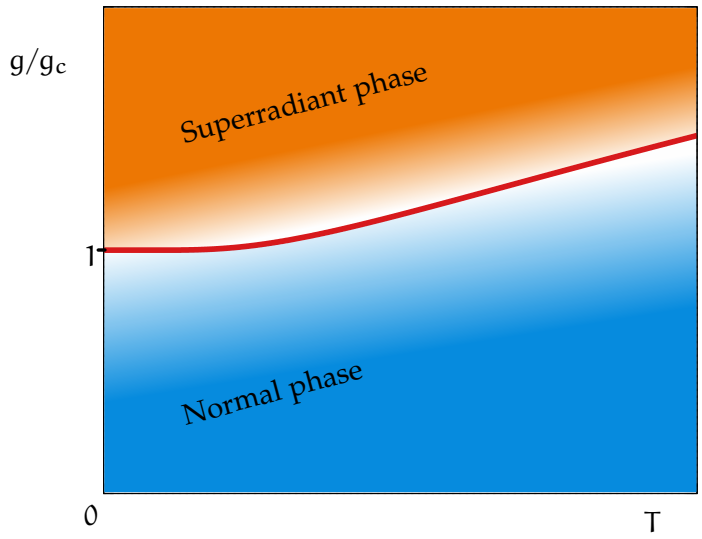

Figure 4.2: Finite-temperature phase diagram of the Dicke model. The superradiant phase exists for all temperatures. High coupling strengths g are needed, though. The phase boundary is parametrised by Eq. (4.21).

To find the value of y_0 which minimises the exponent of the integral of the partition sum, we have so solve Eq. (4.18) numerically, or directly minimise the function $f(y, z)$, Eq. (4.17).

4.1.1 *Expectation Values of Mode Operators*

Mean or expectation values of functions $G(\hat{a}^\dagger, \hat{a})$ of the creation and annihilation operators of the resonator mode only, are calculated in the same manner as the partition sum,

$$\langle G(\hat{a}^\dagger, \hat{a})\rangle = \frac{1}{\mathcal{Z}} \mathrm{Tr}\{G(\hat{a}^\dagger, \hat{a})\, e^{-\beta \hat{H}}\} \tag{4.22}$$

$$= \frac{1}{\mathcal{Z}} \int_{\mathbb{C}} \frac{d^2\alpha}{\pi} G(\alpha^*, \alpha) e^{-\beta\hbar\omega\alpha^*\alpha}\, \mathrm{Tr}\{e^{-\beta \hat{h}(\alpha^*,\alpha)}\}^{\mathcal{N}} \tag{4.23}$$

$$= \frac{1}{\mathcal{Z}} \frac{\mathcal{N}}{\pi} \int_{\mathbb{R}} dy\, G(\sqrt{\mathcal{N}}y, \sqrt{\mathcal{N}}y)\, e^{-\mathcal{N} f(y,0)}. \tag{4.24}$$

In the integrand, the exponential dominates for large $\mathcal{N}$. Hence, the function G can be considered constant and the remaining integral is equal to the partition sum. So we have

$$\langle G(\hat{a}^\dagger, \hat{a})\rangle = G(\sqrt{\mathcal{N}}y_0, \sqrt{\mathcal{N}}y_0). \tag{4.25}$$

For example, the expectation value of the number of excitations in the mode of the resonator is given by $\langle \hat{a}^\dagger \hat{a}\rangle = \mathcal{N} y_0^2$. By finding the minimum of $f(y, z)$ of Eq. (4.17) numerically, we obtain y_0 and therefore $\langle \hat{a}^\dagger \hat{a}\rangle$ which is shown in Fig. 4.3.

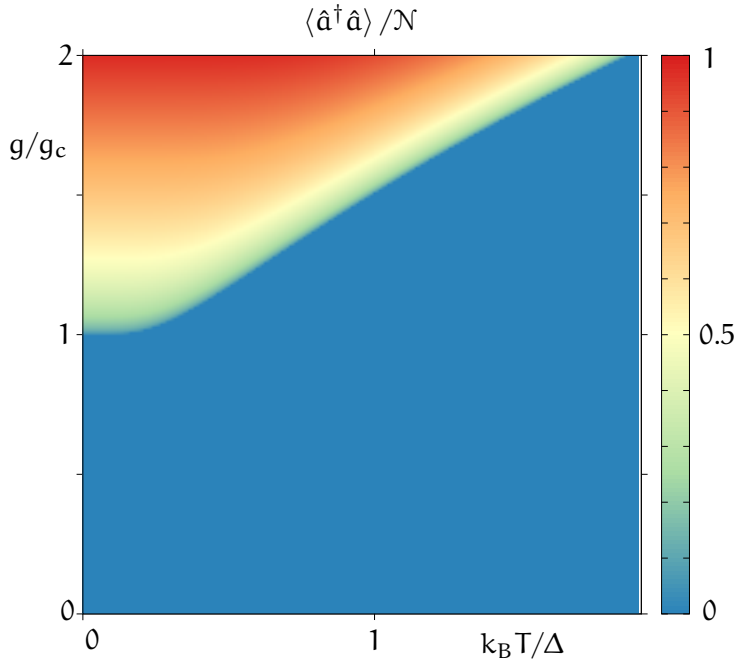

Figure 4.3: Numerical computation of the scaled occupation $\langle \hat{a}^\dagger \hat{a} \rangle / \mathcal{N}$ of the mode of the resonator in the Dicke model, with $\Delta = 1$ and $\hbar\omega = 1$. The units of $\langle \hat{a}^\dagger \hat{a} \rangle$ are arbitrary. The computation has been done in the thermodynamic limit using Laplace's method.

4.1.2 *Expectation Values of Particle Operators*

Expectation values of collective particle degrees of freedom can be calculated in a similar manner. Let $\hat{M}$ be a collective many-particle operator and $\hat{m}^{(n)}$ the corresponding single-particle operator for the n^{th} particle, such that

$$\hat{M} = \sum_{n=1}^{\mathcal{N}} \hat{m}^{(n)}. \tag{4.26}$$

The mean value of $\hat{M}$ is then given by

$$\langle \hat{M} \rangle = \frac{1}{\mathcal{Z}} \mathrm{Tr}\{\hat{M} e^{-\beta \hat{H}}\} \tag{4.27}$$

$$= \frac{1}{\mathcal{Z}} \int_C \frac{d^2\alpha}{\pi} e^{-\beta\hbar\omega\alpha^*\alpha} \sum_{n=1}^{\mathcal{N}} \mathrm{Tr}\left\{ \hat{m}^{(n)} e^{-\beta \hat{h}^{(1)}} \cdot \ldots \cdot e^{-\beta \hat{h}^{(\mathcal{N})}} \right\} \tag{4.28}$$

$$= \frac{1}{\mathcal{Z}} \int_C \frac{d^2\alpha}{\pi} e^{-\beta\hbar\alpha^*\alpha} \mathrm{Tr}\{e^{-\beta\hat{h}}\}^{\mathcal{N}} \mathcal{N} \frac{\mathrm{Tr}\left\{ \hat{m}\, e^{-\beta\hat{h}} \right\}}{\mathrm{Tr}\{e^{-\beta\hat{h}}\}} \tag{4.29}$$

$$= \mathcal{N} \frac{\mathrm{Tr}\left\{ \hat{m}\, e^{-\beta\hat{h}(y_0)} \right\}}{\mathrm{Tr}\{e^{-\beta\hat{h}(y_0)}\}}, \tag{4.30}$$

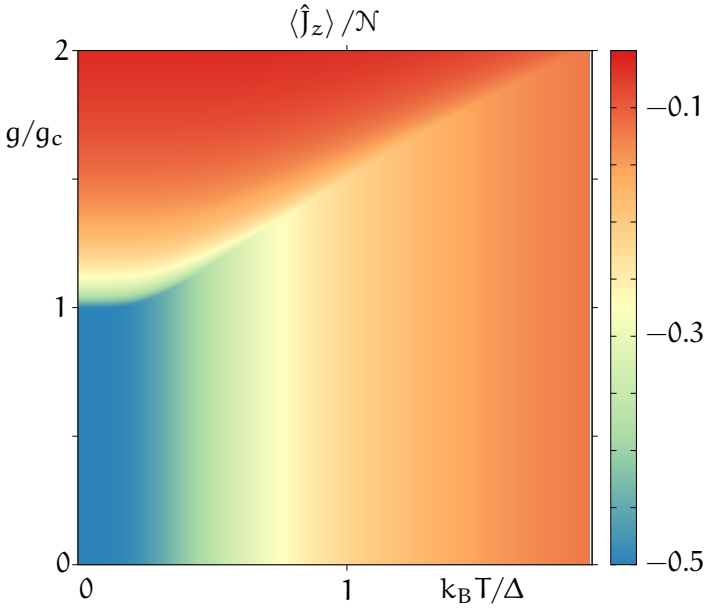

Figure 4.4: Numerical computation of $\langle \hat{J}_z \rangle / \mathcal{N}$ in the Dicke model, with parameters as in Fig. 4.3.

with $\hat{h}^{(n)} = \hat{h}^{(n)}(\alpha^*, \alpha)$ from Eq. (4.7), $\hat{h} = \hat{h}(\alpha^*, \alpha)$ from Eq. (4.9), and $\hat{h}(y_0) = \hat{h}(\sqrt{\mathcal{N}} y_0, \sqrt{\mathcal{N}} y_0)$. The single-particle operator $\hat{m}$ and the traces in the last two lines of the above equations refer to *any* particle. This is because the particle are identical and the coupling to the mode of the resonator is homogeneous.

In conclusion, the many-particle expectation value $\langle \hat{M} \rangle$ is given by $\mathcal{N}$ times the single-particle expectation value $\langle \hat{m} \rangle$ evaluated using the Hamiltonian $\hat{h}(y_0)$. Thus, to compute the expectation value, we need to know y_0 from the minimisation procedure, which, in general, is obtained by a numerical computation.

For relevance regarding the superradiant phase transition in the Dicke model are the collective operators $\hat{J}_z$ and $\hat{J}_x$. The expectation values of both operators can be evaluated explicitly for the Dicke model,

$$\langle \hat{J}_z \rangle = -\frac{\mathcal{N}}{2} \frac{\tanh\left[\frac{\beta\Delta}{2}\Omega(y_0)\right]}{\Omega(y_0)}, \quad \langle \hat{J}_x \rangle = \frac{4gy_0}{\Delta} \langle \hat{J}_z \rangle, \tag{4.31}$$

with $\Omega(y_0)$ from Eq. (4.19). In the normal phase with $y_0 = 0$ and consequently $\Omega(y_0) = 1$, these expectation values reduce to

$$\langle \hat{J}_z \rangle_n = -\frac{\mathcal{N}}{2} \tanh\left[\frac{\beta\Delta}{2}\right], \quad \langle \hat{J}_x \rangle_n = 0. \tag{4.32}$$

In Fig. 4.4 we show $\langle \hat{J}_z \rangle$ as a function of the coupling strength g and temperature T. At $g = g_c$, the phase transition is clearly visible.

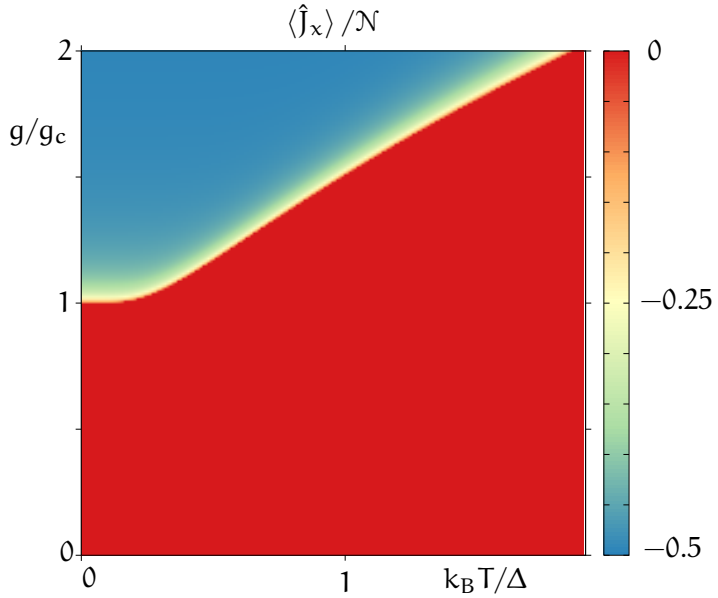

Figure 4.5: Numerical computation of $\langle \hat{J}_x \rangle / \mathcal{N}$ in the Dicke model, with parameters as in Fig. 4.3.

In addition, for low temperatures, the particles occupy their respective ground states, i. e. the collective spin points downwards. In the normal phase, for increasing temperature, more and more particles get excited, resulting in an increase of $\langle \hat{J}_z \rangle$. We note that in the superradiant phase, $\langle \hat{J}_z \rangle$ is rather insensitive with respect to the temperature T, whereas in the normal phase it is independent of the coupling strength g, see Eq. (4.32)

In Fig. 4.5, $\langle \hat{J}_x \rangle$ is shown. Again, the two phase are clearly visible, where the normal phase is characterised by vanishing $\langle \hat{J}_x \rangle$ and the superradiant phase shows finite values for $\langle \hat{J}_x \rangle$. We note that $\langle \hat{J}_x \rangle$ is rather insensitive to T.

4.1.3 *The Free Energy*

The last thermodynamic quantity we want to discuss is the free energy F. In statistical physics, the free energy is given by (Feynman, 1972)

$$F = -k_B T \ln \mathcal{Z}. \tag{4.33}$$

In the thermodynamic limit, this definition is equivalent to the definition, Eq. (1.129), of thermodynamics. By Laplace's method, the partition sum $\mathcal{Z}$ reads

$$\mathcal{Z} = c\, e^{-\mathcal{N} f(y_0, 0)} \tag{4.34}$$

in the thermodynamic limit. Here, c is constant of order $\mathcal{N}^{1/2}$ which stems from the Gaussian integration done in Laplace's method (Ben-

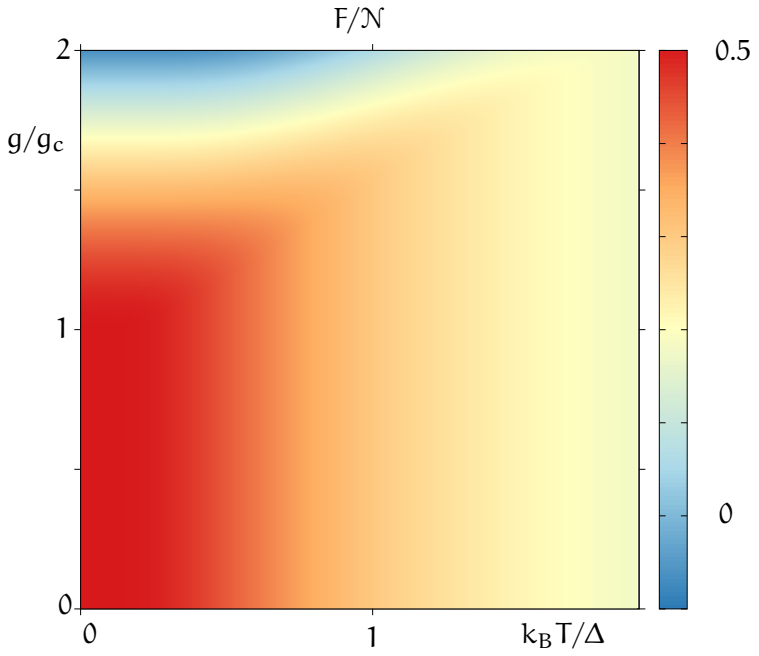

Figure 4.6: Numerical computation of the free energy per particle in the Dicke model, with parameters as in Fig. 4.3. The units of F are arbitrary.

DER and ORSZAG, 1999; JÄNICH, 2001). Hence, the leading contribution to the free energy is given by

$$F = \mathcal{N} k_B T f(y_0, 0) \tag{4.35}$$

and we can interpret $k_B T f(y_0, 0)$ as the free energy per particle. We use Eq. (4.35) to compute the free energy numerically. The free energy for the Dicke model in the thermodynamic limit is shown in Fig. 4.6.

4.1.4 *The Zero-Temperature Limit*

We end this section of the thermodynamics of the superradiant phase transition of the Dicke model by considering the limit of ultra-cold temperatures, $\beta \to \infty$, i. e. the quantum limit. Then, Eq. (4.18) can be solved for y_0 exactly and yields the result

$$y_0 = \pm \frac{g}{\hbar\omega} \sqrt{1 - \left(\frac{g_c}{g}\right)^4}. \tag{4.36}$$

Taking into account the findings of Eq. (4.25), we can identify y_0 with $\langle \hat{a} \rangle = \langle \hat{a}^\dagger \rangle$ which is equal to φ of Eq. (1.133).

The results for the expectation values of $\hat{J}_z$ and $\hat{J}_x$, Eq. (4.31) read in the zero-temperature limit

$$\langle \hat{J}_z \rangle = -\frac{\mathcal{N}}{2}\frac{1}{\Omega(y_0)} = -\frac{\mathcal{N}}{2}\left(\frac{g_c}{g}\right)^2 \tag{4.37}$$

and

$$\langle \hat{J}_x \rangle = 4\frac{g y_0}{\Delta}\frac{\mathcal{N}}{2}\left(\frac{g_c}{g}\right)^2 = \mp\frac{\mathcal{N}}{2}\sqrt{1-\left(\frac{g_c}{g}\right)^4} \tag{4.38}$$

Hence, we reproduce the findings of Eqs. (1.149), (1.155), and (1.156) of the quantum phase transition of the Dicke model analysed in Sec. 1.3.3.3.

Having analysed the original Dicke model at finite temperatures, we proceed to study the Lambda-model at non-zero temperatures.

4.2 FINITE-TEMPERATURE PHASE TRANSITION: LAMBDA-MODEL

In this section we apply and generalise the methods of the previous section to the Lambda-model. The Hamiltonian is given by

$$\begin{aligned}\hat{H} = {} & \delta \hat{A}_2^{\,2} + \Delta \hat{A}_3^{\,3} + \hbar\omega_1 \hat{a}_1^\dagger \hat{a}_1 + \hbar\omega_2 \hat{a}_2^\dagger \hat{a}_2 \\ & + \frac{g_1}{\sqrt{\mathcal{N}}}(\hat{a}_1^\dagger + \hat{a}_1)(\hat{A}_1^{\,3} + \hat{A}_3^{\,1}) + \frac{g_2}{\sqrt{\mathcal{N}}}(\hat{a}_2^\dagger + \hat{a}_2)(\hat{A}_2^{\,3} + \hat{A}_3^{\,2}).\end{aligned} \tag{4.39}$$

As in the calculation of the Dicke model, Sec. 4.1, we expand the collective particle operators $\hat{A}_n^{\,m}$ in single-particle operators $\hat{a}_{n,m}^{(k)}$ (cf. Sec. A.2),

$$\hat{A}_n^{\,m} = \sum_{k=1}^{\mathcal{N}} \hat{a}_{n,m}^{(k)}. \tag{4.40}$$

The operator $\hat{a}_{n,m}^{(k)}$ acts on the degrees of freedom of the k^{th} particle and can be represented by

$$\hat{a}_{n,m}^{(k)} = |n\rangle^{(k)} \langle m|\,. \tag{4.41}$$

In terms of these single-particle operators, the Hamiltonian, Eq. (4.39), of the Lambda-model is given by

$$\begin{aligned}\hat{H} = {} & \delta \sum_{k=1}^{\mathcal{N}} \hat{a}_{2,2}^{(k)} + \Delta \sum_{k=1}^{\mathcal{N}} \hat{a}_{3,3}^{(k)} + \hbar\omega_1 \hat{a}_1^\dagger \hat{a}_1 + \hbar\omega_2 \hat{a}_2^\dagger \hat{a}_2 \\ & + \frac{g_1}{\sqrt{\mathcal{N}}}(\hat{a}_1^\dagger + \hat{a}_1) \sum_{k=1}^{\mathcal{N}} (\hat{a}_{1,3}^{(k)} + \hat{a}_{3,1}^{(k)}) \\ & + \frac{g_2}{\sqrt{\mathcal{N}}}(\hat{a}_2^\dagger + \hat{a}_2) \sum_{k=1}^{\mathcal{N}} (\hat{a}_{2,3}^{(k)} + \hat{a}_{3,2}^{(k)})\end{aligned} \tag{4.42}$$

Again, the central quantity is the partition sum. It is given by

$$\mathcal{Z} = \mathrm{Tr}\{\mathrm{e}^{-\beta\hat{\mathrm{H}}}\} \tag{4.43}$$

$$= \int_{\mathbb{C}} \frac{\mathrm{d}^2\alpha_1}{\pi} \int_{\mathbb{C}} \frac{\mathrm{d}^2\alpha_2}{\pi} \langle\alpha_1, \alpha_2| \left(\prod_{n=1}^{\mathcal{N}} \mathrm{Tr}_n \right) \mathrm{e}^{-\beta\hat{\mathrm{H}}} |\alpha_1, \alpha_2\rangle \,. \tag{4.44}$$

Here, we have already replaced the trace over the bosonic degrees of freedom with two integrals over coherent states (α_1, α_2) and the remaining trace over the particle degrees of freedom has been split into traces over single-particle states. Now, in complete analogy to the steps done for the calculation of the partition sum of the Dicke model, we evaluate the expectation value of the bosonic degrees of freedom. The trace over the particle degrees of freedom factorises as before and we are left with the partition sum

$$\mathcal{Z} = \int_{\mathbb{C}^2} \frac{\mathrm{d}^2\alpha_1 \mathrm{d}^2\alpha_2}{\pi^2} \, \mathrm{e}^{-\beta \sum_{n=1}^{2} \hbar\omega_n |\alpha_n|^2} \mathrm{Tr}\left\{ \mathrm{e}^{-\beta \hat{\mathrm{h}}(\alpha_1^*, \alpha_1, \alpha_2^*, \alpha_2)} \right\}^{\mathcal{N}}. \tag{4.45}$$

Again, the factorisation of the exponentials is valid in the thermodynamic limit only. The single-particle Hamiltonian $\hat{\mathrm{h}}(\alpha_1^*, \alpha_1, \alpha_2^*, \alpha_2)$ is given by

$$\hat{\mathrm{h}}(\alpha_1^*, \alpha_1, \alpha_2^*, \alpha_2) = \delta \hat{a}_{2,2} + \Delta \hat{a}_{3,3} + \frac{g_1}{\sqrt{\mathcal{N}}} (\alpha_1^* + \alpha_1)(\hat{a}_{1,3} + \hat{a}_{3,1}) + \frac{g_2}{\sqrt{\mathcal{N}}} (\alpha_2^* + \alpha_2)(\hat{a}_{2,3} + \hat{a}_{3,2}). \tag{4.46}$$

Since all particles are identical, we have omitted the superindex k at the single-particle operators $\hat{a}^{(k)}_{n,m}$.

In a matrix representation, $\hat{\mathrm{h}}(\alpha_1^*, \alpha_1, \alpha_2^*, \alpha_2)$ reads

$$\hat{\mathrm{h}}(\alpha_1^*, \alpha_1, \alpha_2^*, \alpha_2) = \begin{pmatrix} 0 & 0 & \frac{g_1}{\sqrt{\mathcal{N}}}(\alpha_1^* + \alpha_1) \\ 0 & \delta & \frac{g_2}{\sqrt{\mathcal{N}}}(\alpha_2^* + \alpha_2) \\ \frac{g_1}{\sqrt{\mathcal{N}}}(\alpha_1^* + \alpha_1) & \frac{g_2}{\sqrt{\mathcal{N}}}(\alpha_2^* + \alpha_2) & \Delta \end{pmatrix}. \tag{4.47}$$

The trace over the particle degrees of freedom in the partition sum, Eq. (4.45), is evaluated in an eigenbasis of the single-particle Hamiltonian $\hat{\mathrm{h}}(\alpha_1^*, \alpha_1, \alpha_2^*, \alpha_2)$. Hence, we need to find the eigenvalues of the three-times-three matrix, Eq. (4.47). By virtue of Cardano's formula this can be done exactly[1]. However, the discussion of whether there is a phase transition or not and the analysis of the phase transition, is not very transparent. Therefore, we will pass the general case to a numerical computation and first consider the special case with $\delta = 0$ only, which is amenable to analytical calculations.

1 One can show that Cardano's formula gives indeed three real solutions, as it should be.

4.2.1 *Special Case of Vanishing δ*

For $\delta = 0$, the eigenvalues λ_n of the Hamiltonian matrix, Eq. (4.47), are given by

$$\lambda_0 = 0, \quad \lambda_\pm = \frac{\Delta}{2}\left[1 \pm \Omega(\alpha_1^*, \alpha_1, \alpha_2^*, \alpha_2)\right], \tag{4.48}$$

with

$$\Omega(\alpha_1^*, \alpha_1, \alpha_2^*, \alpha_2) = \sqrt{1 + \frac{4g_1^2}{\Delta^2 \mathcal{N}}\left(\alpha_1^* + \alpha_1\right)^2 + \frac{4g_2^2}{\Delta^2 \mathcal{N}}\left(\alpha_2^* + \alpha_2\right)^2}\,. \tag{4.49}$$

This allows us to sum up the particle degrees of freedom and the partition sum is given by

$$\mathcal{Z} = \int_{\mathbb{C}^2} \frac{d^2\alpha_1 d^2\alpha_2}{\pi^2}\, e^{-\beta \sum_{n=1}^{2} \hbar\omega_n |\alpha_n|^2} \left[1 + 2e^{-\frac{\beta\Delta}{2}} \cosh\Big(\frac{\beta\Delta}{2}\Omega\Big)\right]^{\mathcal{N}}. \tag{4.50}$$

Next, we decompose both α_1 and α_2 in its real and imaginary part as in Eq. (4.12) and scale them with the number $\mathcal{N}$ of particles as in Eq. (4.15),

$$\alpha_n = \sqrt{\mathcal{N}}\, y_n + i\sqrt{\mathcal{N}}\, z_n, \; n = 1, 2. \tag{4.51}$$

Then the partition sum reads

$$\mathcal{Z} = \frac{\mathcal{N}^2}{\pi^2} \int_{\mathbb{R}^2} dy_1 dz_1 \int_{\mathbb{R}^2} dy_2 dz_2\, e^{-\mathcal{N} f(y_1, y_2, z_1, z_2)}, \tag{4.52}$$

with

$$\begin{aligned} f(y_1, y_2, z_1, z_2) = {} & \beta\hbar\omega_1 y_1^2 + \beta\hbar\omega_2 y_2^2 + \beta\hbar\omega_1 z_1^2 + \beta\hbar\omega_2 z_2^2 \\ & - \ln\Big[1 + 2e^{-\beta\Delta/2} \cosh\Big(\frac{\beta\Delta}{2}\Omega\Big)\Big] \end{aligned} \tag{4.53}$$

and a corresponding Ω given by

$$\Omega(y_1, y_2) = \sqrt{1 + 16g_1^2 y_1^2/\Delta^2 + 16g_2^2 y_2^2/\Delta^2}\,. \tag{4.54}$$

The integral in the partition sum of Eq. (4.52) has again the form which is tractable with Laplace's method.

As in the Dicke model, the variable z_n enters only quadratically in f, such that upon minimising f, both z_n need to be zero. Minimising f with respect to y_n yields the two equations ($n = 1, 2$)

$$0 = y_n \left[\Big(\frac{g_{n,c}}{g_n}\Big)^2 \Omega(y_1, y_2) - q(\Omega)\right], \tag{4.55}$$

with

$$q(\Omega) = \frac{2e^{-\beta\Delta/2}\sinh\left[\frac{\beta\Delta}{2}\Omega(y_1,y_2)\right]}{1+2e^{-\beta\Delta/2}\cosh\left[\frac{\beta\Delta}{2}\Omega(y_1,y_2)\right]}, \tag{4.56}$$

and

$$g_{n,c} = \frac{\sqrt{\hbar\omega_n\Delta}}{2}. \tag{4.57}$$

Of course, Eqs. (4.55) are always solved by the trivial solutions $y_1 = y_2 = 0$. But do non-trivial solutions exist, and for which parameter values?

We first observe that the Eqs. (4.55) do not support solutions where both y_1 and y_2 are non-zero. For given y_1 and y_2, the parameter $\Omega(y_1,y_2)$ is fixed. Then the squared bracket cannot be zero for both equations[2]. Hence, the non-trivial solutions are given by one y_n being zero and the other being finite. In the following, the non-zero solution will be called $y_{n,0}$.

To see whether a non-zero $y_{n,0}$ really exists, we have to analyse the equation

$$0 = \left(\frac{g_{n,c}}{g_n}\right)^2\Omega(y_{n,0}) - q\big(\Omega(y_{n,0})\big), \tag{4.58}$$

with

$$\Omega(y_{n,0}) = \sqrt{1+4\frac{\hbar\omega_n}{\Delta}\left(\frac{g_n}{g_{n,c}}\right)^2 y_{n,0}^2}. \tag{4.59}$$

The function $q(\Omega)$ is bounded by one (see left panel of Fig. 4.7) and Ω itself is always greater or equal one. Therefore, for $g_n < g_{n,c}$, Eq. (4.58) has no solution and y_n has to be zero as well.

On the other hand, for $g_n > g_{n,c}$, non-trivial solutions of Eq. (4.58) can exist. In the right panel of Fig. 4.7, both terms of Eq. (4.58) are drawn. We see that for every finite temperature, the two curves always intersect twice, so that Eq. (4.58) always has two solutions. Of course, for a differentiable f, the two solutions cannot both correspond to minima of f. Hence, one solution stems from a maximum and the other from a minimum. Since the right side of Eq. (4.58) is the derivative of f, its sign-change signals whether a maximum (plus-minus sign change) or a minimum (minus-plus sign change) is passed when Ω is increased. Therefore, the first solution corresponds to a maximum and the second to a minimum.

We gain additional insight, if we directly analyse $f(y_n)$ for different coupling strengths[3]. This is shown in Fig. 4.8. We see that for small coupling strengths, $f(y_n)$ has one minimum only which is located

2 An exception is the line parametrised by $\frac{g_1}{g_{1,c}} = \frac{g_2}{g_{2,c}}$.

3 $f(y_n) \equiv f(y_1,0,0,0)$ from Eq. (4.53), w.l.o.g. $n = 1$

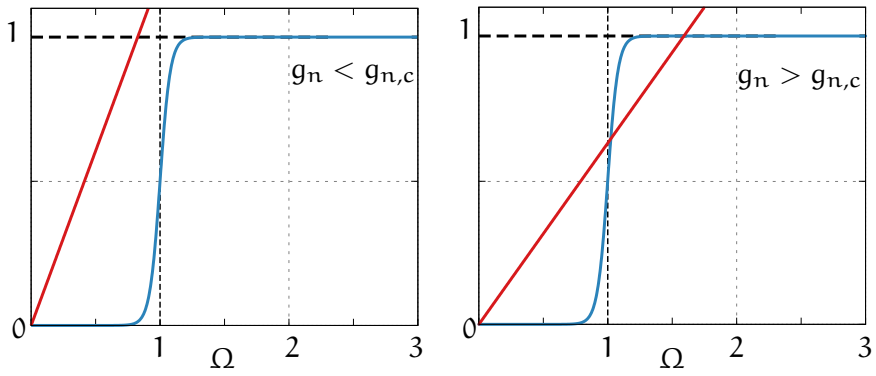

Figure 4.7: Graphical analysis of Eq. (4.58) for $g_n < g_{n,c}$ (left) and $g_n > g_{n,c}$ (right) for a certain n and fixed temperature. The red straight line corresponds to the first term, $\left(\frac{g_{n,c}}{g_n}\right)^2\Omega$, the other blue curved line corresponds to $q(\Omega)$ of Eq. (4.58) involving the hyperbolic functions. Of physical relevance is the region $\Omega > 1$ only. Thus, for $g < g_{n,c}$ no physical solution is possible, whereas for $g_n > g_{n,c}$ a physical solution might exist.

at $y_n = 0$; this is the trivial solution corresponding to the normal phase. If the coupling strength is increased, a maximum-minimum pair forms at finite values of y_n. In general, this minimum at $y_n > 0$ is energetically higher than the minimum of the trivial solution at $y_n = 0$, see Fig. 4.8. Hence, the trivial solution still minimises $f(y_n)$ globally. However, if the coupling strength is increased even further, the local minimum at $y_n > 0$ becomes the global minimum. So we see that the position $y_{n,0}$ of the global minimum jumps at a certain value of the coupling strength from zero to a finite value. As we have seen in the previous section, $y_{n,0}$ measures the occupation of the mode of the resonator. Therefore, the finite-temperature superradiant phase transition in the Lambda-model is a first-order phase transition.

In conclusion, we have shown the existence of three different minima of the function f appearing in the exponent of the integrand of the partition sum. We have also shown that for given temperature T, we can find coupling strengths $g_{1,c}(T), g_{2,c}(T)$, below which the trivial solution minimises f. In this parameter regime, the system is in the normal phase. In addition, above these coupling strengths, f is minimised by non-zero values of either y_1 or y_2. The first corresponds to the blue superradiant phase, the latter to the red superradiant phase of Ch. 2. In contrast to the zero-temperature case of Ch. 2, here all phase transitions are of first order.

The above discussion confines to the case $\delta = 0$. However, for finite δ, the results are qualitatively the same. We discuss the properties of the phase transition for finite δ below.

Next we analyse expectation values of observables. These can be computed just as in the previous section, Sec. 4.1.

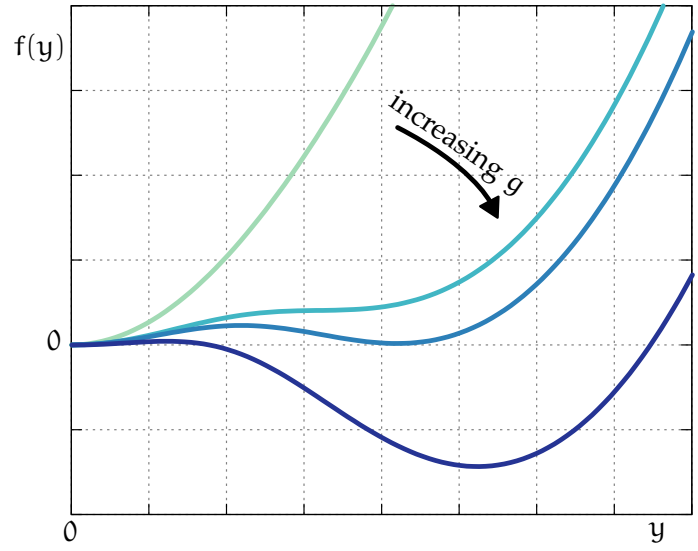

Figure 4.8: The function f of Eq. (4.53) with $z_n = 0 = y_2$, and $y_1 = y$ for fixed temperature. The coupling strength g increases from the upper to the lower curves. The units are arbitrary and f has been rescaled for comparison, such that $f(0) = 0$ for all coupling strengths g. On increasing g, a local minimum forms distant from the origin. For large g this minimum eventually becomes a global minimum.

4.2.2 *Expectation Values of Mode Operators*

For functions G of operators of the two modes of the resonator, the expectation value is given by [cf. the derivation of Eq. (4.25)]

$$\langle G(\hat{a}_1^\dagger, \hat{a}_1, \hat{a}_2^\dagger, \hat{a}_2)\rangle = G(\sqrt{\mathcal{N}}y_{1,0}, \sqrt{\mathcal{N}}y_{1,0}, \sqrt{\mathcal{N}}y_{2,0}, \sqrt{\mathcal{N}}y_{2,0}). \quad (4.60)$$

Then we obtain for the occupation of both modes

$$\langle \hat{a}_n^\dagger \hat{a}_n\rangle = \mathcal{N}y_{n,0}^2. \quad (4.61)$$

Thus we see that for finite temperatures, the character of the normal phase with zero occupation of the resonator modes is preserved. The same holds for the two superradiant phases at non-zero temperatures, as they show only one macroscopically occupied mode of the resonator as well; mode one for the blue superradiant phase and mode two for the red superradiant phase, while the occupation of the other mode is zero. This is due to the fact that at most one of the two y_n can be non-zero simultaneously.

4.2.3 *Expectation Values of Particle Operators*

The expectation values for the collective particle operators $\hat{A}_n^m$ can be traced back to the single-particle operators $\hat{a}_{n,m}$ [cf. the derivation of Eq. (4.30)],

$$\langle \hat{A}_n^m \rangle = \mathcal{N} \frac{\mathrm{Tr}\left\{ \hat{a}_{n,m}\, e^{-\beta \hat{h}(y_{1,0}, y_{2,0})} \right\}}{\mathrm{Tr}\{ e^{-\beta \hat{h}(y_{1,0}, y_{2,0})} \}}, \tag{4.62}$$

with $\hat{h}(y_{1,0}, y_{2,0}) = \hat{h}(\sqrt{\mathcal{N}} y_{1,0}, \sqrt{\mathcal{N}} y_{1,0}, \sqrt{\mathcal{N}} y_{2,0}, \sqrt{\mathcal{N}} y_{2,0})$ [cf. $\hat{h}$ of Eq. (4.47)]. This and the following holds even for non-zero δ. Let ε_n be the eigenvalues and $\boldsymbol{w}_n$ the corresponding eigenvectors of $\hat{h}(y_{1,0}, y_{2,0})$. Then, we evaluate the traces in Eq. (4.62) in this eigenbasis and the expectation values can be written as

$$\langle \hat{A}_n^m \rangle = \mathcal{N} \frac{1}{z} \sum_{k=1}^{3} (\boldsymbol{w}_k^*)_n (\boldsymbol{w}_k)_m\, e^{-\beta \varepsilon_k}. \tag{4.63}$$

Here $z = \mathrm{Tr}\{\exp[-\beta \hat{h}(y_{1,0}, y_{2,0})]\}$ is the partition sum of the single-particle Hamiltonian $\hat{h}(y_{1,0}, y_{2,0})$ and we have used that the matrix elements of $\hat{a}_{n,m}$ are given by zeros, except for the entry of the n^{th} row and m^{th} column, which is one (cf. Sec. A.2).

In the normal phase with $y_{1,0} = y_{2,0} = 0$, the Hamiltonian $\hat{h}(0,0)$ is diagonal and the eigenvectors $\boldsymbol{w}_k$ are given by Cartesian unit vectors. Hence, the expectation value of all collective operators $\hat{A}_n^m$ with $n \neq m$ vanish. Conversely for the diagonal operators $\hat{A}_n^n$, the occupations; their expectation values are given by

$$\langle \hat{A}_1^1 \rangle = \mathcal{N} \frac{1}{1 + e^{-\beta\delta} + e^{-\beta\Delta}}, \tag{4.64}$$

$$\langle \hat{A}_2^2 \rangle = \mathcal{N} \frac{e^{-\beta\delta}}{1 + e^{-\beta\delta} + e^{-\beta\Delta}}, \tag{4.65}$$

and

$$\langle \hat{A}_3^3 \rangle = \mathcal{N} \frac{e^{-\beta\Delta}}{1 + e^{-\beta\delta} + e^{-\beta\Delta}}. \tag{4.66}$$

Here, we explicitly see that in the normal phase the expectation values are independent of the coupling strengths g_1 and g_2. Furthermore, we note that for finite temperatures, in addition to the single-particle ground state $|1\rangle$, the energetically higher lying single-particle states $|2\rangle$ and $|3\rangle$ are macroscopically excited as well. Hence, in contrast to the modes of the resonator, the particle part of the system gets thermally excited. From that point of view, i. e. concerning the populations of the single-particle energy levels, the particle system in the normal phase behaves like a *normal* thermodynamical system.

For the superradiant phases, we cannot give explicit expressions for the expectation values. Neither for finite or vanishing δ. That is

because we need to compute the minimum of f numerically. Though for $\delta = 0$, we can say that some expectation values are exactly zero. This will be done next, separately for the red and the blue superradiant phases.

First consider the blue superradiant phase with $y_{1,0} \equiv y_0 \neq 0$ and $y_{2,0} = 0$. Then, the single-particle Hamiltonian $\hat{h}(y_0, 0)$ reads [cf. Eq. (4.47)]

$$\hat{h}(y_0, 0) = \begin{pmatrix} 0 & 0 & 2g_1 y_0 \\ 0 & 0 & 0 \\ 2g_1 y_1 & 0 & \Delta \end{pmatrix}, \tag{4.67}$$

and its exponential has the form

$$e^{-\beta \hat{h}(y_0,0)} = \begin{pmatrix} a_+ & 0 & b_1 \\ 0 & 1 & 0 \\ b_1 & 0 & a_- \end{pmatrix}. \tag{4.68}$$

The matrix elements $a_\pm$ and b_n are given by[4]

$$a_\pm = e^{-\frac{\beta\Delta}{2}} \left(\cosh\left[\frac{\beta\Delta\Omega}{2}\right] \pm \frac{\sinh\left[\frac{\beta\Delta\Omega}{2}\right]}{\Omega} \right), \tag{4.69}$$

$$b_n = -\frac{4g_n y_n}{\Delta\Omega} e^{-\frac{\beta\Delta}{2}} \sinh\left[\frac{\beta\Delta\Omega}{2}\right]. \tag{4.70}$$

The product of the exponential operator, Eq. (4.68), with matrices of the form

$$\begin{pmatrix} 0 & M_{12} & 0 \\ M_{21} & 0 & M_{23} \\ 0 & M_{32} & 0 \end{pmatrix} \tag{4.71}$$

is traceless. Therefore, the expectation values of the collective operators $\hat{A}_1^2$, $\hat{A}_2^3$ and their Hermitian conjugates are zero, i. e. there is no spontaneous polarisation between both the single-particle states $|1\rangle$ and $|2\rangle$, and the single-particle states $|2\rangle$ and $|3\rangle$. Contrary, the polarisation in the left branch of the Lambda-system, i. e. between the states $|1\rangle$ and $|3\rangle$, is finite and macroscopic.

For the red superradiant case, the discussion is similar. Here we have $y_{2,0} \equiv y_0 \neq 0$ and $y_{1,0} = 0$, and the exponential of the single-particle Hamiltonian reads

$$e^{-\beta \hat{h}(0,y_0)} = \begin{pmatrix} 1 & 0 & 0 \\ 0 & a_+ & b_2 \\ 0 & b_2 & a_- \end{pmatrix}. \tag{4.72}$$

4 The matrix element b_2 is needed below.

The matrix elements are given above, Eqs (4.69), (4.70). Now, the product of the exponential operator, Eq. (4.72), with matrices of the form

$$\begin{pmatrix} 0 & M_{12} & M_{13} \\ M_{21} & 0 & 0 \\ M_{31} & 0 & 0 \end{pmatrix} \tag{4.73}$$

is traceless and thus expectation values of the collective operators $\hat{A}_1{}^2$, $\hat{A}_1{}^3$ and their Hermitian conjugates are zero. On the other hand, the expectation value of the operators $\hat{A}_2{}^3$, $\hat{A}_3{}^2$ is finite and macroscopic. Hence, only the transition in the right branch of the Lambda-system is spontaneously polarised.

In conclusion, we found that in the superradiant phases at finite temperature, only the corresponding branch of the Lambda-system shows spontaneous polarisation; the left branch in the blue superradiant phase and the right branch in the red superradiant phase. In the normal phase, the polarisation is completely absent. Hence, in contrast to the populations of the particle system, the polarisations are not thermally excited and show a genuine quantum character. Thus, both the polarisations and the occupations of the two resonator modes show a similar behaviour in the three phases. Therefore, we have two sets of observables, the polarisations for the particles and the occupations of the modes for the resonator, to detect the superradiant phase transition at finite temperatures.

4.2.4 *General Case of Finite δ*

The above analysis for vanishing δ already shows that the phase transition in the Lambda-model for finite temperatures is a first-order phase transition. This fact renders the calculation of the exact location of the phase transition with our methods impossible. This can be understood with the help of the free energy as follows. In the thermodynamic limit, the global minimum of the free energy defines the thermodynamic phase of the system. We explicitly saw this when we have computed the partition sum. In a phase transition, the system changes from one thermodynamic state to another thermodynamic state. This new state corresponds to a different, now global minimum of the free energy.

For continuous phase transitions, the new minimum evolves continuously from the first minimum[5] and the first minimum changes its character to a maximum. Hence, the continuous phase transition is characterised by a sign-change of the curvature of the free energy at the position of the minimum of the state describing the normal phase. Often, this is tractable analytically.

5 In most cases, two or more new minima appear.

In contrast, in the case of first-order phase transitions, the new global minimum of the free energy appears distant from the old global minimum of the free energy, see Fig. 4.8. There are still two minima and we cannot detect the phase transition by the curvature of the free energy. Thus, to find the phase transition for first-order phase transitions, we first need to find all minima of the free energy and then find the global minima of these. This has to be done numerically here.

For the numerical computation, we do not solve Eq. (4.55), but we test for the minima of $f(y_1, y_2)$, Eq. (4.53), directly. Therefore, we apply a brute-force method, i. e. we look for the smallest value of $f(y_1, y_2)$ on a y_1–y_2 grid. Due to the reflection symmetry of $f(y_1, y_2)$, we can confine the grid to positive values for y_1 and y_2. This yields the position of the minimum $(y_{1,0}, y_{2,0})$. Then we compute the eigenvalues and eigenvectors of the Hamiltonian $\hat{h}(y_{1,0}, y_{2,0})$, Eq. (4.47)[6], at this point and obtain via Eq. (4.60) the expectation values for the operators of the resonator modes, and via Eq. (4.63) the corresponding particle expectation values.

Fig. 4.9, 4.10, 4.11 show the occupation $\langle \hat{a}_n^\dagger \hat{a}_n \rangle$ of the modes of the resonator, the occupation $\hat{A}_n{}^n$ of the single-particle levels of the particles, and the polarisations $\hat{A}_1{}^3$, $\hat{A}_2{}^3$ of the particles for low and high temperatures. All plots have been generated numerically for finite values of δ.

These figures corroborate our findings from the analytical discussion of the partition sum for vanishing δ. We see three phases: a *normal* phase for coupling strengths g_1 and g_2 below the critical coupling strengths $g_{1,c}$ and $g_{2,c}$, a *blue superradiant* phase for large coupling strengths g_1 above the critical coupling strength $g_{1,c}$, and a *red superradiant* phase for coupling strengths g_2 above the critical coupling strength $g_{2,c}$.

The normal phase is characterised by a zero occupation of both modes of the resonator (Fig. 4.9) In addition, the polarisation, or coherence, of the particles is zero in the normal phase (Fig. 4.11).

In contrast to the normal phase, the two superradiant phases are characterised by a macroscopic occupation of only one of the two resonator modes; mode one in the blue superradiant phase and mode two in the red superradiant phase. In addition, the blue (red) superradiant phase shows a spontaneous polarisation only on the transition of the single-particle levels $|1\rangle \leftrightarrow |3\rangle$ ($|2\rangle \leftrightarrow |3\rangle$).

We see that these defining properties remain for increasing temperature (right part of Figs. 4.9-4.11). As discussed in Sec. 4.2.3, we see that the population $\langle \hat{A}_2{}^2 \rangle$ of the single-particle energy level $|2\rangle$ increases for rising temperature. The same is true for the occupation $\langle \hat{A}_3{}^3 \rangle$, though this is not visible in the right part of Fig. 4.10 due to the fact that the temperature is yet too small.

6 Replace α_n and α_n^* by $y_{n,0}$ in $\hat{h}$

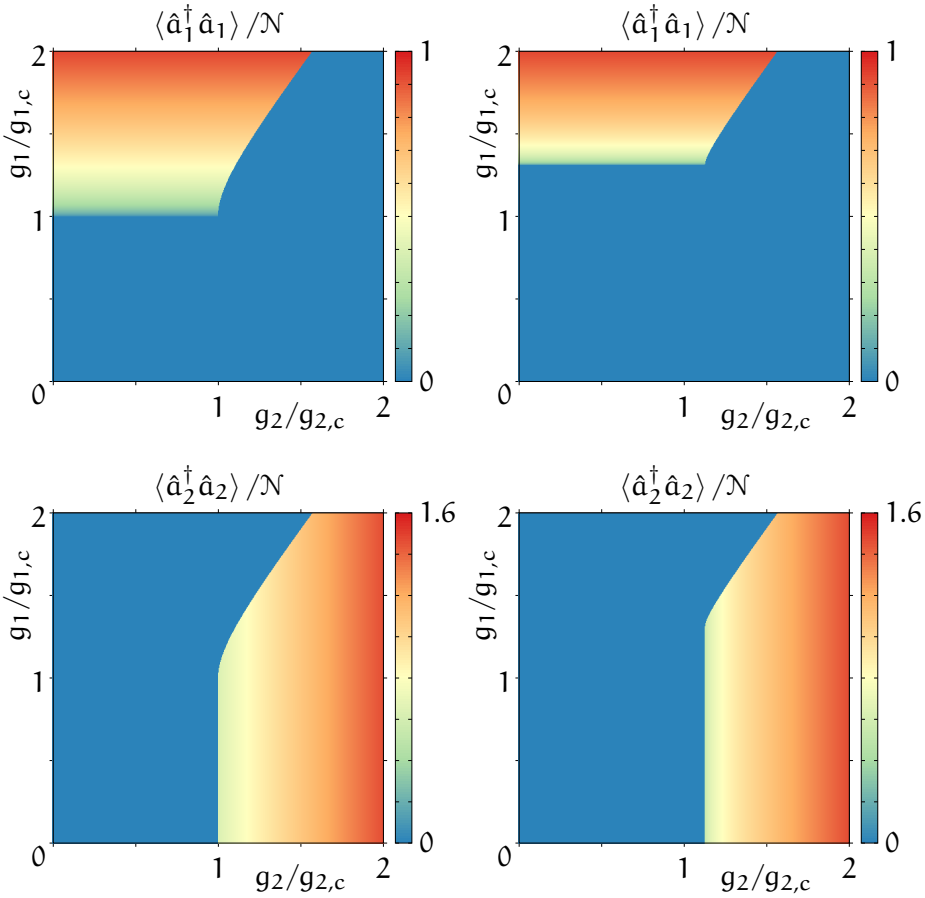

Figure 4.9: Numerical computation of the scaled occupations $\langle \hat{a}_n^\dagger \hat{a}_n \rangle / \mathcal{N}$ of the two bosonic modes for the Lambda-model for $k_B T = 0.001\,\Delta$ (left) and $k_B T = 0.25\,\Delta$ (right). The parameters are set to $\Delta = 1$, $\delta = 0.1$, $\hbar\omega_1 = 1.1$, and $\hbar\omega_2 = 0.8$. The computation has been done in the thermodynamic limit using Laplace's method.

From the Figs. 4.9-4.11 we also see that the shape of the phase boundary remains a straight line between the normal and the two superradiant phases. Between the red and the blue superradiant phases, the form of the phase boundary seems to persist as well. The only effect of the rising temperature is a shift of the phase boundary towards higher values of the coupling strengths g_1 and g_2. This is visualised in Fig. 4.12 where the polarisation $\langle \hat{A}_1{}^3 \rangle$ of the transition $|1\rangle \leftrightarrow |3\rangle$ of the three-level systems is shown for variable coupling strength g_1 and temperature T. The coupling strength of the second mode is fixed to $g_2 = 0.2\,g_{2,c}$. We see that for increasing temperature, the superradiant phase diminishes.

In addition to the shift of the phase boundary, the jump in the observables at this first-order phase transition increases. This is shown in Fig. 4.13 for the occupation $\langle \hat{a}_1^\dagger \hat{a}_1 \rangle$ of the first mode of the resonator. Of course, numerically, jumps are hard to detect since we get a discrete set of points as an output anyway. However, the dotted lines in Fig. 4.13 connect two largely separated points; each of the

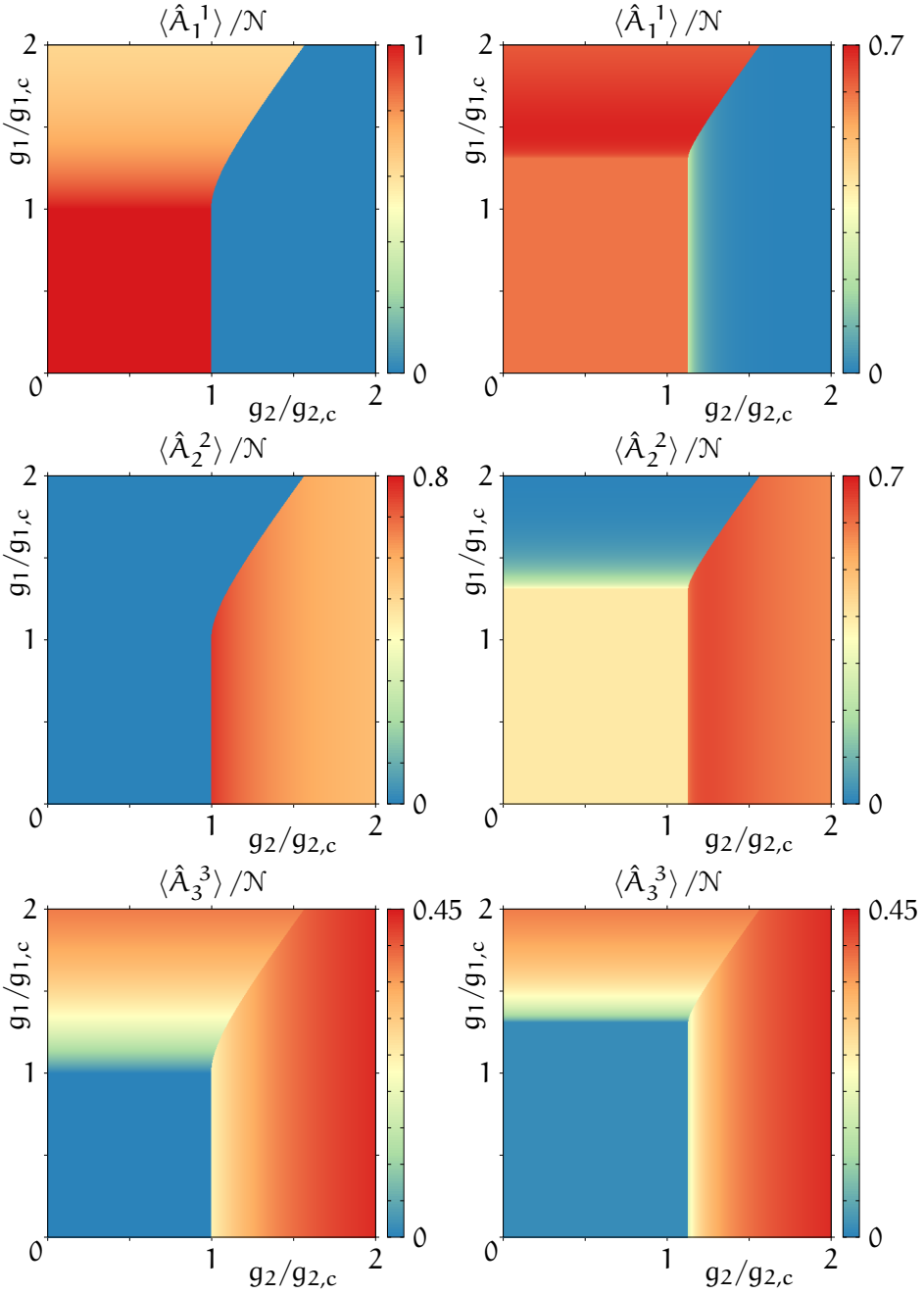

Figure 4.10: Numerical computation of the scaled occupations $\langle \hat{A}_n^n \rangle / \mathcal{N}$ of the single-particle energy levels of the three-level systems for $k_B T = 0.001\,\Delta$ (left) and $k_B T = 0.25\,\Delta$ (right), and other parameters as in Fig. 4.9

lines consists of 1000 data points. Thus, we can really speak of jumps in the observables and thus of a first-order phase transition.

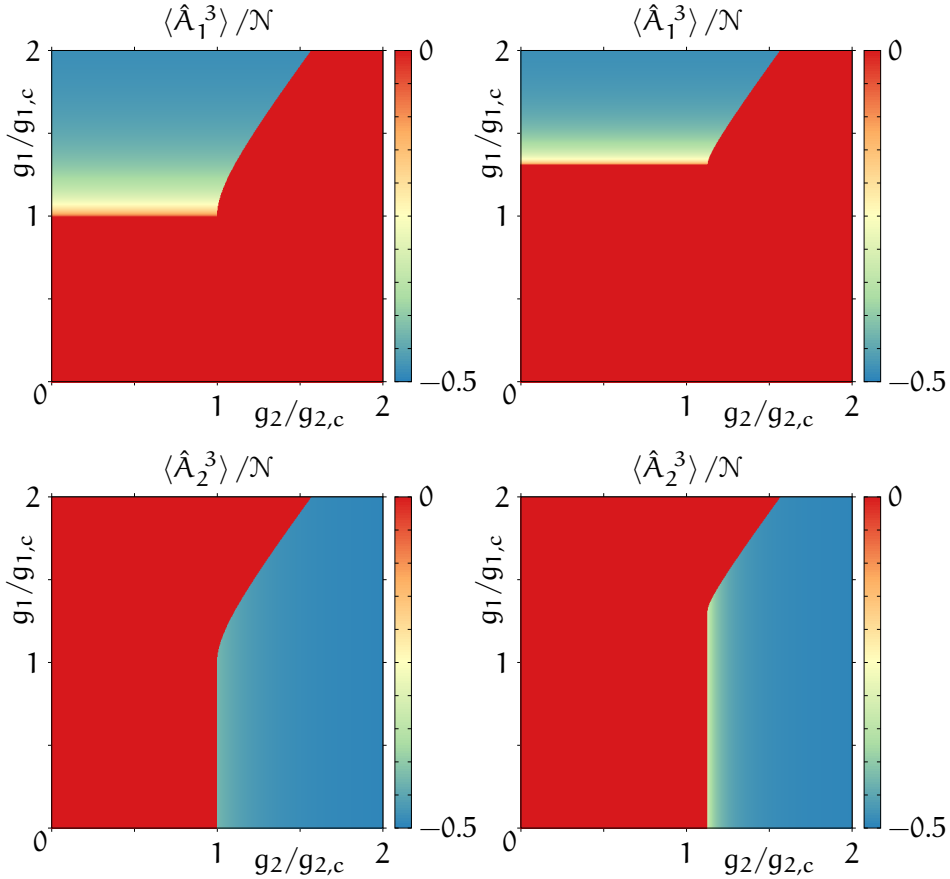

Figure 4.11: Numerical computation of the scaled polarisations $\langle \hat{A}_1^3 \rangle / \mathcal{N}$, $\langle \hat{A}_2^3 \rangle / \mathcal{N}$ of the three-level systems for $k_B T = 0.001\,\Delta$ (left) and $k_B T = 0.25\,\Delta$ (right), and other parameters as in Fig. 4.9

4.2.5 *The Zero-Temperature Limit*

To close this chapter, we analyse the zero-temperature limit of the Lambda-model for $\delta = 0$. For decreasing temperature, the function $q(\Omega)$, Eq. (4.56), becomes more and more step function like. Indeed, for $\beta\Delta \gg 1$, $q(\Omega)$ can be written as a Fermi function, and eventually in the limit $\beta\Delta \to \infty$, $q(\Omega)$ is given by

$$q(\Omega) = \begin{cases} 0 & , \quad \Omega < 1 \\ 1 & , \quad \Omega > 1. \end{cases} \tag{4.74}$$

Hence, at zero temperature, Eq. (4.58) has always a unique solution for coupling strengths $g_n > g_{n,c}$. In addition, since $f(y)$ shows no additional maximum, we have a continuous phase transition in this quantum limit.

Furthermore, we can also compute the position of the minimum of f. In the limit $T \to 0$, Eq. (4.58) reads

$$0 = \left(\frac{g_{n,c}}{g_n}\right)^2 \sqrt{1 + \frac{4\hbar\omega_n}{\Delta}\left(\frac{g_n}{g_{n,c}}\right)^2 y_n^2} - 1. \tag{4.75}$$

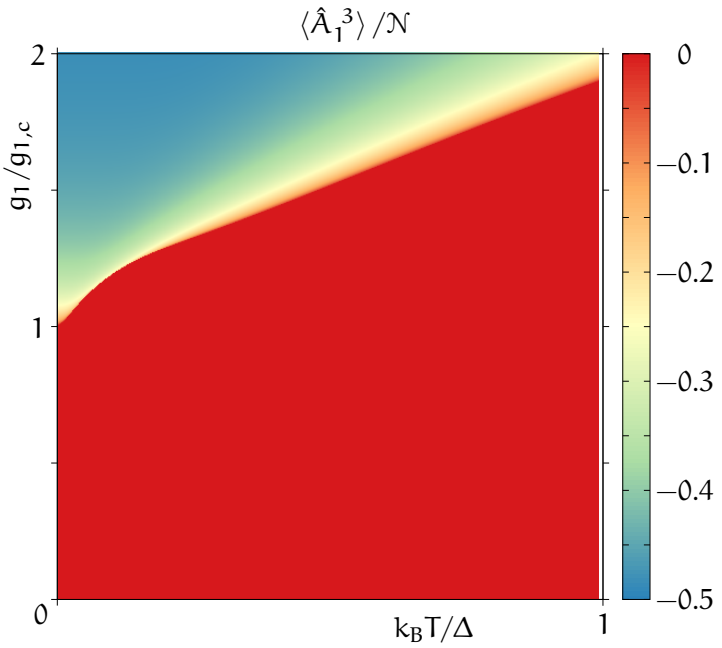

Figure 4.12: Numerical computation of the scaled polarisation $\langle \hat{A}_1^3 \rangle / \mathcal{N}$ of the transition $|1\rangle \leftrightarrow |3\rangle$ of the three-level system. $g_2 = 0.2\, g_{2,c}$ and other parameters as in Fig. 4.9.

Solving for y_n, we obtain

$$y_n = \pm \frac{g}{\hbar\omega_n} \sqrt{1 - \left(\frac{g_{n,c}}{g_n}\right)^4}. \tag{4.76}$$

If we identify, again, y_n with the mean-fields φ_n of Eq. (2.8) of Chap. 2, we reproduce the results of Eqs. (2.23) and (2.25) for the superradiant phases of the quantum phase transition of the Lambda-model.

The mean-fields Ψ_n can be reproduced as well. Consider for instance Ψ_3 which is related to $\langle \hat{A}_3^3 \rangle$ through $\langle \hat{A}_3^3 \rangle = \mathcal{N}\Psi_3^2$, except for a possible phase [cf. Eqs. (2.5) and (2.8)]. Using the results for the Boltzmann operator in the red superradiant phase, Eq. (4.72), plus the above expression for y_1, Eq. (4.76), and finally plug everything into the expectation value of Eq. (4.62), we obtain

$$\langle \hat{A}_3^3 \rangle = \frac{\mathcal{N}}{2} \frac{1 - e^{\beta\Delta\Omega} + \left(1 + e^{\beta\Delta\Omega}\right)\Omega}{\left[1 + e^{\beta\Delta\Omega} + e^{\frac{\beta\Delta}{2}(\Omega+1)}\right]\Omega} \tag{4.77}$$

which in the zero-temperature limit $\beta\Delta \to \infty$ reduces to

$$\langle \hat{A}_3^3 \rangle = \frac{\mathcal{N}}{2} \frac{\Omega - 1}{\Omega}. \tag{4.78}$$

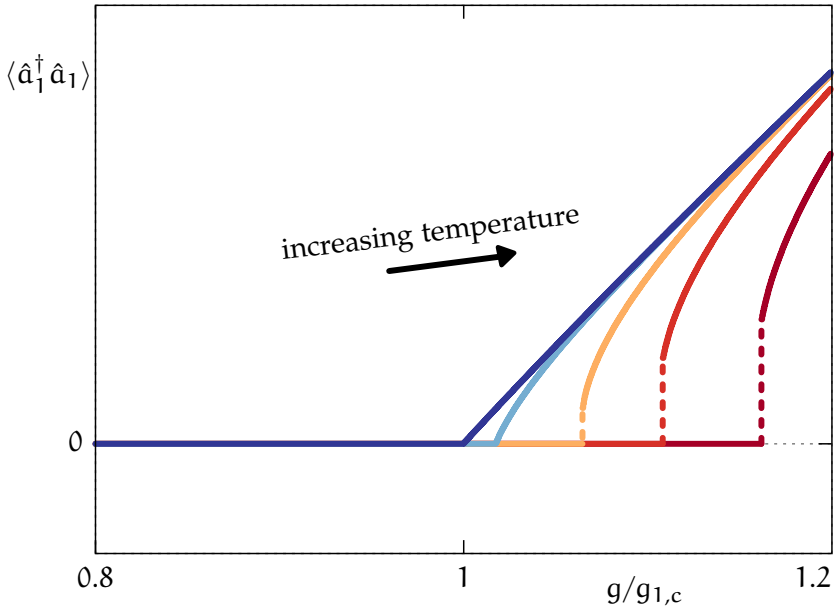

Figure 4.13: Occupations $\langle \hat{a}_1^\dagger \hat{a}_1 \rangle$ of the first mode of the resonator as a function of the coupling strength g_1 for fixed coupling strength $g_2 = 0.2 g_{2,c}$ and rising temperature (left to right, blue to red, respectively). The other parameters are set to $\Delta = 1$, $\delta = 0.1$, $\hbar\omega_1 = 1.1$, and $\hbar\omega_2 = 0.8$.

Here, $\Omega = \Omega(y_1)$ from Eq. (4.59). If we finally insert the position y_1 of the minimum of the free energy, Eq. (4.76), the population of the third single-particle energy level in the zero-temperature limit is given by

$$\langle \hat{A}_3^3 \rangle = \frac{\mathcal{N}}{2}\left[1 - \left(\frac{g_{1,c}}{g_1}\right)^2\right] \tag{4.79}$$

which agrees with the findings of Ch. 2 for Ψ_3, Eqs. (2.23) and (2.25). Applying the same technique, we can obtain the expectation values of all other collective particle operators $\hat{A}_n^m$ in both superradiant phases. This coincides with the results of Ch. 2.

4.3 CONCLUSION

In this section we have analysed the Lambda-model for finite temperatures. Therefore, we have computed the partition sum of the Hamiltonian. We found that at finite temperatures the properties of the phases and phase transition partially persist, compared to the quantum phase transition. Namely, we found a normal and two superradiant phases with the same properties as in the quantum limit, e. g. macroscopic occupation for the modes of the resonator only in the superradiant phases.

In contrast, a new characteristic of the phase transition at finite temperatures is the appearance of first-order phase transitions only. For the quantum phase transition we already found first-order phase transitions between the normal and the red superradiant phase and between the two superradiant phases. Here, for finite temperatures, the phase transition from the normal to the blue superradiant phase becomes a first-order phase transition as well.

5 CONCLUSION

This thesis gives an extensive study of a generalised Dicke model; the interaction of three-level atoms in Lambda-configuration with two modes of a resonator. Though, as modern experiments or their proposals show (Baumann, Guerlin, et al., 2010; Nataf and Ciuti, 2010a; Dimer et al., 2007; Baden et al., 2014), we do not have to restrict to atoms and photons. The atomic system can be any quantum mechanical three-level system and the resonator mode can be represented in principle by any bosonic degree of freedom. The above mentioned experiments and theoretical proposals all consider the original Dicke model. However, we think it is possible, and the conclusions of Baden et al. (2014) leaves us optimistic, that our generalised Dicke model can be *simulated* in a future experiment.

The results of this thesis show that the Lambda-model has a rich phase diagram with a trivial normal phase and two non-trivial superradiant phases. The normal and superradiant phases have the same properties known from the original Dicke model: all atoms occupy the ground state, the atoms show no polarisation, and no photons are present in the resonator for the normal phase; contrary, in the superradiant phases, the atoms as well as the resonator mode are macroscopically excited, and the atoms show a spontaneous polarisation. In addition, the two superradiant phases, blue and red, manifest themselves in one branch of the Lambda-system only. Compared to the original Dicke model, the superradiant phase transition to the blue superradiant phase is qualitatively identical; both are continuous phase transitions and all expectation values like resonator occupation or atomic inversion show the same dependency. However, the transition to the red superradiant phase, i. e. the phase which is connected to the branch of the Lambda-system with the energetically higher single-particle ground state, differs. Here, we found a first-order phase transition which manifests itself in all expectation values as well. A phase with both branches of the Lambda-system being superradiant does not appear. Thus, this generalised Dicke model supports these mutually different superradiant phases which are separated by a first-order phase transition from each other.

We found signatures of STIRAP and dark-state physics, the hallmarks of three-level systems in Lambda-configuration. However, considering the superradiant phase transitions, the dark state is irrelevant and a phase corresponding to a dark state is not stable. Maybe if the low-energy excitations or the excited states are analysed in more detail, the dark state becomes more relevant.

If the three-level systems in our generalised Dicke model represent real atoms, then the coupling strengths of the atom-light interaction are not independent of the diamagnetic term. Thus, in general the diamagnetic term cannot be neglected for real atoms. We showed that the phase diagram of the generalised Dicke model drastically changes, if diamagnetic terms are included. However, the system still undergoes a superradiant phase transition. Comparing to the model without the diamagnetic term, here, the phase transition is of first order only. We emphasise that the model respects the Thomas–Reiche–Kuhn sum rule. This is in contrast to the original Dicke model, where the superradiant phase transition disappears if a diamagnetic term is included in the Hamiltonian. We showed that this can be traced back to the order of the superradiant phase transition; superradiant phase transitions of second order are impossible.

All results found for the quantum phase transition are based on the bosonisation of the generators of the unitary group which naturally appear as collective atomic operators in the Hamiltonian. The bosonisation is done using a generalised Holstein–Primakoff transformation. This transformation results in a non-linear Hamiltonian of interacting oscillators. However, in the thermodynamic limit, the Hamiltonian is expanded and is bi-linear in the creation and annihilation operators of the oscillators representing atomic and resonators degrees of freedom. From this Hamiltonian, we can directly read off the many-body ground-state energy, which is a real number and scales with the number of particles. The analysis of the minima of the ground-state energy gives the phase transition and the properties of the phases. The collective excitations above the many-body ground state are obtained from the part of the Hamiltonian which is bi-linear in the creation and annihilation operators. A Bogoliubov and a canonical transformation yields the corresponding excitation energies.

The last chapter of this thesis addresses the superradiant phase transition in the generalised Dicke model for finite temperatures. We have evaluated the partition sum of the model in the thermodynamic limit using Laplace's method as far as we could. In the case of degenerate single-particle ground-state energies, we made strong statements on the properties of the phase transition and phases: in analogy to the quantum phase transition, there exist at most one superradiant phase for specific values of the coupling constants. These superradiant phases have the same properties as the blue and red superradiant phases of the zero-temperature model. In addition, the phase transition is always a first-order phase transition. We confirmed these findings numerically for the case of non-degenerate single-particle ground states as well. We did not explore the relevance of the diamagnetic term on the phase transition. Since we know that the no-go theorem presented in Ch. 3 does not apply to first-order superradiant phase transition, it is interesting to see whether or not the dia-

magnetic term permits superradiant phase transition for the Lambda-model at finite temperatures.

Other open questions concern (*i*) the ultra-strong coupling limit. How can a polaron transformation for the Lambda-model as in ALCALDE et al. (2012) be constructed? Is there a Lipkin-Meshkov-Glick model corresponding to the Lambda-model? Furthermore, (*ii*) is it possible to go beyond the low-energy excitations obtained via the Holstein–Primakoff transformation? Can the methods for the computation of the partition sum of Ch. 4 be used to analyse the properties of excited-state quantum phase transitions (BRANDES, 2013)?

A

APPENDIX

A.1 THE THOMAS–REICHE–KUHN SUM RULE

For every Hamiltonian $\hat{H}$ with spectrum E_n and eigenbasis $|n\rangle$, the identity

$$\sum_n (E_n - E_l) \langle l|\hat{O}|n\rangle \langle n|\hat{O}|l\rangle = \frac{1}{2} \langle l|\big[\hat{O}, [\hat{H}, \hat{O}]\big]|l\rangle \tag{A.1}$$

is fulfiled. Here, the sum runs over all quantum numbers n. This identity is called sum rule and is proven by expanding the double commutator on the right hand side of Eq. (A.1) plus inserting a completeness relation. The sum rule, Eq. (A.1), is valid for any operator $\hat{O}$ and every quantum number l of the Hamiltonian $\hat{H}$.

For atomic systems with $\mathcal{N}_e$ electrons per atom, position and momentum operators $\hat{\mathbf{r}}_n$ and $\hat{\mathbf{p}}_n$ for each electron, respectively, and a Hamiltonian of the form

$$\hat{H} = \sum_{n=1}^{\mathcal{N}_e} \frac{\hat{\mathbf{p}}_n^2}{2m} + \hat{h}(\hat{\mathbf{r}}_1, \ldots, \hat{\mathbf{r}}_{\mathcal{N}_e}), \tag{A.2}$$

a special sum rule with the operators

$$\hat{O} = \boldsymbol{\varepsilon} \cdot \hat{\mathbf{d}}, \quad \hat{\mathbf{d}} = q \sum_{n=1}^{\mathcal{N}_e} \hat{\mathbf{r}}_n, \quad |\boldsymbol{\varepsilon}| = 1 \tag{A.3}$$

is given by

$$\sum_n (E_n - E_l) \, |\boldsymbol{\varepsilon} \cdot \mathbf{d}_{ln}|^2 = \frac{\hbar^2 q^2 \mathcal{N}_e}{2m}, \quad \mathbf{d}_{nl} = \langle n|\hat{\mathbf{d}}|l\rangle \, . \tag{A.4}$$

This equation holds for all quantum numbers l. Up to now, no approximation has been made. This kind of sum rule for the matrix element $\mathbf{d}_{nl}$ of the dipole operator $\hat{\mathbf{d}}$ is called Thomas–Reiche–Kuhn sum rule (see e. g. Bethe and Jackiw, 1986). Upon inserting the definitions for the real coupling strengths, Eq. (1.88), and the diamagnetic parameter, Eq. (1.92), the Thomas–Reiche–Kuhn sum rule reads,

$$\sum_n \frac{g_{nl,k,s}^2}{E_n - E_l} = \frac{\kappa^2}{\omega_k}. \tag{A.5}$$

SPECIALISATION TO LAMBDA-SYSTEM If the infinite dimensional Hilbert space of a single atom is restricted to three energy levels only and $\mathbf{d}_{12} = 0$ is assumed, as in the Lambda-model, then not all terms in the sum on the left hand side of the Thomas–Reiche–Kuhn sum rule, Eq. (A.5), contribute. Hence, the left hand side is bounded, i.e.

$$\sum_{n}^{3} \frac{g_{nl,k,s}^2}{E_n - E_l} \leqslant \frac{\kappa^2}{\omega_k}, \quad l = 1, 2. \tag{A.6}$$

Eventually, inserting $l = 1, 2$ and bear in mind that $g_{nn,k,s} = g_{12,k,s} = 0$, $g_{31,k,s} = g_1$, $g_{32,k,s} = g_2$, and ω_k needs to be either ω_1 or ω_2, we obtain the two inequalities of the Eqs. (3.5).

A.2 ABOUT THE U(N) & SU(N) GROUP AND ITS GENERATORS

A group consists of a set G plus an operation on two group elements which satisfies (SINGER, 2005):

(*i*) For $g_1, g_2, g_3 \in G$ it holds $(g_1 g_2) g_3 = g_1 (g_2 g_3)$, i. e. associativity of the group operation.

(*ii*) There exists an identity element $I \in G$ such that for all $g \in G$ we have $Ig = gI = g$.

(*iii*) There is an inverse element $g^{-1} \in G$ for every element $g \in G$ such that $g^{-1} g = g g^{-1} = I$.

This definition is at first sight quite abstract. However, in physics in general and in quantum mechanics in special, symmetries play an important role. Symmetry operations leave the state or the physical properties of a physical system invariant, i. e. the action of symmetry operators let the state of the system remain in its corresponding symmetric subspace. In other words, the symmetry operators in quantum mechanics are representations of elements of a group. It is clear that the identity is a symmetry operation and that every symmetry operation can be reversed and thus representing the inverse element. In modern physics, symmetries and the theory of groups are of considerable interest in e. g. high-energy (WEINBERG, 1995) or in solid-state physics (ASHCROFT and MERMIN, 1976).

As a specific example of a group, consider the invertible linear transformations of elements of a N dimensional complex vector space onto itself. These transformations can be described by complex matrices and form a group, the so-called *general linear group*, GL(N, $\mathbb{C}$). The operation of the group is given by matrix multiplication. It is clear that all three group properties are satisfied: (*i*) since matrix multiplication is associative, (*ii*) the identity element is given by the identity matrix, and (iii) since the linear transformations are assumed invertible, hence their corresponding matrix representations have an inverse matrix which gives the inverse element.

The restriction to unitary transformations only, produces another group, the so-called *unitary group* U(N). Unitary matrices $U \in U(N)$ have the property that their inverse is given by their Hermitian conjugate, $U^{-1} = U^{\dagger}$[1]. The unitary transformations are generalisations of orthogonal matrices to complex vector spaces and therefore represent rotations in Hilbert space. In general, the determinant of unitary matrices is a complex number of modulus one, i. e. $\operatorname{Det} U = e^{i\alpha}$, $\alpha \in \mathbb{R}$. Unitary matrices with $\operatorname{Det} U = 1$ also form a group, the so-called special unitary group SU(N)[2]. The groups U(N) and SU(N) are key players in various fields of physics, like atomic, nuclear, or high energy physics.

GENERATORS OF U(N) The elements of the two groups U(N) and SU(N) can be obtained by so-called *generators* via the exponential map (HALL, 2003). For instance, consider the unitary matrix $U \in U(2)$

$$U = \begin{pmatrix} \cos s & i \sin s \\ i \sin s & \cos s \end{pmatrix}. \tag{A.7}$$

This matrix is generated by the Pauli matrix

$$\sigma_x = \begin{pmatrix} 0 & 1 \\ 1 & 0 \end{pmatrix}, \tag{A.8}$$

via $U = \exp[is\sigma_x]$.

The elements of the group U(N) are generated by N^2 generators (HALL, 2003). From the restriction for elements of the special unitary group SU(N) of having a determinant equal to one, their generators need to be traceless. This constraint removes one generator, such that the number of generators for SU(N) is $N^2 - 1$.

Let the generators be denoted by ${\Gamma_n}^m$ where n and m assume the values $1, 2, \ldots, N$. The generators ${\Gamma_n}^m$ of the U(N) group satisfy the commutation relation (HAMERMESH, 1964; OKUBO, 1975)

$$\left[{\Gamma_n}^m, {\Gamma_k}^j\right] = {\Gamma_n}^j \delta_{m,k} - {\Gamma_k}^m \delta_{n,j}. \tag{A.9}$$

Every element g of the groups U(N) and SU(N) can be written in the form

$$g = \exp\left[\sum_{n,m=1}^{N} i s_{n,m} {\Gamma_n}^m\right]. \tag{A.10}$$

For example, well-known generators for the unitary group U(2) are the Pauli matrices plus the identity matrix. For the special unitary group SU(3), the Gell-Mann matrices give the eight generators.

1 The product of two unitary matrices U_1, U_2 is a unitary matrix $U_3 = U_1 U_2$ as well, since the inverse of U_3 needs to be $U_3^{-1} = U_3^{\dagger} = U_2^{\dagger} U_1^{\dagger}$. Then it holds $U_3^{-1} U_3 = U_2^{\dagger} U_1^{\dagger} U_1 U_2 = U_2^{\dagger} U_2 = 1$. Hence, the product $U_1 U_2$ is in fact a unitary matrix.

2 Remember $\operatorname{Det}(U_1 U_2) = \operatorname{Det} U_1 \operatorname{Det} U_2$.

CONNECTION TO COLLECTIVE PARTICLE OPERATORS In Sec. 1.2 we introduced collective particle operators [cf. Eq. (1.91)],

$$\hat{A}_n^{\ m} = \sum_{\nu=1}^{\mathcal{N}} |n\rangle^\nu\langle m|\,, \tag{A.11}$$

where $|n\rangle^\nu$ are the n^{th} single-particle energy eigenstate of the ν^{th} particle. Since the states of different particles are orthogonal, we have

$$\hat{A}_n^{\ m}\hat{A}_k^{\ j} = \sum_{\nu,\mu} |n\rangle^\nu\langle m|k\rangle^\mu\langle j| \tag{A.12}$$

$$= \sum_{\nu} |n\rangle^\nu\langle j|\,\delta_{m,k} \tag{A.13}$$

$$= \hat{A}_n^{\ j}\,\delta_{m,k} \tag{A.14}$$

and analogous

$$\hat{A}_k^{\ j}\hat{A}_n^{\ m} = \hat{A}_k^{\ m}\,\delta_{j,n}, \tag{A.15}$$

or combined

$$\left[\hat{A}_n^{\ m}, \hat{A}_k^{\ j}\right] = \hat{A}_n^{\ j}\,\delta_{m,k} - \hat{A}_k^{\ m}\,\delta_{j,n}, \tag{A.16}$$

i. e., we reproduce the commutation relation, Eq. (A.9). Hence, the operators $\hat{A}_n^{\ m}$ are actually a representation of the generators $\Gamma_n^{\ m}$ of the groups U(N) and SU(N).

For atomic systems, the number N appearing in U(N) and SU(N) corresponds to the number of single-particle energy levels of the atoms. So that in the Hamiltonian of the Dicke model from Sec. 1.2.1, generators of the unitary group U(2) appear, whereas the Lambda-model from Sec. 1.2.2 is described by SU(3) generators.

From their representation, Eq. (A.11), we see that the generators fulfil the relation

$$\left(\hat{A}_n^{\ m}\right)^\dagger = \hat{A}_m^{\ n}. \tag{A.17}$$

We can write the collective particle operators as

$$\hat{A}_n^{\ m} = \sum_{\nu=1}^{\mathcal{N}} \hat{a}_{n,m}^{(\nu)}. \tag{A.18}$$

Here, $\hat{a}_{n,m}^{(\nu)} = |n\rangle^\nu\langle m|$ is the single-particle operator of the ν^{th} particle. One can easily show that theses operators are a representation of the generators $\Gamma_n^{\ m}$ as well. A three-by-three matrix representation of the operators $\hat{a}_{n,m}^{(\nu)}$ reads

$$\left(\hat{a}_{n,m}^{(\nu)}\right)_{ij} = \delta_{i,n}\delta_{j,m}, \quad i,j = 1,2,3. \tag{A.19}$$

This matrix representation is obtained by choosing Cartesian basis vectors as a representation for the single-particle states $|n\rangle^\nu$.

HERMITIAN SUBSETS The generators $\hat{A}_m^n$ with $n \neq m$ are not hermitian. However, one can consider linear combinations of the generators and construct hermitian generators. Consider the $\frac{N(N-1)}{2}$ subsets $\{\hat{A}_k^n, \hat{A}_n^k, \frac{1}{2}(\hat{A}_k^k - \hat{A}_n^n)\}$ of generators of the unitary group U(N), with $n, k \in \{1, 2, \ldots, N\}$ and $n < k$. The operators of each set fulfil the following commutation relations

$$\left[\frac{1}{2}(\hat{A}_k^k - \hat{A}_n^n), \hat{A}_k^n\right] = \frac{1}{2}[\hat{A}_k^k, \hat{A}_k^n] - \frac{1}{2}[\hat{A}_n^n, \hat{A}_k^n] \tag{A.20}$$

$$= \frac{1}{2}\hat{A}_k^n + \frac{1}{2}\hat{A}_k^n = \hat{A}_k^n, \tag{A.21}$$

$$\left[\frac{1}{2}(\hat{A}_k^k - \hat{A}_n^n), \hat{A}_n^k\right] = \frac{1}{2}[\hat{A}_k^k, \hat{A}_n^k] - \frac{1}{2}[\hat{A}_n^n, \hat{A}_n^k] \tag{A.22}$$

$$= -\frac{1}{2}\hat{A}_n^k - \frac{1}{2}\hat{A}_n^k = -\hat{A}_n^k, \tag{A.23}$$

and

$$[\hat{A}_k^n, \hat{A}_n^k] = \hat{A}_k^k - \hat{A}_n^n = 2\frac{1}{2}(\hat{A}_k^k - \hat{A}_n^n). \tag{A.24}$$

These are the commutation relation of spin operators (SAKURAI, 1994). In consequence, we have for each of the $(N-1)!$ transitions of the N-level particle a set of spin operators $\{\hat{X}_{k,n}, \hat{Y}_{k,n}, \hat{Z}_{k,n}\}$ satisfying

$$[\hat{X}_{k,n}, \hat{Y}_{k,n}] = i\,\hat{Z}_{k,n} \tag{A.25}$$

(and cyclic permutation) plus the mapping

$$\hat{X}_{k,n} = \frac{1}{2}\left(\hat{A}_k^n + \hat{A}_n^k\right), \tag{A.26}$$

$$\hat{Y}_{k,n} = \frac{1}{2i}\left(\hat{A}_k^n - \hat{A}_n^k\right), \tag{A.27}$$

and

$$\hat{Z}_{k,n} = \frac{1}{2}\left(\hat{A}_k^k - \hat{A}_n^n\right). \tag{A.28}$$

In general, spin operators corresponding to different transitions but involving one common energy level, do not commute. For instance,

$$[\hat{X}_{2,1}, \hat{X}_{3,2}] = \frac{1}{4}[\hat{A}_2^1 + \hat{A}_1^2, \hat{A}_3^2 + \hat{A}_2^3] \tag{A.29}$$

$$= -\frac{i}{2}\frac{1}{2}\left(\hat{A}_3^1 - \hat{A}_1^3\right) \tag{A.30}$$

$$= -\frac{i}{2}\hat{Y}_{3,1}. \tag{A.31}$$

In the case of two-level systems, $N = 2$, we have only one subset of generators and the mapping

$$\hat{J}_x = \frac{1}{2}\left(\hat{A}_2^1 + \hat{A}_1^2\right) = \frac{1}{2}\left(\hat{J}_+ + \hat{J}_-\right), \tag{A.32}$$

$$\hat{J}_y = \frac{1}{2i}\left(\hat{A}_2^1 - \hat{A}_1^2\right) = \frac{1}{2i}\left(\hat{J}_+ - \hat{J}_-\right), \tag{A.33}$$

and

$$\hat{J}_z = \frac{1}{2}\left(\hat{A}_2{}^2 - \hat{A}_1{}^1\right) \tag{A.34}$$

to the spin operators $\hat{J}_n$, $n \in \{x, y, z\}$. Here we have also identified the spin ladder operators

$$\hat{J}_+ = \hat{A}_2{}^1, \quad \hat{J}_- = \hat{A}_1{}^2. \tag{A.35}$$

We note that the matrix elements of spin operators have a physical dimension, whereas the matrix elements of the collective operators $\hat{A}_n{}^m$ are dimensionless. This can be fixed by including a $\hbar$ on the right-hand side. However, we neglect $\hbar$ here in this thesis.

For the unitary group U(3), i. e. for three-level systems, we have three possible transitions between the single-particle energy levels, and, consequently, there are three subsets of spin operators.

A.3 THE HOLSTEIN–PRIMAKOFF TRANSFORMATION

Mathematically, the matrices or operators of the generators of the unitary group U(N) group can be represented by oscillator, or bosonic operators (Okubo, 1975; Klein and Marshalek, 1991). One bosonic representation for the group SU(2) was introduced by Holstein and Primakoff (1940) and is therefore called Holstein–Primakoff transformation.

HOLSTEIN–PRIMAKOFF TRANSFORMATION OF SU(2) The Fig. A.1 gives an idea, why this mapping of spin states[3] to oscillator states works. The idea of the Holstein–Primakoff transformation is that the ladder of spin states $|J, M\rangle$, with $(M = -J, -J+1, \ldots, J-1, J)$, is mapped onto a finite number of harmonic oscillator states $|n\rangle$ $(n = 0, 1, \ldots, 2J)$; the spin raising and lowering operators $\hat{J}_+$ and $\hat{J}_-$ are mapped onto independent (bosonic) creation and annihilation operators $\hat{b}^\dagger$ and $\hat{b}$ of the oscillator.

This mapping of spin to oscillator operators, i. e. the transformation of Holstein and Primakoff, is given by (Okubo, 1975; Klein and Marshalek, 1991)

$$\hat{J}_+ = \hat{b}^\dagger \sqrt{2J - \hat{b}^\dagger \hat{b}}\,, \quad \hat{J}_- = \sqrt{2J - \hat{b}^\dagger \hat{b}}\,\hat{b}, \quad \hat{J}_z = \hat{b}^\dagger \hat{b} - J. \tag{A.36}$$

The bosonic operators $\hat{b}^\dagger$ and $\hat{b}$ fulfil canonical commutation relations

$$\left[\hat{b}, \hat{b}^\dagger\right] = 1. \tag{A.37}$$

Correspondingly, the mapping of the spin states is given by

$$|J, M\rangle = |J + M\rangle\,. \tag{A.38}$$

3 Remember, SU(2) is the group which is used for describing spin degrees of freedom.

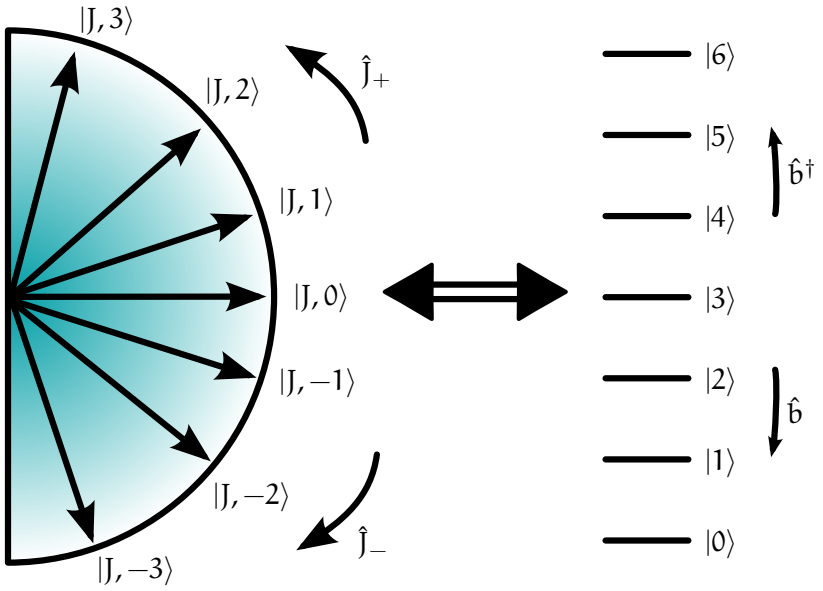

Figure A.1: Mapping of spin states (with $J = 3$) and operators (left) onto harmonic oscillator states and operators (right), $|J, M\rangle \leftrightarrow |M + 3\rangle$ and $\hat{J}_+ \leftrightarrow \hat{b}^\dagger$, $\hat{J}_- \leftrightarrow \hat{b}$.

To be clear, on the left hand side is a spin state, whereas on the right hand side there is an oscillator state. We note that the quantum number J is unchanged by the spin operators considered here.

In order to check the validity of the Holstein–Primakoff transformation, we act with the bosonic representation directly on the oscillator states[4],

$$\hat{J}_+ |J, M\rangle = \hat{b}^\dagger \sqrt{2J - \hat{b}^\dagger \hat{b}}\, |J + M\rangle \tag{A.39}$$
$$= \hat{b}^\dagger \sqrt{2J - (J + M)}\, |J + M\rangle \tag{A.40}$$
$$= \sqrt{J + M + 1}\, \sqrt{J - M}\, |J + M + 1\rangle \tag{A.41}$$
$$= \sqrt{(J - M)(J + M + 1)}\, |J, M + 1\rangle \tag{A.42}$$

analogously for $\hat{J}_-$, and for $\hat{J}_z$ we have

$$\hat{J}_z |J, M\rangle = \left(\hat{b}^\dagger \hat{b} - J\right) |J + M\rangle \tag{A.43}$$
$$= \left(J + M - J\right) |J + M\rangle \tag{A.44}$$
$$= M\, |J, M\rangle\,. \tag{A.45}$$

We see, that the Holstein–Primakoff transformation indeed gives the correct states and prefactors [see e. g. SAKURAI (1994)].

HOLSTEIN–PRIMAKOFF TRANSFORMATION OF U(N) The transformation of Holstein and Primakoff can be generalised to unitary

4 Remember for the creation and annihilation operators $\hat{b}^\dagger$, $\hat{b}$ it holds $\hat{b}^\dagger |n\rangle = \sqrt{n + 1}\, |n + 1\rangle$ and $\hat{b}\, |n\rangle = \sqrt{n}\, |n - 1\rangle$.

groups U(N) with N arbitrary (Okubo, 1975; Klein and Marshalek, 1991). Then, the generators of U(N) are represented as

$$\left.\begin{aligned} \hat{A}_n{}^m &= \hat{b}_n^\dagger\, \hat{b}_m, \\ \hat{A}_n{}^\ell &= \hat{b}_n^\dagger\, \hat{\Theta}_\ell(\mathcal{N}), \\ \hat{A}_\ell{}^m &= \hat{\Theta}_\ell(\mathcal{N})\, \hat{b}_m, \\ \hat{A}_\ell{}^\ell &= \hat{\Theta}_\ell(\mathcal{N})^2 \end{aligned}\right\} \; n, m \neq \ell. \tag{A.46}$$

Here, $n, m, \ell \in \{1, \ldots, N\}$ and ℓ is fixed.

The operator $\hat{\Theta}_\ell(\mathcal{N})$ is a generalisation of the square root operator of the Holstein–Primakoff transformation of SU(2):

$$\hat{\Theta}_\ell(\mathcal{N}) = \sqrt{\mathcal{N} - \sum_{\substack{n=1 \\ n\neq\ell}}^{N} \hat{b}_n^\dagger \hat{b}_n}\,. \tag{A.47}$$

The values of ℓ and $\mathcal{N}$ depend on the physical context. In this thesis $\mathcal{N}$ is the number of particles. For spin systems $\mathcal{N}$ is given by 2J.

The $N-1$ bosonic operators $\hat{b}_n$ fulfil the canonical commutation relations

$$[\hat{b}_n, \hat{b}_m^\dagger] = \delta_{n,m}, \quad [\hat{b}_n, \hat{b}_m] = 0. \tag{A.48}$$

To close this section, we want to show that the generators represented by the Holstein–Primakoff transformation of Eq. (A.46) indeed satisfy the commutation relations (A.9) of the generators of the unitary group U(N).

We first consider generators $\hat{A}_a{}^b$ with $a, b \neq \ell$

$$\begin{aligned} [\hat{A}_n{}^m, \hat{A}_k{}^j] &= [\hat{b}_n^\dagger \hat{b}_m, \hat{b}_k^\dagger \hat{b}_j] = \hat{b}_n^\dagger \hat{b}_j \delta_{m,k} - \hat{b}_k^\dagger \hat{b}_m \delta_{n,j} && \text{(A.49)} \\ &= \hat{A}_n{}^j \delta_{m,k} - \hat{A}_k{}^m \delta_{n,j} && \text{(A.50)} \end{aligned}$$

which agrees with Eq. (A.9).

Next we analyse the commutator with one generator having one index $m = \ell$,

$$\begin{aligned} [\hat{A}_\ell{}^m, \hat{A}_k{}^j] &= [\hat{\Theta}_\ell \hat{b}_m, \hat{b}_k^\dagger \hat{b}_j] = [\hat{\Theta}_\ell, \hat{b}_k^\dagger \hat{b}_j]\hat{b}_m + \hat{\Theta}_\ell \hat{b}_j \delta_{m,k} && \text{(A.51)} \\ &= (\hat{\Theta}_\ell \hat{b}_k^\dagger \hat{b}_j - \hat{b}_k^\dagger \hat{b}_j \hat{\Theta}_\ell)\hat{b}_m + \hat{A}_\ell{}^j \delta_{m,k}. && \text{(A.52)} \end{aligned}$$

In order to evaluate the expression in the parentheses, we use the following identities ($m \neq \ell$)

$$\sqrt{\mathcal{N} - \sum_{\substack{n=1 \\ n\neq\ell}}^{N} \hat{b}_n^\dagger \hat{b}_n}\; \hat{b}_m^\dagger = \hat{b}_m^\dagger \sqrt{\mathcal{N} - \sum_{\substack{n=1 \\ n\neq\ell}}^{N} \hat{b}_n^\dagger \hat{b}_n - 1} \tag{A.53}$$

$$\hat{b}_m \sqrt{\mathcal{N} - \sum_{\substack{n=1 \\ n\neq\ell}}^{N} \hat{b}_n^\dagger \hat{b}_n} = \sqrt{\mathcal{N} - \sum_{\substack{n=1 \\ n\neq\ell}}^{N} \hat{b}_n^\dagger \hat{b}_n - 1}\; \hat{b}_m \tag{A.54}$$

$$[\hat{\Theta}_k, \hat{b}_m^\dagger \hat{b}_m] = 0. \tag{A.55}$$

These equations can easily be checked by applying both sides of the equation to a Fock state. By means of these identities, we can simplify the parentheses in Eq. (A.52),

$$\hat{\Theta}_\ell \hat{b}_k^\dagger \hat{b}_j = \sqrt{\mathcal{N} - \sum_{\substack{n=1 \\ n\neq\ell}}^{N} \hat{b}_n^\dagger \hat{b}_n}\ \hat{b}_k^\dagger \hat{b}_j \tag{A.56}$$

$$= \hat{b}_k^\dagger \sqrt{\mathcal{N} - \sum_{\substack{n=1 \\ n\neq\ell}}^{N} \hat{b}_n^\dagger \hat{b}_n - 1}\ \hat{b}_j \tag{A.57}$$

$$= \hat{b}_k^\dagger \hat{b}_j \sqrt{\mathcal{N} - \sum_{\substack{n=1 \\ n\neq\ell}}^{N} \hat{b}_n^\dagger \hat{b}_n} = \hat{b}_k^\dagger \hat{b}_j\, \hat{\Theta}_\ell \tag{A.58}$$

i. e.

$$\left[\hat{\Theta}_\ell, \hat{b}_k^\dagger \hat{b}_j\right] = 0 \tag{A.59}$$

for arbitrary $k, j \neq \ell$. So, the above commutator, Eq. (A.52) yields

$$\left[\hat{A}_\ell{}^m, \hat{A}_k{}^j\right] = \hat{A}_\ell{}^j \delta_{m,k} \tag{A.60}$$

as it should [see Eq. (A.9)].

Next, we consider the commutator with $n = j = \ell$:

$$\left[\hat{A}_\ell{}^m, \hat{A}_k{}^\ell\right] = \left[\hat{\Theta}_\ell \hat{b}_m, \hat{b}_k^\dagger \hat{\Theta}_\ell\right] = \hat{\Theta}_\ell \hat{b}_m \hat{b}_k^\dagger \hat{\Theta}_\ell - \hat{b}_k^\dagger \hat{\Theta}_\ell^2 \hat{b}_m \tag{A.61}$$

$$= \hat{\Theta}_\ell \hat{b}_k^\dagger \hat{b}_m \hat{\Theta}_\ell + \hat{\Theta}_\ell^2 \delta_{m,k} - \hat{b}_k^\dagger \hat{\Theta}_\ell^2 \hat{b}_m \tag{A.62}$$

$$= \hat{b}_k^\dagger \sqrt{\mathcal{N} - \sum_{\substack{n=1 \\ n\neq\ell}}^{N} \hat{b}_n^\dagger \hat{b}_n - 1} \sqrt{\mathcal{N} - \sum_{\substack{n=1 \\ n\neq\ell}}^{N} \hat{b}_n^\dagger \hat{b}_n - 1}\ \hat{b}_m \tag{A.63}$$

$$+ \hat{\Theta}_\ell^2 \delta_{m,k} - \hat{b}_k^\dagger \left(\mathcal{N} - \sum_{\substack{n=1 \\ n\neq\ell}}^{N} \hat{b}_n^\dagger \hat{b}_n\right) \hat{b}_m \tag{A.64}$$

$$= -\hat{b}_k^\dagger \hat{b}_m + \hat{\Theta}_\ell^2 \delta_{m,k} = \hat{A}_\ell{}^\ell \delta_{m,k} - \hat{A}_k{}^m, \tag{A.65}$$

as desired.

The next case is given by $n = m = \ell$ and is calculated as

$$\left[\hat{A}_\ell{}^\ell, \hat{A}_k{}^j\right] = \left[\hat{\Theta}_\ell^2, \hat{b}_k^\dagger \hat{b}_j\right] = -\left[\hat{b}_k^\dagger \hat{b}_k + \hat{b}_j^\dagger \hat{b}_j, \hat{b}_k^\dagger \hat{b}_j\right] \tag{A.66}$$

$$= -\hat{b}_k^\dagger \hat{b}_j + \hat{b}_k^\dagger \hat{b}_k \delta_{j,k} + \hat{b}_k^\dagger \hat{b}_j - \hat{b}_j^\dagger \hat{b}_j \delta_{j,k} = 0. \tag{A.67}$$

Which is true as well.

Finally, we consider the case with $n = m = k = \ell$:

$$\left[\hat{A}_\ell{}^\ell, \hat{A}_\ell{}^j\right] = \left[\hat{\Theta}_\ell^2, \hat{\Theta}_\ell \hat{b}_j\right] = \hat{\Theta}_\ell \left[\hat{\Theta}_\ell^2, \hat{b}_j\right] \tag{A.68}$$

$$= -\hat{\Theta}_\ell \left[\hat{b}_j^\dagger \hat{b}_j, \hat{b}_j\right] = \hat{\Theta}_\ell \hat{b}_j = \hat{A}_\ell{}^j \tag{A.69}$$

All other combination of operators in the commutator follow from these cases by Hermitian conjugation and renaming of indices. Thus, the Holstein–Primakoff transformation of Eq. (A.46) indeed reproduces the canonical commutation relations Eq. (A.9) for the generators of the unitary group U(N).

A.4 THE BOGOLIUBOV TRANSFORMATION

A.4.1 *Basic Example — Two Interacting Oscillators*

Consider the Hamiltonian

$$\hat{H}/\hbar = \omega_1 \hat{a}_1^\dagger \hat{a}_1 + \omega_2 \hat{a}_2^\dagger \hat{a}_2 + \lambda(\hat{a}_1^\dagger + \hat{a}_1)(\hat{a}_2^\dagger + \hat{a}_2) + \lambda'(\hat{a}_1^\dagger + \hat{a}_1)^2 \quad \text{(A.70)}$$

of two interacting oscillators.

We introduce a transformation to new coordinates $\hat{q}$, $\hat{p}$ via

$$\hat{q} = \sqrt{\frac{1}{2\omega}}(\hat{a}^\dagger + \hat{a}), \quad \text{(A.71)}$$

$$\hat{p} = i\sqrt{\frac{\omega}{2}}(\hat{a}^\dagger - \hat{a}). \quad \text{(A.72)}$$

For the inverse transformation, it holds

$$\hat{a} = \sqrt{\frac{\omega}{2}}(\hat{q} + i\frac{1}{\omega}\hat{p}), \quad \text{(A.73)}$$

$$\hat{a}^\dagger = \sqrt{\frac{\omega}{2}}(\hat{q} - i\frac{1}{\omega}\hat{p}). \quad \text{(A.74)}$$

With that, we have for the commutator and the squares of these new coordinates

$$[\hat{q}, \hat{p}] = i, \quad \text{(A.75)}$$

$$\hat{q}^2 = \frac{1}{2\omega}(\hat{a}^{\dagger 2} + 2\hat{a}^\dagger \hat{a} + 1 + \hat{a}^2), \quad \text{(A.76)}$$

$$\hat{p}^2 = -\frac{\omega}{2}(\hat{a}^{\dagger 2} - 2\hat{a}^\dagger \hat{a} - 1 + \hat{a}^2) \quad \text{(A.77)}$$

and thus

$$\frac{1}{2}\hat{p}^2 + \frac{1}{2}\omega^2 \hat{q}^2 = \omega(\hat{a}^\dagger \hat{a} + 1/2). \quad \text{(A.78)}$$

In addition, it holds

$$\hat{a}^\dagger \hat{a} = \frac{1}{2\omega}\hat{p}^2 + \frac{1}{2}\omega \hat{q}^2 - 1/2, \quad \text{(A.79)}$$

$$\hat{a}^\dagger + \hat{a} = \sqrt{2\omega}\hat{q}. \quad \text{(A.80)}$$

In these new coordinates, the Hamiltonian, Eq. (A.70), of the interacting oscillators reads

$$\hat{H}/\hbar = \frac{1}{2}\hat{p}_1^2 + \frac{1}{2}\hat{p}_2^2 + \frac{1}{2}\omega_1^2\hat{q}_1^2 + \frac{1}{2}\omega_2^2\hat{q}_2^2 + 2\sqrt{\omega_1\omega_2}\lambda\hat{q}_1\hat{q}_2 + 2\omega_1\lambda'\hat{q}_1^2. \quad \text{(A.81)}$$

The q-sector of this Hamiltonian can be written in a matrix-vector notation,

$$\hat{H}/\hbar = \frac{1}{2}\hat{p}_1^2 + \frac{1}{2}\hat{p}_2^2 + \frac{1}{2}(\hat{q}_1, \hat{q}_2) \cdot \begin{pmatrix} \omega_1^2 + 4\omega_1\lambda' & 2\sqrt{\omega_1\omega_2}\lambda \\ 2\sqrt{\omega_1\omega_2}\lambda & \omega_2^2 \end{pmatrix} \cdot \begin{pmatrix} \hat{q}_1 \\ \hat{q}_2 \end{pmatrix}. \quad \text{(A.82)}$$

Diagonalising this matrix gives new uncoupled coordinates $\hat{Q}_n$. Due to the diagonalisation of a symmetric matrix, the operators $\hat{Q}_n$ and $\hat{q}_n$ are related by an orthogonal transformation $\mathbf{U}$,

$$\hat{Q}_n = \sum_m U_{n,m}\hat{q}_m. \quad \text{(A.83)}$$

If we define new canonical momenta $\hat{P}_n$ via

$$\hat{P}_n = \sum_m U_{n,m}\hat{p}_m, \quad \text{(A.84)}$$

the canonical commutation relations are preserved,

$$[\hat{Q}_n, \hat{P}_m] = \sum_{j,k} U_{n,j}U_{m,k}[\hat{q}_j, \hat{p}_k] = i\sum_j U_{n,j}U_{m,j} = i\delta_{n,m}. \quad \text{(A.85)}$$

In the last step, the orthogonality property of $\mathbf{U}$ was used.

In addition, the sum of the squares of the momenta is invariant under the orthogonal transformation $\mathbf{U}$,

$$\sum_m \hat{P}_m^2 = \sum_m \sum_{j,k} U_{m,j}U_{m,k}\hat{p}_j\hat{p}_k = \sum_j \hat{p}_j^2. \quad \text{(A.86)}$$

Finally, the Hamiltonian in these new coordinates reads

$$\hat{H}/\hbar = \frac{1}{2}\hat{P}_1^2 + \frac{1}{2}\hat{P}_2^2 + \frac{1}{2}\varepsilon_1^2\hat{Q}_1^2 + \frac{1}{2}\varepsilon_2^2\hat{Q}_2^2. \quad \text{(A.87)}$$

This is a Hamiltonian of two *non-interacting* oscillators. Here, ε_n^2 are the two eigenvalues of the matrix appearing in the Hamiltonian of Eq. (A.82). These eigenvalues are explicitly given by

$$\varepsilon_{1,2}^2 = \frac{1}{2}\left[\omega_1^2 + 4\omega_1\lambda' + \omega_2^2 \pm \sqrt{[\omega_1^2 + 4\omega_1\lambda' - \omega_2^2]^2 + 16\lambda^2\omega_1\omega_2}\right]. \quad \text{(A.88)}$$

Applying an additional transformation back to new creation and annihilation operators $\hat{e}_n^\dagger$, $\hat{e}_n$, similar as above, Eqs. (A.71), (A.72), we end with a Hamiltonian of two non-interacting oscillators

$$\hat{H} = \hbar\varepsilon_1 \hat{e}_1^\dagger \hat{e}_1 + \hbar\varepsilon_2 \hat{e}_2^\dagger \hat{e}_2, \tag{A.89}$$

with the frequencies ε_n from the diagonalisation procedure. This diagonalisation procedure of interacting oscillators or bosonic degrees of freedom is called *Bogoliubov* transformation.

A.4.2 *Application to Excitations in the Lambda-model*

The Hamiltonian of the Lambda-model reads (cf. Sec. 2.2)

$$\hat{H} = \sum_{n=1}^{3} E_n \hat{A}_n^{\,n} + \sum_{n=1}^{2} \Big[\hbar\omega_n \hat{a}_n^\dagger \hat{a}_n + \frac{g_n}{\sqrt{\mathcal{N}}} \big(\hat{a}_n^\dagger + \hat{a}_n\big)\big(\hat{A}_n^{\,3} + \hat{A}_3^{\,n}\big) \Big]. \tag{A.90}$$

Upon representing the collective $\hat{A}_n^{\,m}$ operators by bosonic operators via the Holstein–Primakoff transformation (cf. Sec. 2.3.1) and introduce mean fields Ψ_n and φ_n, the Hamiltonian can be written in powers of $1/\sqrt{\mathcal{N}}$ (cf. Sec. 2.3.2). Of interest here is the $\hat{h}_m^{(2)}$ part of the Hamiltonian, since it defines the collective excitations of the system (Emary and Brandes, 2003a). The index m signals different instances of the Holstein–Primakoff transformation. For the normal and blue superradiant phase, $m = 1$ is suitable. The Hamiltonian is given in Eq. (2.18)

Next, we introduce new names for the creation and annihilation operators,

$$\hat{a}_1 = \hat{c}_1, \tag{A.91}$$
$$\hat{a}_2 = \hat{c}_2, \tag{A.92}$$
$$\hat{a}_3 = \hat{d}_2, \text{ and} \tag{A.93}$$
$$\hat{a}_4 = \hat{d}_3, \tag{A.94}$$

for the frequencies

$$\hbar\omega_3 = \delta - 2\, g_1\, \varphi_1\, \Psi_3/\psi_1, \text{ and} \tag{A.95}$$
$$\hbar\omega_4 = \Delta - 2\, g_1\, \varphi_1\, \Psi_3/\psi_1, \tag{A.96}$$
$$\tag{A.97}$$

and for the couplings

$$\hbar\lambda_{33} = -\frac{1}{2} g_1 \varphi_1 \Psi_2^2 \Psi_3/\psi_1^3 \tag{A.98}$$

$$\hbar\lambda_{44} = -g_1 \varphi_1 \Psi_3/\psi_1 \left(1 + \tfrac{1}{2}\Psi_3^2/\psi_1^2\right) \tag{A.99}$$

$$\hbar\lambda_{34} = -g_1 \varphi_1 \Psi_2/\psi_1 \left(1 + \Psi_3^2/\psi_1^2\right) \tag{A.100}$$

$$\hbar\lambda_{34'} = 2\, g_2 \varphi_2 \tag{A.101}$$

$$\hbar\lambda_{13} = -g_1 \Psi_2 \Psi_3/\psi_1 \tag{A.102}$$

$$\hbar\lambda_{14} = g_1 \psi_1 \left(1 - \Psi_3^2/\psi_1^2\right) \tag{A.103}$$

$$\hbar\lambda_{23} = g_2 \Psi_3 \tag{A.104}$$

$$\hbar\lambda_{24} = g_2 \Psi_2. \tag{A.105}$$

With that, the Hamiltonian of Eq. (2.18) assumes the form

$$\begin{aligned}\hat{h}^{(2)}_{m=1}/\hbar = {} & \omega_1 \hat{a}_1^\dagger \hat{a}_1 + \omega_2 \hat{a}_2^\dagger \hat{a}_2 + \omega_3 \hat{a}_3^\dagger \hat{a}_3 + \omega_4 \hat{a}_4^\dagger \hat{a}_4 \\ & + \lambda_{33}\left(\hat{a}_3^\dagger + \hat{a}_3\right)^2 + \lambda_{44}\left(\hat{a}_4^\dagger + \hat{a}_4\right)^2 \\ & + \lambda_{34}\left(\hat{a}_3^\dagger + \hat{a}_3\right)\left(\hat{a}_4^\dagger + \hat{a}_4\right) + \lambda_{34'}\left(\hat{a}_4^\dagger \hat{a}_3 + \hat{a}_3^\dagger \hat{a}_4\right) \\ & + \lambda_{13}\left(\hat{a}_1^\dagger + \hat{a}_1\right)\left(\hat{a}_3^\dagger + \hat{a}_3\right) + \lambda_{14}\left(\hat{a}_1^\dagger + \hat{a}_1\right)\left(\hat{a}_4^\dagger + \hat{a}_4\right) \\ & + \lambda_{23}\left(\hat{a}_2^\dagger + \hat{a}_2\right)\left(\hat{a}_3^\dagger + \hat{a}_3\right) + \lambda_{24}\left(\hat{a}_2^\dagger + \hat{a}_2\right)\left(\hat{a}_4^\dagger + \hat{a}_4\right).\end{aligned} \tag{A.106}$$

In the following, we specialise this Hamiltonian to the three phases of the Lambda-model: the normal and the two superradiant phases.

NORMAL PHASE For the normal Phase, it holds (cf. Sec. 2.3.3)

$$\Psi_2 = 0, \Psi_3 = 0, \psi_1 = 1, \varphi_1 = 0, \varphi_2 = 0. \tag{A.107}$$

Then, the coupling $\lambda_{14} = g_1/\hbar$ is non-zero only, the frequencies simplify to

$$\hbar\omega_3 = \delta \tag{A.108}$$

$$\hbar\omega_4 = \Delta \tag{A.109}$$

and the Hamiltonian is given by

$$\begin{aligned}\hat{h}^{(2)}_{m=1} = {} & \hbar\omega_1 \hat{a}_1^\dagger \hat{a}_1 + \hbar\omega_2 \hat{a}_2^\dagger \hat{a}_2 + \hbar\omega_3 \hat{a}_3^\dagger \hat{a}_3 + \hbar\omega_4 \hat{a}_4^\dagger \hat{a}_4 \\ & + \hbar\lambda_{14}\left(\hat{a}_1^\dagger + \hat{a}_1\right)\left(\hat{a}_4^\dagger + \hat{a}_4\right).\end{aligned} \tag{A.110}$$

Using the findings of the previous section, the excitation energies are given by

$$\begin{aligned}\varepsilon_{1,4}^2 = \frac{1}{2}\Bigg[& \omega_1^2 + \left(\Delta/\hbar\right)^2 \\ & \pm \sqrt{[\omega_1^2 - \left(\Delta/\hbar\right)^2]^2 + 16\left(g_1/\hbar\right)^2 \omega_1 \Delta/\hbar}\Bigg],\end{aligned} \tag{A.111}$$

$$\varepsilon_2 = \delta/\hbar, \tag{A.112}$$

$$\varepsilon_3 = \omega_2. \tag{A.113}$$

BLUE SUPERRADIANT PHASE Now, consider the blue superradiant phase (cf. Sec. 2.3.3),

$$\Psi_2 = 0, \Psi_3 = \sqrt{\frac{1}{2}}\sqrt{1-\left(\frac{g_{1,c}}{g_1}\right)^2}, \tag{A.114}$$

$$\varphi_1 = -\frac{g_1}{\hbar\omega_1}\sqrt{1-\left(\frac{g_{1,c}}{g_1}\right)^4}\,\varphi_2 = 0. \tag{A.115}$$

We introduce new names for the creation and annihilation operators as above.

Furthermore, it holds

$$\begin{aligned} 2g_1\varphi_1\Psi_3/\psi_1 &= -2\frac{g_1^2}{\hbar\omega_1}\sqrt{1-\left(\frac{g_{1,c}}{g_1}\right)^4}\,\frac{\sqrt{1-\left(\frac{g_{1,c}}{g_1}\right)^2}}{\sqrt{1+\left(\frac{g_{1,c}}{g_1}\right)^2}} \\ &= -2\frac{g_1^2}{\hbar\omega_1}\left[1-\left(\frac{g_{1,c}}{g_1}\right)^2\right] \\ &= -\frac{\Delta}{2}\left(\frac{g_1}{g_{1,c}}\right)^2\left[1-\left(\frac{g_{1,c}}{g_1}\right)^2\right] \\ &= \frac{\Delta}{2}\left[1-\left(\frac{g_1}{g_{1,c}}\right)^2\right] \end{aligned} \tag{A.116}$$

and we define

$$\eta_1 = \left(\frac{g_1}{g_{1,c}}\right)^2, \quad \eta_2 = \left(\frac{g_2}{g_{2,c_1}}\right)^2, \tag{A.117}$$

with the critical coupling strengths

$$g_{1,c} = \frac{\sqrt{\Delta\hbar\omega_1}}{2} \text{ and } g_{2,c_1} = \frac{\sqrt{(\Delta-\delta)\hbar\omega_2}}{2}. \tag{A.118}$$

With that, the frequencies in the Hamiltonian are given by,

$$\hbar\omega_3 = \delta + \frac{\Delta}{2}\Big(\eta_1 - 1\Big), \tag{A.119}$$

$$\hbar\omega_4 = \frac{\Delta}{2}\Big(\eta_1 + 1\Big) \tag{A.120}$$

and the non-zero couplings are given by

$$\begin{aligned}\hbar\lambda_{44} &= -\frac{\Delta}{4}\Big[1-\Big(\frac{g_1}{g_{1,c}}\Big)^2\Big]\Big[1+\frac{1}{2}\frac{1-\left(\frac{g_{1,c}}{g_1}\right)^2}{1+\left(\frac{g_{1,c}}{g_1}\right)^2}\Big] \\ &= \frac{\Delta}{8}\frac{(\eta_1-1)(3\eta_1+1)}{\eta_1+1}, \end{aligned} \tag{A.121}$$

$$\begin{aligned}\hbar\lambda_{14} &= g_1\sqrt{\frac{1}{2}}\sqrt{1+\Big(\frac{g_{1,c}}{g_1}\Big)^2}\Big[1-\frac{1-\left(\frac{g_{1,c}}{g_1}\right)^2}{1+\left(\frac{g_{1,c}}{g_1}\right)^2}\Big] \\ &= \frac{g_{1,c}\sqrt{2}}{\sqrt{\eta_1+1}}, \end{aligned} \tag{A.122}$$

$$\hbar\lambda_{23} = g_2\sqrt{\frac{1}{2}}\sqrt{1-1/\eta_1} = g_2\sqrt{\frac{1}{2}}\sqrt{\frac{\eta_1-1}{\eta_1}}. \tag{A.123}$$

The Hamiltonian is given by

$$\begin{aligned}\hat{h}^{(2)}_{m=1} &= \hbar\omega_1\hat{a}_1^\dagger\hat{a}_1+\hbar\omega_2\hat{a}_2^\dagger\hat{a}_2+\hbar\omega_3\hat{a}_3^\dagger\hat{a}_3+\hbar\omega_4\hat{a}_4^\dagger\hat{a}_4 \\ &+\hbar\lambda_{14}(\hat{a}_1^\dagger+\hat{a}_1)(\hat{a}_4^\dagger+\hat{a}_4)+\hbar\lambda_{23}(\hat{a}_2^\dagger+\hat{a}_2)(\hat{a}_3^\dagger+\hat{a}_3) \\ &+\hbar\lambda_{44}(\hat{a}_4^\dagger+\hat{a}_4)^2. \end{aligned} \tag{A.124}$$

We see, that the first and fourth, and second and third oscillator are coupled, respectively. Thus, the excitation energies of the diagonalised Hamiltonian are given by

$$\varepsilon^2_{1,4} = \frac{1}{2}\Bigg[\omega_1^2+\omega_4^2+4\omega_4\lambda_{44} \tag{A.125}$$

$$\pm\sqrt{[\omega_1^2-\omega_4^2-4\omega_4\lambda_{44}]^2+16\lambda_{14}^2\omega_1\omega_4}\Bigg], \tag{A.126}$$

$$\varepsilon^2_{2,3} = \frac{1}{2}\Big[\omega_2^2+\omega_3^2\pm\sqrt{[\omega_2^2-\omega_3^2]^2+16\lambda_{23}^2\omega_2\omega_3}\Big]. \tag{A.127}$$

RED SUPERRADIANT PHASE At last, consider the red superradiant phase. The Hamiltonian for the excitations, with $m = 2$ as a reference state, is given by

$$\begin{aligned}\hat{h}^{(2)}_{m=2} &= \hat{a}_1^\dagger\,\hat{a}_1\left[-\delta - 2\,g_2\,\varphi_2\,\Psi_3/\psi_2\right] \\ &+ \hat{a}_3^\dagger\,\hat{a}_3\left[\Delta - \delta - 2\,g_2\,\varphi_2\,\Psi_3/\psi_2\right] + \hbar\omega_1\,\hat{c}_1^\dagger\,\hat{c}_1 + \hbar\omega_2\,\hat{c}_2^\dagger\,\hat{c}_2 \\ &- \left(\hat{a}_1^\dagger + \hat{a}_1\right)^2 \frac{1}{2} g_2\,\varphi_2\,\Psi_1^2\,\Psi_3/\psi_2^3 \\ &- \left(\hat{a}_3^\dagger + \hat{a}_3\right)^2 g_2\,\varphi_2\,\Psi_3/\psi_2\left(1 + \tfrac{1}{2}\Psi_3^2/\psi_2^2\right) \\ &- \left(\hat{a}_1^\dagger + \hat{a}_1\right)\left(\hat{a}_3^\dagger + \hat{a}_3\right) g_2\,\varphi_2\,\Psi_1/\psi_2\left(1 + \Psi_3^2/\psi_2^2\right) \\ &+ \left(\hat{a}_3^\dagger\,\hat{a}_1 + \hat{a}_1^\dagger\,\hat{a}_3\right) 2\,g_1\,\varphi_1 \\ &- \left(\hat{c}_2^\dagger + \hat{c}_2\right)\left(\hat{a}_1^\dagger + \hat{a}_1\right) g_2\,\Psi_1\,\Psi_3/\psi_2 \\ &+ \left(\hat{c}_2^\dagger + \hat{c}_2\right)\left(\hat{a}_3^\dagger + \hat{a}_3\right) g_2\,\psi_2\left(1 - \Psi_3^2/\psi_2^2\right) \\ &+ \left(\hat{c}_1^\dagger + \hat{c}_1\right)\left(\hat{a}_1^\dagger + \hat{a}_1\right) g_1\,\Psi_3 \\ &+ \left(\hat{c}_1^\dagger + \hat{c}_1\right)\left(\hat{a}_3^\dagger + \hat{a}_3\right) g_1\,\Psi_1. \end{aligned} \tag{A.128}$$

Here, we have defined $\psi_2 = \sqrt{1 - \Psi_1^2 - \Psi_3^2}$.

We define new operators

$$\hat{a}_1 = \hat{c}_1, \tag{A.129}$$
$$\hat{a}_2 = \hat{c}_2, \tag{A.130}$$
$$\hat{a}_3 = \hat{a}_1, \tag{A.131}$$
$$\hat{a}_4 = \hat{a}_3, \tag{A.132}$$

new frequencies

$$\hbar\omega_3 = -\delta - 2\,g_2\,\varphi_2\,\Psi_3/\psi_2, \tag{A.133}$$
$$\hbar\omega_4 = \Delta - \delta - 2\,g_2\,\varphi_2\,\Psi_3/\psi_2, \tag{A.134}$$

and new couplings

$$\hbar\lambda_{33} = -\frac{1}{2} g_2\,\varphi_2\,\Psi_1^2\,\Psi_3/\psi_2^3, \tag{A.135}$$
$$\hbar\lambda_{44} = -g_2\,\varphi_2\,\Psi_3/\psi_2\left(1 + \tfrac{1}{2}\Psi_3^2/\psi_2^2\right), \tag{A.136}$$
$$\hbar\lambda_{34} = -g_2\,\varphi_2\,\Psi_1/\psi_2\left(1 + \Psi_3^2/\psi_2^2\right), \tag{A.137}$$
$$\hbar\lambda'_{34} = 2g_1\varphi_1, \tag{A.138}$$
$$\hbar\lambda_{23} = -g_2\Psi_1\Psi_3/\psi_2, \tag{A.139}$$
$$\hbar\lambda_{24} = g_2\psi_2(1 - \Psi_3^2/\psi_2^2), \tag{A.140}$$
$$\hbar\lambda_{13} = g_1\Psi_3, \tag{A.141}$$
$$\hbar\lambda_{14} = g_1\Psi_1. \tag{A.142}$$

For the red superradiant state, it holds (cf. Sec. 2.3.3)

$$\Psi_1 = 0, \Psi_3 = \sqrt{\frac{1}{2}}\sqrt{1-\left(\frac{g_{2,c_1}}{g_2}\right)^2}, \tag{A.143}$$

$$\varphi_1 = 0, \varphi_2 = -\frac{g_2}{\hbar\omega_2}\sqrt{1-\left(\frac{g_{2,c_1}}{g_2}\right)^4}, \tag{A.144}$$

such that λ_{44}, λ_{24}, and λ_{13} are non-zero only.

We have

$$2g_2\varphi_2\Psi_3/\psi_2 = -\frac{\Delta-\delta}{2}\left[\left(\frac{g_2}{g_{2,c_1}}\right)^2 - 1\right], \tag{A.145}$$

$$g_2\varphi_2\Psi_3/\psi_2(1+\tfrac{1}{2}\Psi_3^2/\psi_2^2) = -\frac{\Delta-\delta}{8}\frac{\left[\left(\frac{g_2}{g_{2,c_1}}\right)^2 - 1\right]\left[3\left(\frac{g_2}{g_{2,c_1}}\right)^2 + 1\right]}{1+\left(\frac{g_2}{g_{2,c_1}}\right)^2}, \tag{A.146}$$

$$g_2\psi_2(1-\Psi_3^2/\psi_2^2) = \sqrt{2}g_{2,c_1}\sqrt{\frac{1}{1+\left(\frac{g_2}{g_{2,c_1}}\right)^2}}. \tag{A.147}$$

With that, we have for the frequencies

$$\hbar\omega_3 = -\delta + \frac{\Delta-\delta}{2}(\eta_2 - 1), \tag{A.148}$$

$$\hbar\omega_4 = \frac{\Delta-\delta}{2}(\eta_2 + 1), \tag{A.149}$$

and for the couplings

$$\hbar\lambda_{13} = g_1\sqrt{\frac{1}{2}}\sqrt{1-1/\eta_2} = g_1\sqrt{\frac{1}{2}}\sqrt{\frac{\eta_2-1}{\eta_2}}, \tag{A.150}$$

$$\hbar\lambda_{24} = g_{2,c_1}\sqrt{2}\sqrt{\frac{1}{\eta_2+1}}, \tag{A.151}$$

$$\hbar\lambda_{44} = \frac{\Delta-\delta}{8}\frac{(\eta_2-1)(3\eta_2+1)}{\eta_2+1}. \tag{A.152}$$

The Hamiltonian is given by

$$\begin{aligned}\hat{h}^{(2)}_{m=2} = {}& \hbar\omega_1\hat{a}_1^\dagger\hat{a}_1 + \hbar\omega_2\hat{a}_2^\dagger\hat{a}_2 + \hbar\omega_3\hat{a}_3^\dagger\hat{a}_3 + \hbar\omega_4\hat{a}_4^\dagger\hat{a}_4 \\ & + \hbar\lambda_{13}(\hat{a}_1^\dagger + \hat{a}_1)(\hat{a}_3^\dagger + \hat{a}_3) + \hbar\lambda_{24}(\hat{a}_2^\dagger + \hat{a}_2)(\hat{a}_4^\dagger + \hat{a}_4) \\ & + \hbar\lambda_{44}(\hat{a}_4^\dagger + \hat{a}_4)^2.\end{aligned} \tag{A.153}$$

Thus, the excitation energies are given by

$$\varepsilon^2_{1,4} = \frac{1}{2}\left[\omega_1^2 + \omega_3^2 \pm \sqrt{\left[\omega_1^2 - \omega_3^2\right]^2 + 16\lambda_{13}^2\omega_1\omega_3}\right], \tag{A.154}$$

$$\begin{aligned}\varepsilon^2_{2,3} = \frac{1}{2}\Big[{}& \omega_2^2 + \omega_4^2 + 4\omega_4\lambda_{44} \\ & \pm \sqrt{\left[\omega_2^2 - \omega_4^2 - 4\omega_4\lambda_{44}\right]^2 + 16\lambda_{24}^2\omega_2\omega_4}\Big].\end{aligned} \tag{A.155}$$

We note, that we have chosen a different naming of the indices of the excitation energies here.

In conclusion, we have for the excitation energies of the collective excitations for the Lambda-model in the respective phases:

NORMAL PHASE

$$\varepsilon_{1,4} = \sqrt{\frac{1}{2}\left[\omega_1^2 + \left(\Delta/\hbar\right)^2 \pm \sqrt{[\omega_1^2 - \left(\Delta/\hbar\right)^2]^2 + 64\left(g_1/\hbar\right)^2\left(g_{1,c}/\hbar\right)^2}\right]} \tag{A.156}$$

$$\varepsilon_2 = \delta/\hbar \tag{A.157}$$

$$\varepsilon_3 = \omega_2. \tag{A.158}$$

BLUE SUPERRADIANT PHASE

$$\varepsilon_{1,4}^2 = \frac{1}{2}\left[\omega_1^2 + \left[\frac{\Delta/\hbar}{2}\left(\eta_1+1\right)\right]^2 + \left(\frac{\Delta/\hbar}{2}\right)^2\left(\eta_1-1\right)\left(3\eta_1+1\right)\right. \tag{A.159}$$
$$\left. \pm \sqrt{\left[\omega_1^2 - \left[\frac{\Delta/\hbar}{2}\left(\eta_1+1\right)\right]^2 - \left(\frac{\Delta/\hbar}{2}\right)^2\left(\eta_1-1\right)\left(3\eta_1+1\right)\right]^2 + 64\left(g_{1,c}/\hbar\right)^4}\right]$$

$$\varepsilon_{2,3}^2 = \frac{1}{2}\left[\omega_2^2 + \left[\delta/\hbar + \frac{\Delta/\hbar}{2}\left(\eta_1-1\right)\right]^2\right. \tag{A.160}$$
$$\left. \pm \sqrt{\left[\omega_2^2 - \left[\delta/\hbar + \frac{\Delta/\hbar}{2}\left(\eta_1-1\right)\right]^2\right]^2 + 8\left(g_2/\hbar\right)^2\frac{\eta_1-1}{\eta_1}\left[\delta/\hbar + \frac{\Delta/\hbar}{2}\left(\eta_1-1\right)\right]\omega_2}\right]$$

RED SUPERRADIANT PHASE

$$\varepsilon_{1,4}^2 = \frac{1}{2}\left[\omega_1^2 + \left[-\delta/\hbar + \frac{(\Delta-\delta)/\hbar}{2}\left(\eta_2-1\right)\right]^2\right. \tag{A.161}$$
$$\left. \pm \sqrt{\left[\omega_1^2 - \left[-\delta/\hbar + \frac{(\Delta-\delta)/\hbar}{2}\left(\eta_2-1\right)\right]^2\right]^2 + 8\left(g_1/\hbar\right)^2\frac{\eta_2-1}{\eta_2}\left[-\delta/\hbar + \frac{(\Delta-\delta)/\hbar}{2}\left(\eta_2-1\right)\right]\omega_1}\right]$$

$$\varepsilon_{2,3}^2 = \frac{1}{2}\left[\omega_2^2 + \left[\frac{(\Delta-\delta)/\hbar}{2}\left(\eta_2+1\right)\right]^2 + \left[\frac{(\Delta-\delta)/\hbar}{2}\right]^2\left(\eta_2-1\right)\left(3\eta_2+1\right)\right. \tag{A.162}$$
$$\left. \pm \sqrt{\left[\omega_2^2 - \left[\frac{(\Delta-\delta)/\hbar}{2}\left(\eta_2+1\right)\right]^2 - \left[\frac{(\Delta-\delta)/\hbar}{2}\right]^2\left(\eta_2-1\right)\left(3\eta_2+1\right)\right]^2 + 64\left(g_{2,c_1}/\hbar\right)^4}\right]$$

The notation $\eta_1 = \left(g_1/g_{1,c}\right)^2$, $\eta_2 = \left(g_2/g_{2,c_1}\right)^2$ is used. The critical coupling strengths are given by $g_{1,c} = \sqrt{\Delta\hbar\omega_1}/2$ and $g_{2,c_1} = \sqrt{\left(\Delta-\delta\right)\hbar\omega_2}/2$. It is clear that the excitation energies are positive.

BIBLIOGRAPHY

Abramowitz, Milton and Irene A. Stegun, eds. (1972): *Handbook of Mathematical Functions with Formulas, Graphs, and Mathematical Tables*. 9. Ed. New York, NY: Dover. ISBN: 0-486-61272-4.

Agarwal, G. S. (1971): *Rotating-Wave Approximation and Spontaneous Emission*, Phys. Rev. A **4**, pp. 1778–1781. DOI: 10.1103/PhysRevA.4.1778.

Alcalde, M. Aparicio, M. Bucher, C. Emary, and T. Brandes (2012): *Thermal phase transitions for Dicke-type models in the ultrastrong-coupling limit*, Phys. Rev. E **86**, p. 012101. DOI: 10.1103/PhysRevE.86.012101.

Altland, Alexander and Fritz Haake (2012): *Quantum Chaos and Effective Thermalization*, Phys. Rev. Lett. **108**, p. 073601. DOI: 10.1103/PhysRevLett.108.073601.

Altland, Alexander and Berry Simons (2010): *Condensed Matter Field Theory*. 2. Ed. Cambridge [u.a.]: Cambridge University Press. ISBN: 978-0-521-76975-4.

Arecchi, F. T., Eric Courtens, Robert Gilmore, and Harry Thomas (1972): *Atomic Coherent States in Quantum Optics*, Phys. Rev. A **6**, p. 2211. DOI: 10.1103/PhysRevA.6.2211.

Arimondo, E. (1996). "V Coherent Population Trapping in Laser Spectroscopy". In: ed. by E. Wolf. Vol. 35. Progress in Optics. Elsevier, p. 257. DOI: 10.1016/S0079-6638(08)70531-6.

Ashcroft, Neil W. and N. David Mermin (1976): *Solid State Physics*. Philadelphia: W. B. Saunders Company. ISBN: 0-03-049346-3.

Baden, Markus P., Kyle J. Arnold, Arne L. Grimsmo, Scott Parkins, and Murray D. Barrett (2014): *Realization of the Dicke Model Using Cavity-Assisted Raman Transitions*, Phys. Rev. Lett. **113**, p. 020408. DOI: 10.1103/PhysRevLett.113.020408.

Bakemeier, L., A. Alvermann, and H. Fehske (2012): *Quantum phase transition in the Dicke model with critical and noncritical entanglement*, Phys. Rev. A **85**, p. 043821. DOI: 10.1103/PhysRevA.85.043821.

Bakemeier, L., A. Alvermann, and H. Fehske (2013): *Dynamics of the Dicke model close to the classical limit*, Phys. Rev. A **88**, p. 043835. doi: 10.1103/PhysRevA.88.043835.

Baksic, Alexandre, Pierre Nataf, and Cristiano Ciuti (2013): *Superradiant phase transitions with three-level systems*, Phys. Rev. A **87**, p. 023813. doi: 10.1103/PhysRevA.87.023813.

Bastidas, V. M., C. Emary, B. Regler, and T. Brandes (2012): *Nonequilibrium Quantum Phase Transitions in the Dicke Model*, Phys. Rev. Lett. **108**, p. 043003. doi: 10.1103/PhysRevLett.108.043003.

Baumann, K., R. Mottl, F. Brennecke, and T. Esslinger (2011): *Exploring Symmetry Breaking at the Dicke Quantum Phase Transition*, Phys. Rev. Lett. **107**, p. 140402. doi: 10.1103/PhysRevLett.107.140402.

Baumann, Kristian, Christine Guerlin, Ferdinand Brennecke, and Tilman Esslinger (2010): *Dicke quantum phase transition with a superfluid gas in an optical cavity*, Nature (London) **464**, p. 1301. doi: 10.1038/nature09009.

Bender, Carl M. and Steven A. Orszag (1999): *Advanced Mathematical Methods for Scientists and Engineers*. New York [u.a.]: Springer. isbn: 0-387-98931-5.

Bergmann, K., H. Theuer, and B. W. Shore (1998): *Coherent population transfer among quantum states of atoms and molecules*, Rev. Mod. Phys. **70**, p. 1003. doi: 10.1103/RevModPhys.70.1003.

Bethe, Hans Albrecht and Roman W. Jackiw (1986): *Intermediate quantum mechanics*. 3. Ed. Menlo Park, Calif: Benjamin/Cummings. isbn: 0-8053-0757-5.

Bhaseen, M. J., J. Mayoh, B. D. Simons, and J. Keeling (2012): *Dynamics of nonequilibrium Dicke models*, Phys. Rev. A **85**, p. 013817. doi: 10.1103/PhysRevA.85.013817.

Bialynicki-Birula, Iwo and Kazimierz Rzążewski (1979): *No-go theorem concerning the superradiant phase transition in atomic systems*, Phys. Rev. A **19**, pp. 301–303. doi: 10.1103/PhysRevA.19.301.

Blais, Alexandre, Ren-Shou Huang, Andreas Wallraff, S. M. Girvin, and R. J. Schoelkopf (2004): *Cavity quantum electrodynamics for superconducting electrical circuits: An architecture for quantum computation*, Phys. Rev. A **69**, p. 062320. doi: 10.1103/PhysRevA.69.062320.

Braak, D. (2011): *Integrability of the Rabi Model*, Phys. Rev. Lett. **107**, p. 100401. doi: 10.1103/PhysRevLett.107.100401.

Brandes, Tobias (2013): *Excited-state quantum phase transitions in Dicke superradiance models*, Phys. Rev. E **88**, p. 032133. doi: 10.1103/PhysRevE.88.032133.

Bronstein, I. N., K. A. Semendjajew, G. Musiol, and H. Mühlig (2001): *Taschenbuch der Mathematik*. 5. Ed. Thun [u.a.]: Verlag Harri Deutsch. isbn: 3-8171-2005-2.

Carmichael, H. J., C. W. Gardiner, and D. F. Walls (1973): *Higher order corrections to the Dicke superradiant phase transition*, Physics Letters A **46**, pp. 47–48. doi: 10.1016/0375-9601(73)90679-8.

Champeney, D. C. (1973): *Fourier Transforms and their Physical Applications*. London and New York: Academic Press. isbn: 0-12-167450-9.

Chen, Gang, Zidong Chen, and Jiuqing Liang (2007): *Simulation of the superradiant quantum phase transition in the superconducting charge qubits inside a cavity*, Phys. Rev. A **76**, p. 055803. doi: 10.1103/PhysRevA.76.055803.

Chen, Gang, Juqi Li, and J.-Q. Liang (2006): *Critical property of the geometric phase in the Dicke model*, Phys. Rev. A **74**, p. 054101. doi: 10.1103/PhysRevA.74.054101.

Ciuti, Cristiano and Pierre Nataf (2012): *Comment on "Superradiant Phase Transitions and the Standard Description of Circuit QED"*, Phys. Rev. Lett. **109**, p. 179301. doi: 10.1103/PhysRevLett.109.179301.

Cohen-Tannoudji, Claude, Jaques Dupont-Roc, and Gilbert Grynberg (1989): *Photons & Atoms: Introduction to Quantum Electrodynamics*. New York [u.a.]: Wiley. isbn: 0-471-84526-4.

Dembiński, S. T. and A. Kossakowski (1974): *Laser and superradiant phase transitions in the Dicke model of a dynamical system*, Physics Letters A **49**, pp. 331–332. doi: 10.1016/0375-9601(74)90834-2.

Dicke, Robert Henry (1954): *Coherence in Spontaneous Radiation Processes*, Phys. Rev. **93**, p. 99. doi: 10.1103/PhysRev.93.99.

Dimer, F., B. Estienne, A. S. Parkins, and H. J. Carmichael (2007): *Proposed realization of the Dicke-model quantum phase transition in an optical cavity QED system*, Phys. Rev. A **75**, p. 013804. doi: 10.1103/PhysRevA.75.013804.

Dirac, P. A. M. (1958): *The Principles of Quantum Mechanics*. 4. Ed. London [u.a.]: Oxford University Press.

Emary, Clive and Tobias Brandes (2003a): *Chaos and the quantum phase transition in the Dicke model*, Phys. Rev. E **67**, p. 066203. doi: 10.1103/PhysRevE.67.066203.

Emary, Clive and Tobias Brandes (2003b): *Quantum Chaos Triggered by Precursors of a Quantum Phase Transition: The Dicke Model*, Phys. Rev. Lett. **90**, p. 044101. doi: 10.1103/PhysRevLett.90.044101.

Engelhardt, G., V. M. Bastidas, W. Kopylov, and T. Brandes (2015): *Excited-state quantum phase transitions and periodic dynamics*, Phys. Rev. A **91**, p. 013631. doi: 10.1103/PhysRevA.91.013631.

Feynman, R. P. (1972): *Statistical Mechanics — A Set of Lectures*. Frontiers in Physics. Reading, Massachusetts: W. A. Benjamin, Inc. isbn: 0-805-32509-3.

Fisher, Matthew P. A., Peter B. Weichman, G. Grinstein, and Daniel S. Fisher (1989): *Boson localization and the superfluid-insulator transition*, Phys. Rev. B **40**, pp. 546–570. doi: 10.1103/PhysRevB.40.546.

Garraway, Barry M. (2011): *The Dicke model in quantum optics: Dicke model revisited*, Phil. Trans. R. Soc. A **369**, pp. 1137–1155. doi: 10.1098/rsta.2010.0333.

Genway, Sam, Weibin Li, Cenap Ates, Benjamin P. Lanyon, and Igor Lesanovsky (2014): *Generalized Dicke Nonequilibrium Dynamics in Trapped Ions*, Phys. Rev. Lett. **112**, p. 023603. doi: 10.1103/PhysRevLett.112.023603.

Gilmore, R. (1976): *Persistence of the phase transition in the Dicke model with external fields and counter-rotating terms*, Physics Letters A **55**, pp. 459–460. doi: 10.1016/0375-9601(76)90220-6.

Glauber, Roy J. (1963): *Coherent and Incoherent States of the Radiation Field*, Phys. Rev. **131**, pp. 2766–2788. doi: 10.1103/PhysRev.131.2766.

Glick, A. J., H. J. Lipkin, and N. Meshkov (1965): *Validity of many-body approximation methods for a solvable model: (III). Diagram summations*, Nuclear Physics **62**, pp. 211–224. doi: 10.1016/0029-5582(65)90864-3.

Goban, A., C.-L. Hung, J. D. Hood, S.-P. Yu, J. A. Muniz, O. Painter, and H. J. Kimble (2015): *Superradiance for Atoms Trapped along a Photonic Crystal Waveguide*, Phys. Rev. Lett. **115**, p. 063601. doi: 10.1103/PhysRevLett.115.063601.

Goldenfeld, Nigel (2010): *Lectures on phase transitions and the renormalization group*. reprint. Frontiers in physics 85. Boulder, Colorado: Westview Press. isbn: 0-201-55409-7.

Goldstein, Herbert (1980): *Classical Mechanics*. 2. Ed. Reading, Massachusetts [u.a.]: Addison-Wesley. isbn: 0-201-02969-3.

Greiner, Markus, Olaf Mandel, Tilman Esslinger, Theodor W. Hänsch, and Immanuel Bloch (2002): *Quantum phase transition from a superfluid to a Mott insulator in a gas of ultracold atoms*, Nature **415**, p. 39. doi: 10.1038/415039a.

Griffin, A., D. W. Snoke, and S. Stringari, eds. (1995): *Bose–Einstein Condensation*. Cambridge [u.a.]: Cambridge University Press. isbn: 0-521-46473-0.

Gross, M., C. Fabre, P. Pillet, and S. Haroche (1976): *Observation of Near-Infrared Dicke Superradiance on Cascading Transitions in Atomic Sodium*, Phys. Rev. Lett. **36**, pp. 1035–1038. doi: 10.1103/PhysRevLett.36.1035.

Gross, M. and S. Haroche (1982): *Superradiance: An essay on the theory of collective spontaneous emision*, Phys. Rep. **93**, p. 301. doi: 10.1016/0370-1573(82)90102-8.

Gross, M., J. M. Raimond, and S. Haroche (1978): *Doppler Beats in Superradiance*, Phys. Rev. Lett. **40**, pp. 1711–1714. doi: 10.1103/PhysRevLett.40.1711.

Guerin, William, Michelle O. Araújo, and Robin Kaiser (2016): *Subradiance in a Large Cloud of Cold Atoms*, Phys. Rev. Lett. **116**, p. 083601. doi: 10.1103/PhysRevLett.116.083601.

Hall, Brian C. (2003): *Lie Groups, Lie Algebras, and Representations — An Elementary Introduction*. New York: Springer. isbn: 978-1-4419-2313-4. doi: 10.1007/978-0-387-21554-9.

Hamermesh, Morton (1964): *Group Theory*. Second Printing. Reading, Massachusetts [u.a.]: Addison-Wesley.

Hepp, Klaus and Elliott H. Lieb (1973a): *Equilibrium Statistical Mechanics of Matter Interacting with the Quantized Radiation Field*, Phys. Rev. A **8**, p. 2517. DOI: 10.1103/PhysRevA.8.2517.

Hepp, Klaus and Elliott H. Lieb (1973b): *On the superradiant phase transition for molecules in a quantized radiation field: the dicke maser model*, Ann. Phys. **76**, p. 360. DOI: 10.1016/0003-4916(73)90039-0.

Hepp, Klaus and Elliott H. Lieb (1973c): *Phase Transition in Reservoir-Driven Open Systems with Applications to Lasers and Superconductors*, Helvetica Physica Acta **46**, p. 573. DOI: 10.5169/seals-114496.

Hioe, F. T. (1973): *Phase Transitions in Some Generalized Dicke Models of Superradiance*, Phys. Rev. A **8**, pp. 1440–1445. DOI: 10.1103/PhysRevA.8.1440.

Holstein, T. and H. Primakoff (1940): *Field Dependence of the Intrinsic Domain Magnetization of a Ferromagnet*, Phys. Rev. **58**, p. 1098. DOI: 10.1103/PhysRev.58.1098.

Hopfield, J. J. (1958): *Theory of the Contribution of Excitons to the Complex Dielectric Constant of Crystals*, Phys. Rev. **112**, p. 1555. DOI: 10.1103/PhysRev.112.1555.

Huang, Kerson (1964): *Statistische Mechanik III*. Mannheim: BI Hochschultaschenbücher-Verlag.

Jackson, John David (1999): *Classical Electrodynamics*. 3. Ed. New York [u.a.]: John Wiley & Sons. ISBN: 0-471-30932-X.

Jaeger, Gregg (1998): *The Ehrenfest Classification of Phase Transitions: Introduction and Evolution*, Archive for History of Exact Sciences **53**, pp. 51–81. DOI: 10.1007/s004070050021.

Jaksch, D., C. Bruder, J. I. Cirac, C. W. Gardiner, and P. Zoller (1998): *Cold Bosonic Atoms in Optical Lattices*, Phys. Rev. Lett. **81**, pp. 3108–3111. DOI: 10.1103/PhysRevLett.81.3108.

Jaksch, D. and P. Zoller (2005): *The cold atom Hubbard toolbox*, Annals of Physics **315**. Special Issue, pp. 52–79. DOI: http://dx.doi.org/10.1016/j.aop.2004.09.010.

Jänich, Klaus (2001): *Analysis für Physiker und Ingenieure*. 4. Ed. Berlin [u.a.]: Springer. ISBN: 3-540-41985-3.

Jaynes, E. T. and Frederick W. Cummings (1963): *Comparison of quantum and semiclassical radiation theories with application to the beam*

maser, Proceedings of the IEEE **51**, pp. 89–109. DOI: 10.1109/PROC.1963.1664.

KEELING, J., M. J. BHASEEN, and B. D. SIMONS (2010): *Collective Dynamics of Bose-Einstein Condensates in Optical Cavities*, Phys. Rev. Lett. **105**, p. 043001. DOI: 10.1103/PhysRevLett.105.043001.

KLEIN, Abraham and E. R. MARSHALEK (1991): *Boson realizations of Lie algebras with applications to nuclear physics*, Rev. Mod. Phys. **63**, p. 375. DOI: 10.1103/RevModPhys.63.375.

KNIGHT, J. M., Y. AHARONOV, and G. T. C. HSIEH (1978): *Are superradiant phase transitions possible?*, Phys. Rev. A **17**, pp. 1454–1462. DOI: 10.1103/PhysRevA.17.1454.

KNIGHT, P. L. and L. ALLEN (1973): *Rotating-Wave Approximation in Coherent Interactions*, Phys. Rev. A **7**, pp. 368–370. DOI: 10.1103/PhysRevA.7.368.

KOPYLOV, Wassilij, Clive EMARY, and Tobias BRANDES (2013): *Counting statistics of the Dicke superradiance phase transition*, Phys. Rev. A **87**, p. 043840. DOI: 10.1103/PhysRevA.87.043840.

KOPYLOV, Wassilij, Clive EMARY, Eckehard SCHÖLL, and Tobias BRANDES (2015): *Time-delayed feedback control of the Dicke–Hepp–Lieb superradiant quantum phase transition*, New Journal of Physics **17**, p. 013040. DOI: 10.1088/1367-2630/17/1/013040.

LAMBERT, Neil, Yueh-Nan CHEN, Robert JOHANSSON, and Franco NORI (2009): *Quantum chaos and critical behavior on a chip*, Phys. Rev. B **80**, p. 165308. DOI: 10.1103/PhysRevB.80.165308.

LARSON, Jonas (2007): *Dynamics of the Jaynes–Cummings and Rabi models: old wine in new bottles*, Physica Scripta **76**, p. 146. DOI: 10.1088/0031-8949/76/2/007.

LAURENT, T., Y. TODOROV, A. VASANELLI, A. DELTEIL, C. SIRTORI, I. SAGNES, and G. BEAUDOIN (2015): *Superradiant Emission from a Collective Excitation in a Semiconductor*, Phys. Rev. Lett. **115**, p. 187402. DOI: 10.1103/PhysRevLett.115.187402.

LEWENSTEIN, Maciej, Anna SANPERA, Veronica AHUFINGER, Bogdan DAMSKI, Aditi SEN(DE), and Ujjwal SEN (2007): *Ultracold atomic gases in optical lattices: mimicking condensed matter physics and beyond*, Advances in Physics **56**, p. 243. DOI: 10.1080/00018730701223200.

Liberti, Giuseppe, Francesco Plastina, and Franco Piperno (2006): *Scaling behavior of the adiabatic Dicke model*, Phys. Rev. A **74**, p. 022324. doi: 10.1103/PhysRevA.74.022324.

Lipkin, H. J., N. Meshkov, and A. J. Glick (1965): *Validity of many-body approximation methods for a solvable model: (I). Exact solutions and perturbation theory*, Nuclear Physics **62**, pp. 188–198. doi: 10.1016/0029-5582(65)90862-X.

Mallory, William R. (1969): *Solution of a Multiatom Radiation Model Using the Bargmann Realization of the Radiation Field*, Phys. Rev. **188**, pp. 1976–1987. doi: 10.1103/PhysRev.188.1976.

Meshkov, N., A. J. Glick, and H. J. Lipkin (1965): *Validity of many-body approximation methods for a solvable model: (II). Linearization procedures*, Nuclear Physics **62**, pp. 199–210. doi: 10.1016/0029-5582(65)90863-1.

Meystre, Pierre (1992). "V Cavity Quantum Optics and the Quantum Measurement Process". In: ed. by E. Wolf. Vol. 30. Progress in Optics. Elsevier, pp. 261–355. doi: 10.1016/S0079-6638(08)70100-8.

Mlynek, J. A., A. A. Abdumalikov, C. Eichler, and A. Wallraff (2014): *Observation of Dicke superradiance for two artificial atoms in a cavity with high decay rate*, Nat. Commun. **5**, p. 5186. doi: 10.1038/ncomms6186.

Nagy, D., G. Kónya, G. Szirmai, and P. Domokos (2010): *Dicke-Model Phase Transition in the Quantum Motion of a Bose-Einstein Condensate in an Optical Cavity*, Phys. Rev. Lett. **104**, p. 130401. doi: 10.1103/PhysRevLett.104.130401.

Nataf, Pierre and Cristiano Ciuti (2010a): *No-go theorem for superradiant quantum phase transitions in cavity QED and counter-example in circuit QED*, Nat. Commun. **1**, p. 72. doi: 10.1038/ncomms1069.

Nataf, Pierre and Cristiano Ciuti (2010b): *Vacuum Degeneracy of a Circuit QED System in the Ultrastrong Coupling Regime*, Phys. Rev. Lett. **104**, p. 023601. doi: 10.1103/PhysRevLett.104.023601.

Nielsen, Michael A. and Isaac L. Chuang (2002): *Quantum computation and quantum information*. Cambridge University Press. isbn: 0-521-63503-9.

Nussenzveig, H. Moysés (1973): *Introduction to Quantum Optics*. London [u.a.]: Gordon and Breach Science Publishers. ISBN: 0-677-03900-X.

Okubo, Susumu (1975): *Algebraic identities among U(n) infinitesimal generators*, J. Math. Phys. (N.Y.) **16**, p. 528. DOI: 10.1063/1.522550.

Orszag, Miguel (1977): *Phase transition of a system of two-level atoms*, Journal of Physics A: Mathematical and General **10**, p. 1995. DOI: 10.1088/0305-4470/10/11/025.

Rabi, I. I. (1937): *Space Quantization in a Gyrating Magnetic Field*, Phys. Rev. **51**, pp. 652–654. DOI: 10.1103/PhysRev.51.652.

Ribeiro, Pedro, Julien Vidal, and Rémy Mosseri (2008): *Exact spectrum of the Lipkin-Meshkov-Glick model in the thermodynamic limit and finite-size corrections*, Phys. Rev. E **78**, p. 021106. DOI: 10.1103/PhysRevE.78.021106.

Röhlsberger, Ralf, Kai Schlage, Balaram Sahoo, Sebastien Couet, and Rudolf Rüffer (2010): *Collective Lamb Shift in Single-Photon Superradiance*, Science **328**, p. 1248. DOI: 10.1126/science.1187770.

Rzażewski, K. and K. Wódkiewicz (1976): *Thermodynamics of two-level atoms interacting with the continuum of electromagnetic field modes*, Phys. Rev. A **13**, pp. 1967–1969. DOI: 10.1103/PhysRevA.13.1967.

Rzażewski, K., K. Wódkiewicz, and W. Żakowicz (1975): *Phase transitions, two-level atoms, and the A^2 Term*, Phys. Rev. Lett. **35**, p. 432. DOI: 10.1103/PhysRevLett.35.432.

Rzażewski, K., K. Wódkiewicz, and W. Żakowicz (1976): *Remark on the superradiant phase transition*, Physics Letters A **58**, pp. 211–212. DOI: 10.1016/0375-9601(76)90074-8.

Sachdev, Subir (1999): *Quantum Phase Transitions*. Cambridge [u.a.]: Cambridge University Press. ISBN: 0-521-58254-7.

Sakurai, Jun John (1967): *Advanced Quantum Mechanics*. Reading, Massachusetts [u.a.]: Addison-Wesley.

Sakurai, Jun John (1994): *Modern Quantum Mechanics*. Reading, Massachusetts [u.a.]: Addison-Wesley. ISBN: 0-201-53929-2.

Scharf, G. (1970): *On a quantum mechanical maser model*, Helvetica Physica Acta **43**, p. 806. DOI: 10.5169/seals-114194.

Scheibner, Michael, Thomas Schmidt, Lukas Worschech, Alfred Forchel, Gerd Bacher, Thorsten Passow, and Detlef Hommel (2007): *Superradiance of quantum dots*, Nature Physics **3**, p. 106. doi: 10.1038/nphys494.

Schwinger, J. S. (1952): *On Angular Momentum*. url: http://www.osti.gov/accomplishments/display_biblio.jsp?id=ACC0111.

Scully, Marlan O. (2015): *Single Photon Subradiance: Quantum Control of Spontaneous Emission and Ultrafast Readout*, Phys. Rev. Lett. **115**, p. 243602. doi: 10.1103/PhysRevLett.115.243602.

Shore, Bruce W. and Peter L. Knight (1993): *The Jaynes-Cummings Model*, Journal of Modern Optics **40**, pp. 1195–1238. doi: 10.1080/09500349314551321.

Silver, A. O., M. Hohenadler, M. J. Bhaseen, and B. D. Simons (2010): *Bose-Hubbard models coupled to cavity light fields*, Phys. Rev. A **81**, p. 023617. doi: 10.1103/PhysRevA.81.023617.

Singer, Stephanie Frank (2005): *Linearity, Symmetry, and Prediction in the Hydrogen Atom*. New York: Springer. isbn: 0-387-24637-1. doi: 10.1007/b136359.

Skribanowitz, N., I. P. Herman, J. C. MacGillivray, and M. S. Feld (1973): *Observation of Dicke Superradiance in Optically Pumped HF Gas*, Phys. Rev. Lett. **30**, pp. 309–312. doi: 10.1103/PhysRevLett.30.309.

Slyusarev, V. A. and R. P. Yankelevich (1979): *On the impossibility of a phase transition to the superradiant state in a thermodynamically equilibrium gauge-invariant system*, Theoretical and Mathematical Physics **40**, pp. 641–644. doi: 10.1007/BF01019248.

Tavis, Michael and Frederick W. Cummings (1968): *Exact Solution for an* N*-Molecule—Radiation-Field Hamiltonian*, Phys. Rev. **170**, pp. 379–384. doi: 10.1103/PhysRev.170.379.

Tavis, Michael and Frederick W. Cummings (1969): *Approximate Solutions for an* N*-Molecule-Radiation-Field Hamiltonian*, Phys. Rev. **188**, pp. 692–695. doi: 10.1103/PhysRev.188.692.

Thompson, B. V. (1975): *The phase transition in a modified Dicke model*, Journal of Physics A: Mathematical and General **8**, p. 126. doi: 10.1088/0305-4470/8/1/019.

Vertogen, G. and A. S. De Vries (1974): *The dicke maser model*, Physics Letters A **48**, pp. 451–453. doi: 10.1016/0375-9601(74)90620-3.

Viehmann, Oliver, Jan von Delft, and Florian Marquardt (2011): *Superradiant Phase Transitions and the Standard Description of Circuit QED*, Phys. Rev. Lett. **107**, p. 113602. doi: 10.1103/PhysRevLett.107.113602.

Viehmann, Oliver, Jan von Delft, and Florian Marquardt (2012). "Reply to Comment on "Superradiant Phase Transitions and the Standard Description of Circuit QED"".

von Neumann, John (1932): *Mathematische Grundlagen der Quantenmechanik*. Reprint. Berlin [u.a.]: Springer. isbn: 3-540-59207-5.

Walls, D. F. (1972): *Higher order effects in the single atom field mode interaction*, Physics Letters A **42**, pp. 217–218. doi: http://dx.doi.org/10.1016/0375-9601(72)90867-5.

Wang, Y. K. and F. T. Hioe (1973): *Phase Transition in the Dicke Model of Superradiance*, Phys. Rev. A **7**, p. 831. doi: 10.1103/PhysRevA.7.831.

Weinberg, Steven (1995): *The Quanumt Theory of Fields I, II, III*. Cambridge: Cambridge University Press. isbn: 0-521-55001-7.

ACKNOWLEDGMENTS

Ein großer Dank geht an Prof. Tobias Brandes, dafür dass er soviel Vertrauen in mich hatte und mir die Möglichkeit gegeben hat in seiner Arbeitsgruppe an diesem Thema zu forschen und am Fachbereich aktiv in der Lehre mitzuwirken.

Ein Dank geht auch Prof. Cristiano Ciuti dafür, dass er das Zweitgutachten meiner Arbeit übernimmt. Danke auch an Prof. Ulrike Woggon dafür, dass sie dem Promotionsausschuß meiner Verteidigung vorsitzt.

Ein großes Dankeschön geht an die aktuellen und ehemaligen Leute unserer Arbeitsgruppe. Besonders an Philipp Zedler, Anja Metelmann, Christian Nietner, Victor Bastidas, Martin Aparicio Alcalde, Malte Vogl, Wassilij Kopylov, Clive Emary, Emily Wiegand und Philipp Strasberg. Vielen lieben Dank an Heike Klemz und Julia Eckert für die große Hilfe bei vielen organisatorischen Angelegenheiten.

Ein besonderes Dankeschön geht an meine Familie, meinen Eltern und ganz speziell an meine Frau Sophie. Danke, dass du es in den letzten Wochen in diesen besonderen Umständen mit mir ausgehalten hast und meine Arbeit unermüdlich gelesen hast. Liebe Luisa und lieber Anton, auch euch ein herzliches Dankeschön, dass ihr mir die letzte nötige Motivation gegeben habt, diese Arbeit fertig zu stellen.

Vielen Dank!